a ARD-AR-304

AGARD

ADVISORY GROUP FOR AEROSPACE RESEARCH & DEVELOPMENT

7 RUE ANCELLE 92200 NEUILLY SUR SEINE FRANCE

**AGARD ADVISORY REPORT 304**
**Fluid Dynamics Panel Working Group 15**

# Quality Assessment for Wind Tunnel Testing

(L'Appréciation de la Qualité pour les Essais en Soufflerie)

*This Advisory Report has been pre*
*of the Fluid Dynamics Panel of A(*



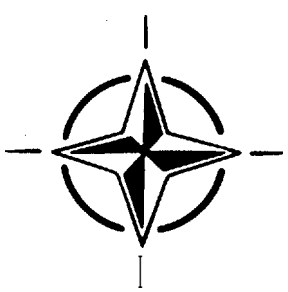

**NORTH ATLANTIC TREATY ORGANIZATION**

Published July **1994**

*Distribution and Availability on Back Cover*

AGARD-AR-304

AGARD

ADVISORY GROUP FOR AEROSPACE RESEARCH & DEVELOPMENT
7 RUE ANCELLE 92200 NEUILLY SUR SEINE FRANCE

**AGARD ADVISORY REPORT 304**
**Fluid Dynamics Panel Working Group 15**

# Quality Assessment for Wind Tunnel Testing

(L'Appréciation de la Qualité pour
les Essais en Soufflerie)

This Advisory Report has been prepared at the request
of the Fluid Dynamics Panel of AGARD.

North Atlantic Treaty Organization
*Organisation du Traite de l'Atlantique Nord*

# The Mission of AGARD

According to its Charter, the mission of AGARD is to bring together the leading personalities of the NATO nations in the fields of science and technology relating to aerospace for the following purposes:

- Recommending effective ways for the member nations to use their research and development capabilities for the common benefit of the NATO community;
- Providing scientific and technical advice and assistance to the Military Committee in the field of aerospace research and development (with particular regard to its military application);
- Continuously stimulating advances in the aerospace sciences relevant to strengthening the common defence posture;
- Improving the co-operation among member nations in aerospace research and development;
- Exchange of scientific and technical information;
- Providing assistance to member nations for the purpose of increasing their scientific and technical potential;
- Rendering scientific and technical assistance, as requested, to other NATO bodies and to member nations in connection with research and development problems in the aerospace field.

The highest authority within AGARD is the National Delegates Board consisting of officially appointed senior representatives from each member nation. The mission of AGARD is carried out through the Panels which are composed of experts appointed by the National Delegates, the Consultant and Exchange Programme and the Aerospace Applications Studies Programme. The results of AGARD work are reported to the member nations and the NATO Authorities through the AGARD series of publications of which this is one.

Participation in AGARD activities is by invitation only and is normally limited to citizens of the NATO nations.



Published July 1994



ISBN 92-835-0753-3

*Printed by Specialised Printing Services Limited*
***40** Chigwell Lane, Loughton, Essex IG10 3TZ*

# Recent Publications of the Fluid Dynamics Panel

AGARDOGRAPHS (AG)

Scale Effects on Aircraft and Weapon Aerodynamics
AGARD AG-323, July 1994

Design and Testing of High-Performance Parachutes
AGARD AG-319, November 1991

Experimental Techniques in the Field of Low Density Aerodynamics
AGARD AG-318 (E), April 1991

Techniques Expbimentales Liées à l'Aérodynamique à Basse Densité
AGARD AG-318 (FR), April 1990

A Survey of Measurements and Measuring Techniques in Rapidly Distorted Compressible Turbulent Boundary Layers
AGARD AG-315, May 1989

REPORTS (R)

Missile Aerodynamics
AGARD R-804, Special Course Notes, June 1994

Progress in Transition Modelling
AGARD R-793, Special Course Notes, April 1994

Shock-Wave/Boundary-Layer Interactions in Supersonic and Hypersonic Flows
AGARD R-792, Special Course Notes, August 1993

Unstructured Grid Methods for Advection Dominated Flows
AGARD R-787, Special Course Notes, May 1992

Skin Friction Drag Reduction
AGARD R-786, Special Course Notes, March 1992

ADVISORY REPORTS (AR)

Air Intakes for High Speed Vehicles
AGARD AR-270, Report of WG13, September 1991

Appraisal of the Suitability of Turbulence Models in Flow Calculations
AGARD AR-291, Technical Status Reveiw, July 1991

Rotary-Balance Testing for Aircraft Dynamics
AGARD AR-265, Report of WG11, December 1990

Calculation of 3D Separated Turbulent Flows in Boundary Layer Limit
AGARD AR-255, Report of WG10, May 1990

Adaptive Wind Tunnel Walls: Technology and Applications
AGARD AR-269, Report of WG12, April 1990

CONFERENCE PROCEEDINGS (CP)

Computational and Experimental Assessment of Jets in Cross Flow
AGARD CP-534, November 1993

High-Lift System Aerodynamics
AGARD CP-515, September 1993

Theoretical and Experimental Methods in Hypersonic Flows
AGARD CP-514, April 1993

Aerodynamic Engine/Airframe Integration for High Performance Aircraft and Missiles
AGARD CP-498, September 1992

Effects of Adverse Weather on Aerodynamics
AGARD CP-496, December 1991

Manoeuvring Aerodynamics
AGARD CP-497, November 1991

Vortex Flow Aerodynamics
AGARD CP-494, July 1991

Missile Aerodynamics
AGARD CP-493, October 1990

Aerodynamics of Combat Aircraft Controls and of Ground Effects
AGARD CP-465, April 1990

Computational Methods for Aerodynamic Design (Inverse) and Optimization
AGARD CP-463, March 1990

Applications of Mesh Generation to Complex 3-D Configurations
AGARD CP-464, March 1990

Fluid Dynamics of Three-Dimensional Turbulent Shear Flows and Transition
AGARD CP-438, April 1989

Validation of Computational Fluid Dynamics
AGARD CP-437, December 1988

Aerodynamic Data Accuracy and Quality: Requirements and Capabilities in Wind Tunnel Testing
AGARD CP-429, July 1988

Aerodynamics of Hypersonic Lifting Vehicles
AGARD CP-428, November 1987

Aerodynamic and Related Hydrodynamic Studies Using Water Facilities
AGARD CP-413, June 1987

Applications of Computational Fluid Dynamics in Aeronautics
AGARD CP-412, November 1986

Store Airframe Aerodynamics
AGARD CP-389, August 1986

Unsteady Aerodynamics — Fundamentals and Applications to Aircraft Dynamics
AGARD CP-386, November 1985

Aerodynamics and Acoustics of Propellers
AGARD CP-366, February 1985

Improvement of Aerodynamic Performance through Boundary Layer Control and High Lift Systems
AGARD CP-365, August 1984

Wind Tunnels and Testing Techniques
AGARD CP-348, February 1984

Aerodynamics of Vortical Type Flows in Three Dimensions
AGARD CP-342, July 1983

Missile Aerodynamics
AGARD CP-336, February 1983

Prediction of Aerodynamic Loads on Rotorcraft
AGARD CP-334, September 1982

Wall Interference in Wind Tunnels
AGARD CP-335, September 1982

Fluid Dynamics of Jets with Applications to V/STOL
AGARD CP-308, January 1982

Aerodynamics of Power Plant Installation
AGARD CP-301, September 1981

# Preface

At the Fluid Dynamics Panel symposium on Aerodynamic Data Accuracy and Quality: Requirements and Capabilities in Wind Tunnel Testing in October 1987, (Conference Proceedings 429, published July 1988) continuing important problems related to aerodynamic data quality were noted. The technical evaluator suggested that improved treatment of data uncertainty would help alleviate some problems. The panel approved an examination of data quality assessment methodologies with the intent of recommending specific improvements.

Measurement uncertainty is a complex subject involving both statistical techniques and engineering judgment. The method reported here was adapted from currently accepted practices by Working Group 15 of the Fluid Dynamics Panel. The objective of the Group was to define a rational and practical framework for quantifying and reporting uncertainty in wind tunnel test data. The quantitative assessment method was to be compatible with existing methodologies within the technical community. Uncertainties that are difficult to quantify were to be identified and guidelines given on how to report these uncertainties.

The Working Group members were:

Canada

Mr Robin D. Galway
National Research Council **of** Canada
Institute for Aerospace Research
Ottawa

France

Mr Claude Armand
ONERA
Centre de Modane Avrieux

Mr Claude Quemard
ONERA
Centre du Fauga-Mauzac

Germany

Dr Gunter Viehweger
DLR
Koln

The Netherlands

Mr Jan H.A. te Boekhorst
NLR
Amsterdam

United Kingdom

Dr David S. Woodward
DRA-Farnborough

Mr Keith Pallister
ARA
Bedford

United States

Mr Travis Binion
Calspan-AEDC
Arnold AFB, Tennessee

Mr David Cahill
Calspan-AEDC
Amold AFB, Tennessee

Dr Hugh Coleman
University of Alabama in Huntsville
Huntsville, Alabama

Dr Keith Kushman (Chairman)
USAF-AEDC
Amold AFB, Tennessee

Dr Frank Steinle
NASA Ames
Moffett Field, California

# Préface

Lors du symposium "Précision et qualité des données aérodynamiques: Besoins et capacités des essais en soufflerie" organisé par le Panel AGARD de la Dynamique des fluides au mois d'octobre 1987, (Conference Proceedings 429, publié juillet 1988)un certain nombre de problèmes importants et persistants concemant la qualité des données aérodynamiques ont été notés.

L'évaluateur technique a suggéré que l'amélioration des techniques de traitement de l'incertitude des données pourrait contribuer à l'allègement de certains problbmes. Le Panel a approuvé un examen des mkthodologies d'évaluation de la qualité des données en vue de la recommandation d'améliorations spkcifiques.

Les approximations des mesures est un sujet complexe qui met en jeu à la fois des techniques statistiques et le jugement de l'ingénieur. La mkthode décrite ici représente une adaptation des pratiques courantes, réalisée par le groupe de travail No.15 du Panel AGARD de la Dynamique des fluides. Le groupe s'est donné comme objectif de définir un cadre de travail rationnel et pratique pour la quantification et l'analyse des approximations dans les résultats des essais en soufflerie. La méthode d'évaluation quantitative devait être compatible avec les mkthodologies en vigueur au sein de la communauté technique. Les approximations qui s'avkraient difficiles 1 quantifier devaient être identifiées et des directives établies pour rendre compte de celles-ci.

Les membres du groupe de travail étaient:

**Canada**

Mr Robin D. Galway
National Research Council of Canada
Institute for Aerospace Research
Ottawa

**France**

Mr Claude Armand
ONERA
Centre de Modane Avrieux

Mr Claude Quemard
ONERA
Centre du Fauga-Mauzac

**Allemagne**

Dr Gunter Viehweger
DLR
Koln

**Les Pays-Bas**

Mr Jan H.A. te Boekhorst
NLR
Amsterdam

**Royaume-Uni**

Dr David **S.** Woodward
DRA-Famborough

Mr Keith Pallister
ARA
Bedford

**Etats-Unis**

Mr Travis Binion
Calspan-AEDC
Amold AFB, Tennessee

Mr David Cahill
Calspan-AEDC
Amold AFB, Tennessee

Dr Hugh Coleman
University of Alabama in Huntsville
Huntsville, Alabama

Dr Keith Kushman (président)
USAF-AEDC
Amold AFB, Tennessee

Dr Frank Steinle
NASA Ames
Moffett Field, California

# Contents

## Annexes

## 1.0 INTRODUCTION

Wind tunnel data are often presented without reference to the quality of the results. When data uncertainty is considered, it is normally in the form of repeatability from a few supposedly identical tests. Only rarely are estimates of uncertainty based on professional calibrations of facilities and instrumentation, a thorough review of the process producing the data, and comprehensive accounting of significant biases inherent in the experiment.

The development of new and modified aircraft is frequently compromised by inadequate consideration of experimental error. References 1.1 through 1.4 are some of the AGARD publications that have reported important problems over the past 20 years. An AGARD Symposium in 1987 (Ref. 1.5) entitled "Aerodynamic Data Accuracy and Quality: Requirements and Capabilities in Wind Tunnel Testing" highlighted continuing problems. Two important improvements in data quality assessment practices are clearly needed. The first is to adopt a consistent approach for integrating uncertainty analyses into all phases of a test. The second is to provide a complete professional analysis and documentation of uncertainty for each test. This report describes an engineering approach to wind tunnel data quality assessment that can alleviate many of the problems documented in Ref. 1.5. The method developed in this report is general. Aircraft aerodynamic testing was selected as a specific example application to provide a focus for describing and applying the method.

An important concern of an aircraft developer is the risk inherent in predicting the flight performance of a full-scale system. There are numerous contributors to the uncertainty of flight predictions, as shown in Fig. 1.1. Note that some of the contributions occur as the result of analyses that use wind tunnel data as the starting point. Model protuberance, propulsion temperature effects, and extrapolation from reference conditions are examples of such analyses. Other contributions to data uncertainty are directly related to the wind tunnel test. While the method presented applies to any contribution, the scope of this report is limited to those associated with the wind tunnel test. The discussion is pointed toward providing the uncertainty of data for an unsupported rigid model in free air at the wind tunnel test conditions (Mach number, Reynolds number, boundary-layer state...), commonly known as the aerodynamic reference condition. Figure 1.2 illustrates typical contributors to uncertainty within the scope of this report. A well-defined, useful reference condition and related uncertainty analysis should be reported by wind tunnel facilities for all tests, regardless of type.

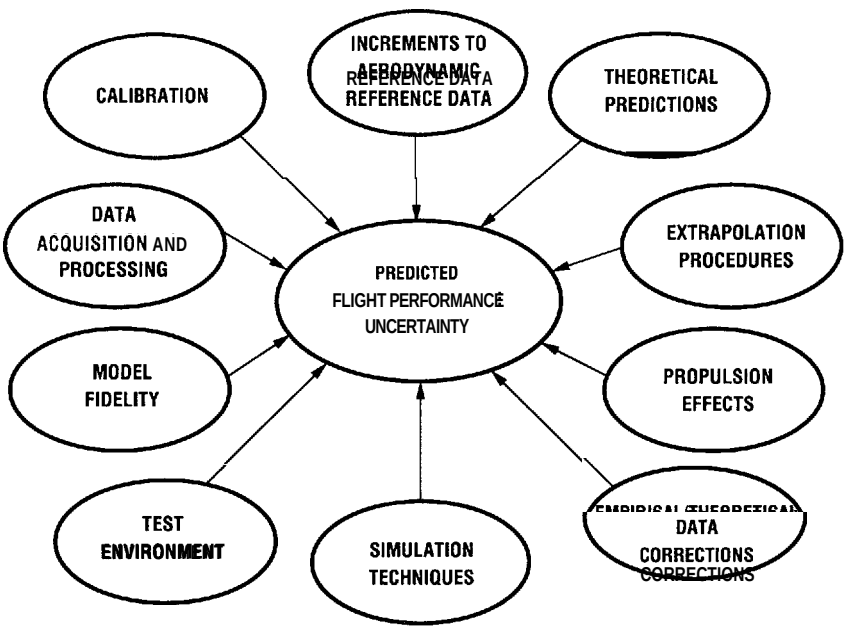


Fig. 1.1 Contributions to predicted flight performance uncertainty.

The terms "data quality" and "uncertainty" are used interchangeably throughout this report to reinforce the concept that intelligent design, execution, and documentation of a test adds great value to the results and must be done in a structured, consistent framework to gain the greatest benefit. It is clear that the risk involved in predicting flight performance is directly related to how well tests are designed to provide useful simulations of flight and suitably accurate data. Risk is managed by

careful objective and subjective reasoning about the primary sources of error in the prediction processes. Experimentalists know that a comprehensive uncertainty analysis uses quantitative estimates that are developed in a structured manner with as much rigor as is appropriate and possible. An assessment of the system development and test processes involves judgments about the "quality" of the results produced. A major component of such judgments must be an uncertainty estimate.

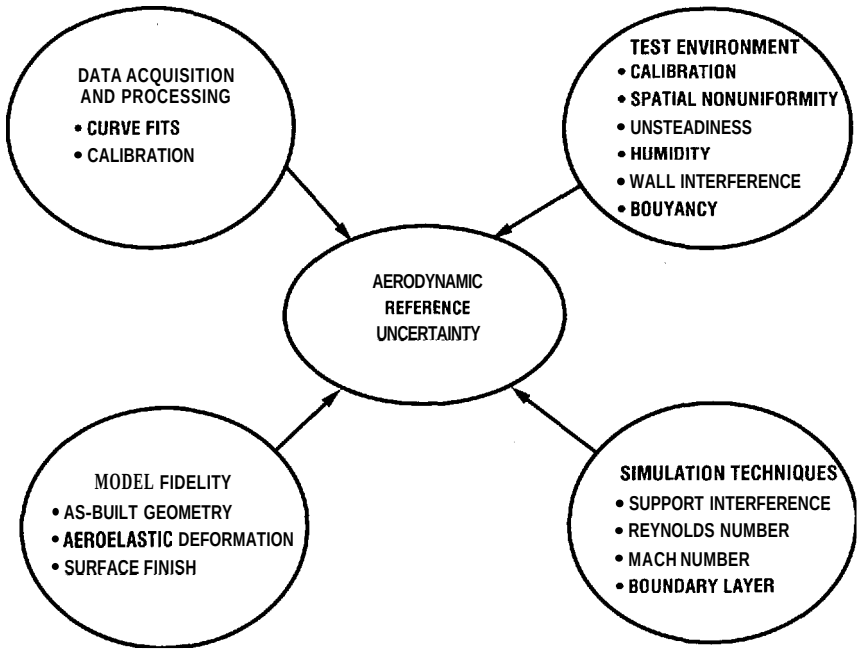


Fig. 1.2 Contributions to Aerodynamic Reference Uncertainty.

Data quality assessment should be a key part *of* the entire wind tunnel testing process. A simple schematic of the process (Fig. 1.3) shows considerations for uncertainty influencing the decision whether to test or not, the design of the experiment, and the conduct of the test. Figure 1.3 also shows the important step of proper analysis and documentation of the uncertainty of final results. This report addresses the entire process shown in Figure 1.3. Chapter Two focuses on the analysis and reporting method. Chapter Three overviews the test process for wind tunnels and provides insight about possible error sources and their significance. Chapter Four presents a specific example of the method applied to wind tunnel testing. Key points are summarized and recommendations are presented in Chapter .Five.

A few considerations were prominent in development of this uncertainty method:

1. Simplification *of* the analyses to permit the greatest possible insight with the least possible effort is important. The method is general enough to apply to any test. The importance of focusing only on significant error sources is stressed, as is the use of "end to end" calibrations to avoid needlessly determining uncertainty contributions of every element in a process.

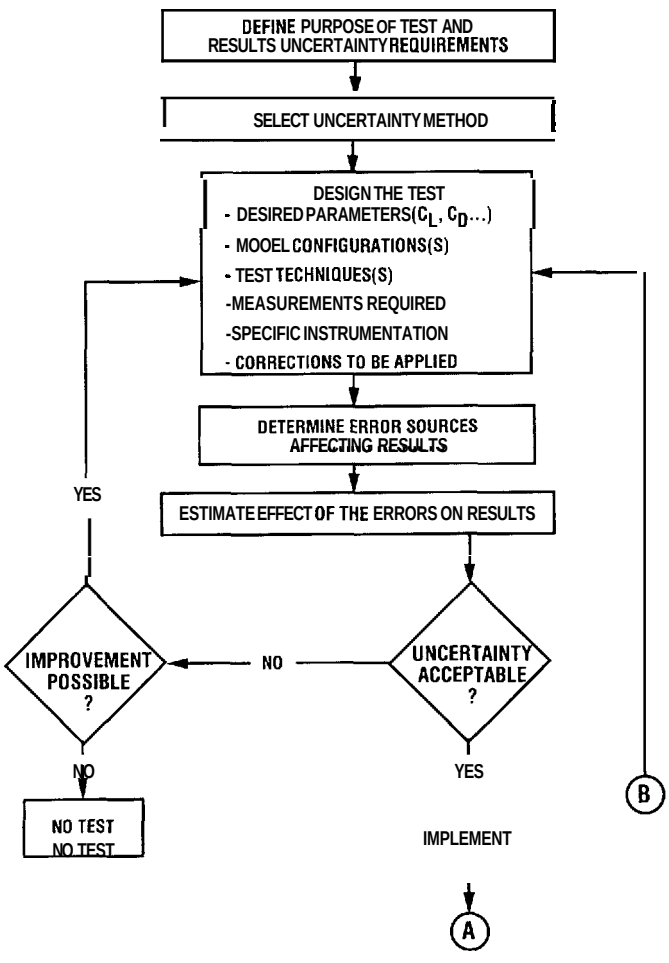


Fig. 1.3 Integration of uncertainty considerations in an experimental process.

2. Recent technical contributions to the practice of uncertainty analysis have been incorporated. Therefore, correlated bias errors and an improved way to treat errors for small sample sizes are discussed in Chapter Two. The entire method is consistent with concepts developed and evolving in international standards committees (Ref. 2.2).

3. The method should provide a basis for meaningful and efficient communication of quality assessments. A standard confidence level and process are recommended, and a consistent reporting procedure, including precision and bias limits and total uncertainty, is described. In the body of the report, the methodology for uncertainty estimates based on large sample sizes is discussed. This method can be used in most wind tunnel testing, and uncertainty estimates should be those appropriate over long sampling times.

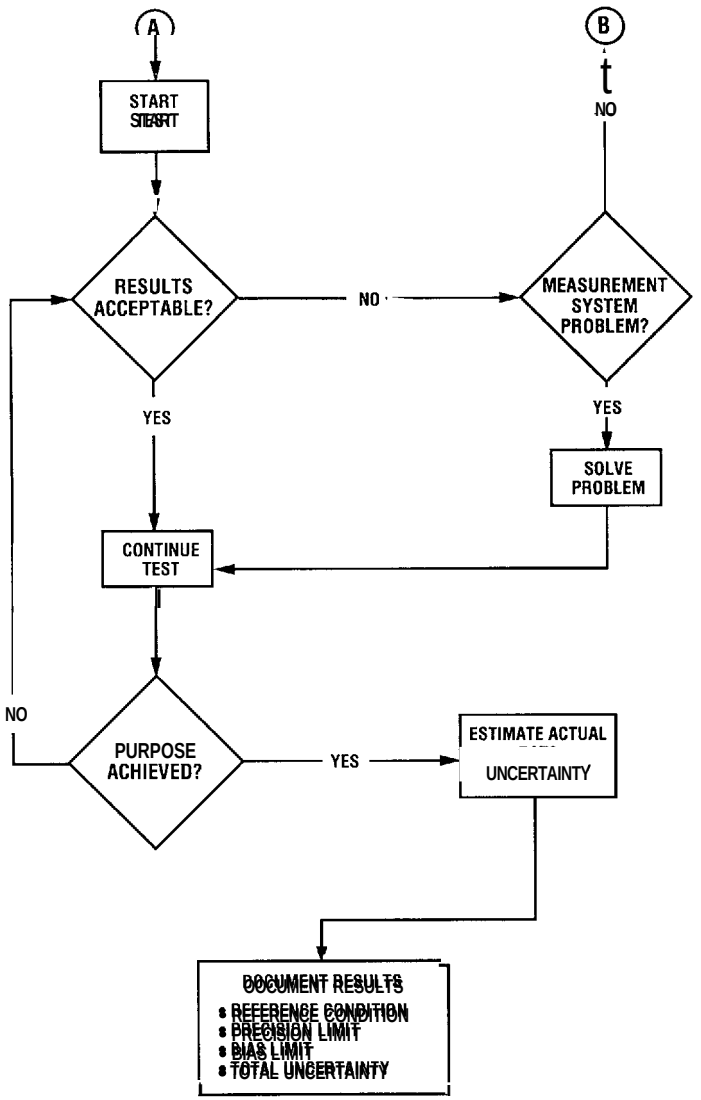


Fig. 1.3 Concluded.

This report assumes the reader is familiar with wind tunnel testing and desires an improved understanding of uncertainty analysis techniques. References describing techniques and testing experiences in detail are cited, but only information essential to the report is included in the text. Readers are encouraged to develop an appreciation of the importance of a professional treatment of data uncertainty and to accept the challenge of improving the quality of their experiments and data.

## REFERENCES

1.1. Kuchemann, D., "Problems in Wind Tunnel Testing Techniques." AGARD-R-601, November 1972.

1.2. Carter, E.S. and Poisson-Quinton, Ph., "Flight/Ground Testing Facilities Correlation." AGARD-CP-187, April 1976.

1.3. Dietz, R.O. and Laster, M.L., "Wind Tunnel Corrections for High Angle of Attack Models." AGARD R-692, February 1981.

1.4. Ohman, L.H., "Wind Tunnel and Testing Techniques." AGARD-CP-348, February 1988.

1.5. Monnerie, B. and Ohman L., "Aerodynamic Data Accuracy and Quality: Requirements and Capabilities in Wind Tunnel Testing." AGARD-CP-429.

## 2.0 UNCERTAINTY ASSESSMENT METHODOLOGY

The methodology for estimating the uncertainties in measurements, and in the experimental results calculated from them, must be structured to combine statistical and engineering concepts in a manner that can be systematically applied to each step in the data uncertainty assessment determination. In this chapter, an uncertainty analysis methodology is presented, and its application in the different phases of an experimental program is discussed. The methodology is based primarily on material from Ref. 2.1 and is consistent with the most current drafts of international guidelines and standards [Refs. 2.2, and 2.31. Definitions of specific terms are made as required in the following text, and the international vocabulary of metrological terms (VIM) is incorporated herein as Ref. 2.4.

### 2.1 OVERVIEW

The word accuracy is generally used to indicate the closeness of the agreement between an experimentally determined value of a quantity and its true value. Error is the difference between the experimentally determined value and the truth. Accuracy is said to increase as error approaches zero. The true values of standard measurement quantities (e.g., mass, length, time, volts, etc.) generally only reside in national standards laboratories. Only in rare instances is the true value of a quantity known. Thus, one is forced to estimate error, and that estimate is called an uncertainty, $U$. In general, the uncertainty of a quantity is a function of the value of that quantity. However, it is common practice to quote the same value of uncertainty for a range of values of the quantity, e.g., percent of full scale of an instrument. In this document, all estimates are assumed to be made at a 95-percent confidence level, meaning that the true value of the quantity is expected to be within the $\pm U$ interval about the experimentally determined value 95 times out of 100.

Errors can be considered to be composed of two components: a precision (random) component and a bias (systematic) component. An error is classified as precision if it contributes to the scatter of the data; otherwise, it is a bias error. It is assumed that corrections have been made for all systematic errors whose values are known. The remaining bias errors are thus equally as likely to be positive as negative.

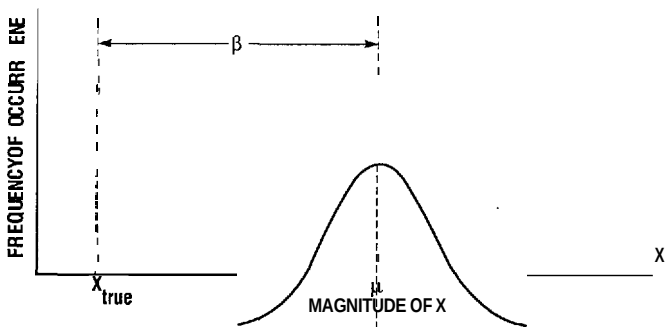


Fig. 2.1 Errors in the measurement of a variable X.

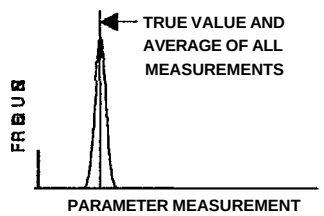


a. Unbiased, precise, accurate

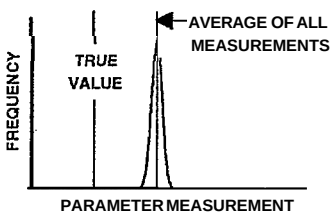


b. Biased, precise, inaccurate

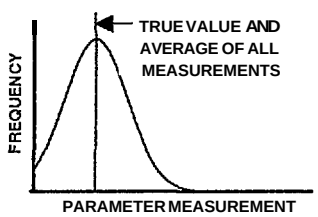


c. Unbiased, imprecise, inaccurate

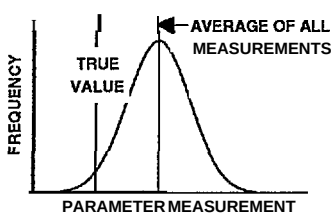


d. Biased, imprecise, inaccurate

Fig. 2.2 Measurement error (bias, precision, and accuracy).

The effects of such errors on multiple readings of a variable X are illustrated in Fig. 2.1, where the bias error is denoted by $\beta$. The qualitative influence of various combinations of large and small precision and bias errors on accuracy is depicted in Fig. 2.2. For example, an accurate value is one with small bias and precision errors (Fig. 2.2a), whereas one may have small precision errors but inaccurate values (Fig. 2.2b).

Estimates of error are meaningful only when considered in the context of the process leading to the value of the quantity under consideration. In order to identify and quantify error sources, two factors must be considered: (1) the steps used in the processes to obtain the measurement of the quantity, and (2) the environment in which the steps were accomplished. Each factor influences the outcome.

In nearly all experiments, the measured values of different quantities are combined using a data reduction equation to form some desired result. A good example is the experimental determination of drag coefficient of a particular vehicle configuration in a wind tunnel test. Defining drag coefficient as

$$C_D = \frac{2F_A}{\rho V^2 A} \tag{2-1}$$

one can envision that errors in the values of the variables on the right-hand side of Eq. (2-1) will cause errors in the experimental result $C_D$.

A more general representation of a data reduction equation is

$$r = r(X_1, X_2, \ldots, X_J) \tag{2-2}$$

where r is the experimental result determined from J measured variables Xi. If B and P are taken as estimates of the magnitude of bias and precision errors, respectively, the experimental situation is represented schematically in Fig. 2.3.

Each of the measurement systems used to measure the value of an individual variable $X_i$ is influenced by a large number of elemental error sources. The effects of these elemental errors are manifested as a bias error (estimated by $B_i$) and a precision error (estimated by $P_i$) in the measured values of the variable. These errors in the measured values then propagate through the data reduction equation, thereby generating the bias and precision errors in the experimental result, r.

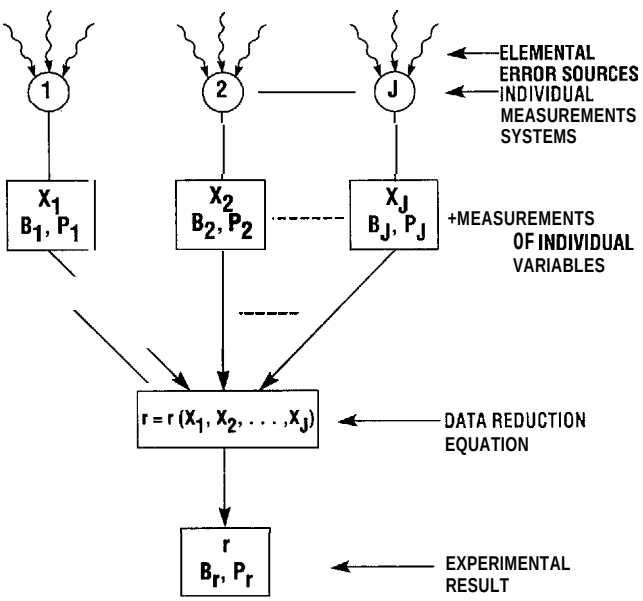


Fig. 2.3 Propagation of errors into an experimental result.

In performing an uncertainty analysis, it is convenient to consider the things which could produce errors in a measurement as **elements.** For example, the elements associated with a pressure measurement could be the unsteady test conditions, orifice, tubing, transducer, transducer environment, signal amplifier, power supply, analog-to-digital converter, and recording device. In typical wind tunnel experimental programs, it is generally not cost effective to try to estimate the precision errors of each elemental error source. It is usually far more effective to estimate the precision of a group of elements (such as the output of the entire measurement system for $X_J$ — the $P_J$ level in Fig. 2.3). This way, the measurement system precision is considered an element contributing to the total uncertainty of pressure measurements. Better yet would be to compute directly the precision of the result ($P_r$ in Fig. 2.3) if multiple results at the same set point are available.

Bias errors, on the other hand, are generally easiest to estimate at a smaller elemental level. For example, the bias caused by imperfect orifices would not be identified in any single set of experimental data and thus must be estimated. However, this should not be taken to imply that bias estimates must

be made for each component of the measurement system. Each measurement system should be calibrated in as large a piece as possible (ideally, an end-to-end calibration under operating conditions). In most situations, such an approach removes the need to estimate the bias errors of individual components of measurement systems. The examples in Chapter 4 describe ways to estimate the bias and precision of a measurement system.

In Section 2.2, the methodology for obtaining estimates of the precision errors and bias errors in the measured variables $X_i$ is presented, and in Section 2.3 the methodology for obtaining estimates of the precision errors and bias errors in the experimental results determined from the $X_i$ is presented. The methodology discussed in the body of this chapter assumes that error distributions are well-approximated by the Gaussian distribution, that uncertainty estimates are made at a 95-percent confidence level using large sample size techniques', and that all precision errors are uncorrelated. In Annex 2-A, a more comprehensive (and more complex) methodology (Ref. 2.2) that is valid for either small or large sample sizes and either Gaussian or non-Gaussian error distributions is discussed. In Annex 2-B, a method for identification of outliers in samples is presented.

## 2.2 ESTIMATING UNCERTAINTY COMPONENTS IN MEASURED VARIABLES

In this section, the methodology for obtaining estimates of the precision errors and bias errors **in the measured variables** $X_i$ is presented. The methodology for obtaining estimates of the precision errors and bias errors **in the experimental results** r, computed using the measured variables in data reduction equations of the form of Eq. (2-2), is discussed in Section 2.3.

### 2.2.1 Definitions

To estimate the magnitude of the precision errors in measurements of a variable Xi, a **precision limit** $P_i$ is defined. As illustrated in Fig. 2.4, the $\pm P_i$ interval about a measurement of $X_i$ is the band within which the (biased) mean value, $\mu$, of the variable would fall 95 times out of 100 if the experiment were repeated many times under the same conditions using the same equipment. The precision limit is thus an estimate of the lack of measurement repeatability caused by random errors, unsteadiness, inability to reset experimental conditions exactly, etc.

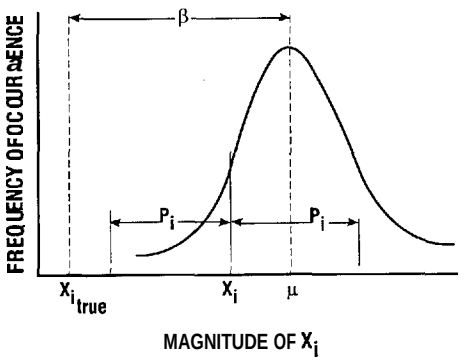


Fig. 2.4 95-percent confidence precision limit interval around a single reading of a variable Xi.

To estimate the magnitude of the bias errors in measurements of a variable Xi, a **bias limit** $B_i$ is defined. The bias limit is estimated with the understanding that the experimenter is 95-percent confident that the true value of the bias error, if known, would be less than $|B_i|$.

The $\pm U_i$ **uncertainty** interval about the measured value of $X_i$ is the band within which the experimenter is 95-percent confident the true value of the variable lies. The 95-percent confidence uncertainty is given by

$$U_i = \left(B_i^2 + P_i^2\right)^{\frac{1}{2}} \qquad (2\text{-}3)$$

---

[1] A discussion of what constitutes "large" sample sizes is given in Annex **2-A.** In most practical wind tunnel test situations. if the dominant uncertainties are estimated based on 10 or more readings, then use of large sample size methodology is justified. (Of course, it is always desirable to have as many readings as possible so that a better estimate can be made of the true variance of the distribution from which the sample readings are taken.)

### 2.2.2 Estimating Precision Limits

The precision limit for a measured variable $X_i$ is given by

$$P_i = KS_i \tag{2-4}$$

where K is the coverage factor and equals 2 for a 95-percent confidence level, $S_i$ is the standard deviation of the sample of $N_i$ readings of the variable $X_i$ and is defined as

$$S_i = \left( \sum_{k=1}^{N_i} \frac{[(X_i)_k - \bar{X}_i]^2}{N_i - 1} \right)^{\frac{1}{2}} \tag{2-5}$$

and the mean value is defined as

$$\bar{X}_i = \frac{1}{N_i} \sum_{k=1}^{N_i} (X_i)_k \tag{2-6}$$

An interpretation of the $\pm P_i$ interval is shown in Fig. 2.4.

The use of K = 2 assumes a large sample size and Gaussian error distribution. It is instructive to note, however, a 1993 policy statement (Ref. 2.5) by the U. S. National Institute of Standards and Technology (NIST): "To be consistent with current international practice, the value of K to be used at NIST for calculating U is, by convention, K = 2. Values of K other than 2 are only to be used for specific applications dictated by established and documented requirements." A discussion of estimating the coverage factor K for "small" sample sizes is presented in Annex 2-A. Also discussed in that annex is the method for combining precision limits estimated at the elemental error source level (Fig. 2.3).

When a mean (averaged) value of $X_i$ is to be used in Eq. (2-2) to determine the result r, the appropriate precision limit is the precision limit of the mean defined by

$$P_{\bar{X}_i} = \frac{P_i}{\sqrt{N_i}} \tag{2-7}$$

An interpretation of this precision limit is shown in Fig. 2.5.

Two questions that often arise in evaluating a precision limit from a sample of $N_i$ readings are

1. What should be done with those data points (outliers) that are far from the majority of the points in the sample?

2. How should data variations that occur because of system unsteadiness rather than from random error sources be evaluated?

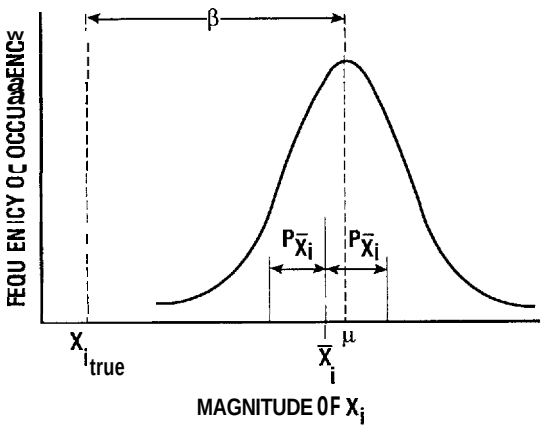


Fig. 2.5 95-percent confidence precision limit interval around the mean value of a sample of readings of variable $X_i$.

Procedures for identifying outliers are discussed in Annex 2-B. Note that apparent outliers can be due to two basic causes — truly spurious events not connected with the test, or phenomenologically relevant data variations that, though improbable, occur during the first $N_i$ readings taken. Aerodynamic folklore is full of stories about vehicles which "discovered" adverse events during flight tests only to find the same event in the ground test data which was erroneously considered to be an outlier. (Note that outliers can only be identified in relation to a mean value computed from a number of samples taken at the same test conditions.) To avoid such occurrences, all outliers should be examined for relevance to the phenomena being investigated.

Consideration of the appropriate time interval for collection of the $N_i$ readings is critical if appropriate precision limits are to be estimated. Consider, for example, an experiment in which some of the test variables have a time variation such as that shown in Fig. 2.6. If the question in the experiment is "what is the result for time interval At?", then M multiple sets of readings of the $(X_1, \ldots, X_J)$ taken over that interval can be used in the data reduction equation [Eq. (2-2)] to determine M values of the result r, and the mean result and appropriate precision limit can be computed using the techniques discussed below in Section 2.3.2.1.

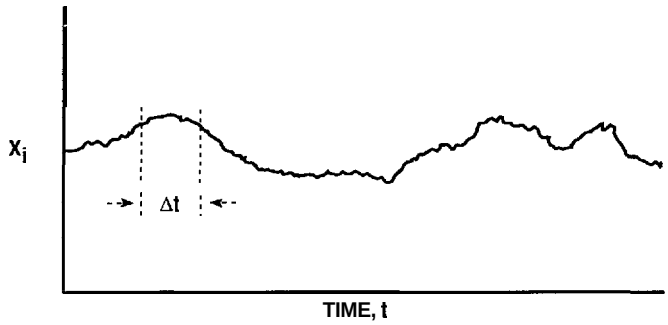


Fig. *2.6* Variation of a variable $X_i$ with time for a "steady" experimental condition.

A more typical situation in wind tunnel testing occurs when the test data are taken at "steady" conditions, but the actual variation of the Xi's with time is similar to that shown in Fig. *2.6.* In this case, one typically desires the result determined using the data reduction equation to be indicative of the value of the result over the interval during which several complete variations in the variables occur. However, it is usually not possible to take measurements over that entire interval, as some of the variations may have periods of hours or even days and others may not be cyclic at all, but vary binarily. In most wind tunnel tests, measurements are taken over a short period with the full understanding that the interval for variation of some of the variables is much longer than the measurement time. In such a case, a value of $X_i$ determined over such a relatively short At should be considered as **a single reading** and the appropriate precision limit is estimated by Eq. (2-4), not by Eq. (2-7). Note that this interpretation holds whether the value of $X_i$ is the average of 10, $10^3$ or $10^6$ readings taken during At.

One may obtain an appropriate estimate of the sample standard deviation [Eq. (2-5)] during the testing process by taking repeat data provided that all of the error sources contributing to the total precision are allowed to vary during the repeat process. For example, taking multiple-samples of data as a function of only time while holding all other conditions constant merely identifies the precision associated with the measurement system and the unsteadiness of the test conditions. The precision associated with other precision error sources, e.g., repeating test conditions, model positions, configuration variables, etc, must also be included to determine the proper precision limit for the variable of interest.

In a given test, the value for the precision limit to be assigned to a single reading would have to be based on **previous information** about that measurement **obtained over the appropriate time interval** (Ref. *2.6).* If such previous information consists of $N_i$ repeated readings for each of the $X_i$ variables, the precision limit for each variable can be determined from the $N_i$ previous readings using Eqs. (2-4) and (2-5). If previous readings of a variable over an appropriate interval are not available, then the experimenter must estimate a value for $P_i$ using the best information available at that time.

The concept of a precision limit is very useful in all phases of an experimental program. For example, in the design phase of an experiment, a 95-percent confidence estimate of the "scatter" expected

for a given measurement based on past experience with the measurement technique may be all that is available. In the debugging phase of the experiment, the comparison of the precision limits estimated in the design phase and the precision limits actually calculated from multiple samples in the debugging phase allows the experimenter to verify that all the factors that influence the precision of the measured variables have been properly taken into account (Ref. 2.1).

### 2.2.3 Estimating Bias Limits

A useful approach to estimating the magnitude of a bias error is to assume that it belongs to some assumed statistical distribution. For example, if a thermistor manufacturer specifies that 95-percent of samples of a given model are within $\pm 0.5°C$ of the reference resistance-temperature (R-T) curve supplied, then one might assume that the systematic errors (the difference between the actual R-T curves of various thermistors and the reference curve) belong to a normal distribution with a standard deviation $b_T$ equal to $(0.5°C)/2$, corresponding to a bias limit estimate $B_T = 2b_T$ (analogous to Eq. (2-4)) or $0.5°C$.

More discussion of assumed bias error distributions is given in Annex 2-A. In the following, all bias errors are assumed to be normally distributed and the coverage factor $K = 2$, as before.

One might separate the bias errors which influence the measurement of a variable into different categories: calibration errors, data acquisition errors, data reduction errors, test technique errors, etc. Within each category, there may be several elemental sources of bias, as indicated schematically in Fig. 2.3. For instance, if for the Jth variable, $X_J$, there are M elemental bias errors identified as significant and whose bias limits are estimated as

$$(B_J)_1, (B_J)_2, \ldots, (B_J)_M$$

then the bias limit for the measurement of $X_J$ is calculated as the root-sum-square (RSS) combination of the elemental limits

$$B_J = \left[ \sum_{k=1}^{M} (B_J)_k^2 \right]^{\frac{1}{2}} \tag{2-8}$$

The elemental bias limits, $(B_i)_k$, must be estimated for each variable $X_i$ using the best information one has available at the time. In the design phase of an experimental program, manufacturer's specifications, analytical estimates, and previous experience will typically provide the basis for most of the estimates. As the experimental program progresses, equipment is assembled, and calibrations are conducted, these estimates can be updated using the additional information gained about the accuracy of the calibration standards, errors associated with calibration process and curvefit procedures, and perhaps analytical estimates of installation errors (such as wall interference effects, sting effects, etc).

As Moffat (Ref. 2.7) suggests, there can be additional conceptual bias errors resulting from not measuring the variable whose symbol appears in the data reduction equation. An example would be a free-stream velocity value measured at a particular axial position on the tunnel centerline and used as "the" free-stream velocity at that cross section in determining $C_D$, but there may be a cross-sectional gradient of velocity at that location causing the "average" value to be different.

## 2.3 ESTIMATING UNCERTAINTY COMPONENTS FOR EXPERIMENTAL RESULTS

In the previous section, the methodology for obtaining estimates of the precision errors and bias errors in the measured variables $X_i$ was discussed. In this section, the methodology is presented for obtaining estimates of the precision errors and bias errors in the experimental results r computed using those measured variables in data reduction equations of the form of Eq. (2-2).

### 2.3.1 Definitions

To estimate the magnitude of the precision component of uncertainty in an experimental result, the **precision limit of a result** P, is defined. The $\pm P$, interval about a result is the band within which the (biased) mean result, $\mu_r$, would fall 95 percent of the time if the experiment were repeated many times under the same conditions using the same equipment. The precision limit is representative of the scatter (or lack of repeatability) caused by random errors, unsteadiness, inability to reset experimental conditions exactly, etc.

To estimate the magnitude of the bias component of uncertainty in an experimental result, the **bias limit of a result** B, is defined. The bias limit is estimated with the understanding that the experimenter is 95-percent confident that the true value of the bias error, if known, would be less than $|B_r|$.

The $\pm U_r$ **uncertainty interval** about the result is the band within which the experimenter is 95-percent confident the true value of the result lies. The 95-percent confidence uncertainty is defined as

$$U_r = \left(B_r^2 + P_r^2\right)^{\frac{1}{2}} \tag{2-9}$$

### 2.3.2 Propagation of Precision Limits into an Experimental Result

#### 2.3.2.1 Multiple Tests

If a test is repeated a number of times so that multiple results at the same set point are available, then the best estimate of the result r would be $\bar{r}$ where

$$\bar{r} = \frac{1}{M}\sum_{k=1}^{M} r_k \tag{2-10}$$

and where M is the number of separate test results. The precision limit for this result would be $P_{\bar{r}} = P_{\bar{r}}$ calculated as

$$P_{\bar{r}} = \frac{KS_r}{\sqrt{M}} \tag{2-11}$$

where K is the coverage factor and is taken as 2, as before. $S_r$ is the standard deviation of the sample of M results and is defined as

$$S_r = \left[\sum_{k=1}^{M} \frac{(r_k - \bar{r})^2}{M-1}\right]^{\frac{1}{2}} \tag{2-12}$$

Obviously, this cannot be computed until multiple results are obtained.

Also note that the precision limit computed is only applicable for those random error sources that were "active" during the repeat measurements. For example, if the model was not disassembled and reassembled between the multiple results, then the precision limit calculated would not account for the fact that the model may not be assembled exactly the same way every time to represent the full-scale article. Further, if the test conditions were not changed and then reestablished between the multiple results, the variability due to resetting to a given test condition would not be accounted for.

#### 2.3.2.2 Single Test with Single Readings

The often-encountered situation, discussed in Section 2.2.2, is when measurements of the variables are averaged over a period that is small compared to the periods of the factors causing variability in the experiment. A proper precision limit cannot be calculated from readings taken over such a small time interval. For such data, the measurement(s) of a variable $X_i$ should be considered a single reading, and the precision limit must be estimated based on previously determined information (calibration data, previous testing in the same facility, previous testing using similar equipment, etc). Once estimates are obtained for the precision limits of all of the measured variables, the precision limit for the result is calculated using

$$P_r = \left[ \sum_{i=1}^{J} (\theta_i P_i)^2 \right]^{\frac{1}{2}} \tag{2-13}$$

where

$$\theta_i = \frac{\partial r}{\partial X_i} \tag{2-14}$$

Here the precision limits are assumed to be based on large sample sizes. Procedures for small sample estimates are discussed in Annex 2-A. Equation (2-13) is an approximate equation that can be derived (Ref. 2.1) using a Taylor series expansion and neglecting all terms higher than first order.

#### 2.3.2.3 Single Test with Averaged Readings

If a test is performed in such a manner that some, but not all, of the Xi's in Eq. (2-2) are determined as averages over appropriate time periods, then Eq. (2-13) should be used with the precision limits for the averaged variables being computed from Eq. (2-7). If a test is run such that all of the Xi's could be determined as averages over appropriate time periods, then multiple individual test results can be determined, and the method of Section 2.3.2.1 should be used.

### 2.3.3 Propagation of Bias Limits into an Experimental Result

When a result is given by

$$r = r(X_1, X_2, \ldots, X_J) \tag{2-15}$$

the bias limit of that result is related to the bias limits $B_i$ of the measurements of the separate variables $X_i$ by

$$B_r^2 = \left( \sum_{i=1}^{J} \theta_i^2 B_i^2 \right) + 2\theta_m \theta_n B_m' B_n' \tag{2-16}$$

where the quantities $B_m'$ and $B_n'$ are the portions of the bias limits for measurements of variables $X_m$ and $X_n$ that arise from the same sources and are presumed to be perfectly correlated (Ref. 2.1), and the bias limits $B_i$ are estimates at 95-percent confidence of the magnitude of the bias errors in the measurements of the separate variables $X_i$ as previously discussed. Equation (2-16) is an approximate equation that can be derived (Ref. 2.1) using a Taylor series expansion and neglecting all terms higher than first order. There is a term similar to the final term in Eq. (2-16) for each (m,n) pair of measured variables whose bias errors are correlated.

For example, if

$$r = r(X_1, X_2, X_3) \tag{2-17}$$

and it is possible for portions of the bias limits $B_1$, $B_2$, and $B_3$ to arise from the same source(s), then

$$B_r^2 = \theta_1^2 B_1^2 + \theta_2^2 B_2^2 + \theta_3^2 B_3^2 + 2\theta_1\theta_2 B_1' B_2' + 2\theta_1\theta_3 B_1' B_3' + 2\theta_2\theta_3 B_2' B_3' \tag{2-18}$$

If, for instance, the measurements of $X_1$ and $X_2$ are each influenced by 4 elemental error sources and sources 2 and 3 are the same for both $X_1$ and $X_2$, then

$$B_1^2 = (B_1)_1^2 + (B_1)_2^2 + (B_1)_3^2 + (B_1)_4^2 \tag{2-19}$$

$$B_2^2 = (B_2)_1^2 + (B_2)_2^2 + (B_2)_3^2 + (B_2)_4^2 \tag{2-20}$$

and

$$B_1' B_2' = (B_1)_2 (B_2)_2 + (B_1)_3 (B_2)_3 \tag{2-21}$$

Correlated bias errors are those that are not independent of each other. It is not unusual for the uncertainties in the results of experimental programs in the fluid and thermal sciences to be influenced by the effects of correlated bias errors in the measurements of several of the variables. A typical example occurs when different variables are measured using the same transducer, such as multiple pressures sequentially ported to and measured with the same transducer, or temperatures at different positions in a flow measured with a single probe that is traversed across the flow field. Obviously, the bias errors in the variables measured with the same transducer are not independent of one another. Another common example occurs when different variables are measured using different transducers, all of which have been calibrated against the same standard, a situation typical of electronically scanned pressure (ESP) measurement systems. In such a case, at least a part of the bias error arising from the calibration procedure will be the same for each transducer, and thus some of the elemental bias error contributions in the measurements of the variables will be correlated. Treatment of these situations is illustrated in Chapter 4.

A comparative test program is another obvious instance where correlated bias error effects are of great importance. If a test article is tested sequentially at the same free-stream conditions and orientation with and without a configuration change, and the difference in lift coefficients is the experimental result, then most (if not all) of the elemental errors in the measurement of an individual variable will arise from the same source in the two tests. Note that the axiom "bias errors subtract out in comparative tests" is not generally correct, even though that is commonly accepted as a truism. The partial derivatives in Eq. (2-16) are evaluated at the particular values of the measured variables, some of which are different in the two tests in a comparative program. Also, the bias limits can be functions of the measured value of a variable — this occurs when bias limits are of the "% of reading" type rather than the "% of full scale" type, for instance.

Depending on the particular .experimental approach, the effect of correlated bias errors in the measurements of different variables can lead either to increased or to decreased uncertainty in the final experimental result as compared to the same approach with no correlated bias errors. Consider the final term in Eq. (2-16) — if some bias errors are correlated ($B_m' B_n'$ not equal to zero) and the partial derivatives ($\theta_m$ and $\theta_n$) are of the same sign, the term is positive and $B_r$ is increased. On the other hand, if some bias errors are correlated and the partial derivatives are of opposite signs, the term is negative and $B_r$ is decreased. This observation suggests that the effect of correlated bias errors can sometimes be used to advantage if the proper strategies are applied in planning and designing the

experiment — sometimes one would want to force correlation of bias errors using appropriate calibration approaches, sometimes not.

Reference 2.1 presents a derivation of the propagation equation for bias errors, including the effects of correlated elemental bias sources and discussions of the approximation of such terms in practical applications.

## 2.4 SUMMARY OF METHODOLOGY

The uncertainty assessment methodology is summarized schematically in Fig. 2.7. For each experimental result, the data reduction equation [Eq. (2-2)] must be determined. Once this has been done, the $X_i$'s that must be considered are known, and the sources of uncertainty for each $X_i$ should be identified. (Note that a math model for a correction, such as for blockage or wall interference effects, is an $X_i$ whose uncertainty must also be considered.)

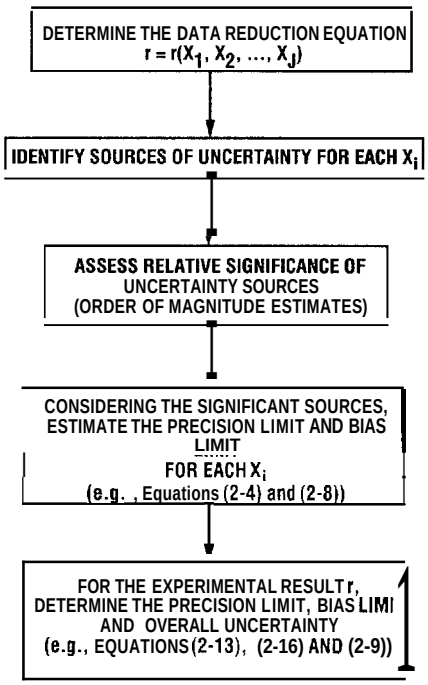


Fig. 2.7 Summary of the uncertainty assessment methodology.

Once the sources of uncertainty have been identified, their relative significance should be established. This is often done using order of magnitude estimates of the sources. As a "rule of thumb" for a given Xi, those uncertainty sources that are smaller that 1/4 or 1/5 of the largest sources are usually considered negligible. Resources can then be concentrated on obtaining estimates of those uncertainties of most importance.

For each $X_i$, estimates of the precision limit and the bias limit are then made. In most wind tunnel tests, it is generally not cost effective or necessary to try to estimate precision limits at the elemental error source level. It is far more effective to estimate the precision of the measurement systems (at the $P_i$ level in Fig. 2.3 and as defined by Eq. (2-4)) or, even better, the precision of the mean result as given by Eq. (2-11) if multiple results at the same set point are available. Of course, if one encounters unacceptably large P's, the elemental sources' contributions must be examined to see which need to be (or can be) improved. It is generally easiest to obtain an estimate of the bias limit for $X_i$ by estimating the bias limits of the significant elemental sources and using Eq. (2-8).

The precision limit, bias limit, and overall uncertainty for the experimental result, r, are then found using Eqs. (2-13) [or (2-11)], (2-16) and (2-9). Note that the partial derivatives can be numerically approximated (using finite difference techniques, for example) if one prefers that to finding them analytically.

## 2.5 REPORTING UNCERTAINTIES

For each experimental result, the bias limit, precision limit, and overall uncertainty should be reported. For situations in which the large sample assumption is not applicable, the small sample methodology used should be reported and discussed. If outliers are rejected, the circumstances and rationale used in rejecting them should be reported.

Details of the uncertainty assessments (as outlined in Fig. 2.7) should be documented either in an appendix to the primary test report or in a separate document that can be referenced in the primary test report.

## REFERENCES

2.1 Coleman, H. W. and Steele, W. G., *Experimentation and Uncertainty Analysis for Engineers.* John Wiley & Sons, Inc., New York, NY, 1989.

2.2 "Guide to the Expression of Uncertainty in Measurement," ISO, First edition, ISBN 92-67-10188-9, 1993.

2.3 "Measurement Uncertainty," ISO/TC 69/SC 6 draft dated April 1992.

2.4 "International Vocabulary of Basic and General Terms in Metrology," ISO, Second edition, ISBN 92-67-01075-1, 1993.

2.5 Taylor, B. N. and Kuyatt, C. E., "Guidelines for Evaluating and Expressing the Uncertainty of NIST Measurement Results," NIST Technical Note 1297, January 1993.

2.6 Steele, W. G., Taylor, R. P., Burrell, R. E., and Coleman, H. W. "The Use of Data from Previous Experience to Estimate the Precision Uncertainty *of* Small Sample Experiments," *AIAA Journal,* Vol. 31, No. 10, 1993.

2.7 Moffat, R. J., "Describing the Uncertainties in Experirnental Results," *Experimental Thermal and Fluid Science,* Vol. 1, 1988.

## ANNEX 2-A: A COMPREHENSIVE UNCERTAINTY ANALYSIS METHODOLOGY

In this Annex, a comprehensive uncertainty analysis methodology is presented and discussed. This methodology is applicable for either large or small sample sizes and for either Gaussian or non-Gaussian error distributions.

Consider the situation in which the experimental result is determined from

$$r = r(X_1, X_2, \ldots, X_J) \tag{2-A-1}$$

where the Xi's are the values of the measured variables. Then the **combined standard uncertainty** $u_c$ (Ref. 2.2) is given by

$$u_c^2 = \sum_{i=1}^{J}\left(\theta_i^2 b_i^2 + \sum_{k=1}^{J} \theta_i \theta_k \rho_{b_{ik}} b_i b_k (1 - \delta_{ik})\right) + \sum_{i=1}^{J}\left(\theta_i^2 S_i^2 + \sum_{k=1}^{J} \theta_i \theta_k \rho_{S_{ik}} S_i S_k (1 - \delta_{ik})\right) \tag{2-A-2}$$

In Eq. (2-A-21, the $(S_i)^2$ are the variances of the precision error distributions of the Xi, the $(b_i)^2$ are the variances of the (assumed) bias error distributions of the Xi, the $\rho_{S_{ik}}$ are the correlation coefficients appropriate for the precision errors in variables $X_i$ and $X_k$, the $\rho_{b_{ik}}$ are the correlation coefficients appropriate for the bias errors in variables $X_i$ and $X_k$, $\delta_{ik}$ is the Kronecker delta defined to equal 1 when $i = k$ and 0 when $i \neq k$, and

$$\theta_i = \frac{\partial r}{\partial X_i} \tag{2-A-3}$$

Eq. (2-A-2) is an approximate equation obtained using a Taylor series expansion and neglecting all terms higher than first order. A derivation is given in Appendix B of Ref. 2.1. No assumptions about type(s) of error distributions are made to obtain Eq. (2-A-2). To obtain an uncertainty $U_r$ at some specified confidence level (such as the 95 percent chosen for use in this document) the combined standard uncertainty $u_c$ must be multiplied by a coverage factor, K,

$$U_r = K u_c \tag{2-A-4}$$

It is in choosing K that assumptions about the type(s) of the error distributions must be made

An argument is presented in Ref. 2.2 that the error distribution of the result, r, in Eq. (2-A-1), may often be considered Gaussian because of the Central Limit Theorem, even if the error distributions of the $X_i$ are not normal. In fact, the same argument can be made for approximate normality of the error distributions of the $X_i$ since the errors typically are composed of a combination of errors from a number of elemental sources. If it is assumed that the error distribution of the result, r, is normal, then the value of K for 95-percent coverage corresponds to the 95-percent confidence level value (Table 2-A-I) from the t distribution so that

$$U_r^2 = t^2 \sum_{i=1}^{J}\left(\theta_i^2 b_i^2 + \sum_{k=1}^{J} \theta_i \theta_k \rho_{b_{ik}} b_i b_k (1 - \delta_{ik})\right) + t^2 \sum_{i=1}^{J}\left(\theta_i^2 S_i^2 + \sum_{k=1}^{J} \theta_i \theta_k \rho_{S_{ik}} S_i S_k (1 - \delta_{ik})\right) \tag{2-A-5}$$

The effective number of degrees of freedom $\nu_r$ for determining t is given (approximately) by the so-called Welch-Satterthwaite formula (Ref. 2.2) as

$$\nu_r = \frac{u_c^4}{\sum_{i=1}^{J} \left( [(\theta_i S_i)^4 / \nu_{S_i}] + [(\theta_i b_i)^4 / \nu_{b_i}] \right)} \qquad (2\text{-A-}6)$$

with

$$\nu_{S_i} = N_i - 1 \qquad (2\text{-A-}7)$$

for the number of degrees of freedom associated with the Si. For the number of degrees of freedom $\nu_{bi}$ to associate with a non-statistical estimate of $b_i$, it is suggested in Ref. 2.2 that one might use the approximation

$$\nu_{b_i} \approx \frac{1}{2}\left(\frac{\Delta b_i}{b_i}\right)^{-2} \qquad (2\text{-A-}8)$$

where the quantity in parenthesis is the relative uncertainty of $b_i$. For example, if one thought that the estimate of $b_i$ was reliable to within ± 25 percent, then

$$\nu_{b_i} \approx \frac{1}{2}(0.25)^{-2} \approx 8 \qquad (2\text{-A-}9)$$

Table 2-A-I. The t Distribution[a]

| ν \ C | 0.900 | 0.950 | 0.990 | 0.995 | 0.999 |
|---|---|---|---|---|---|
| 1 | 6.314 | 12.706 | 63.657 | 127.321 | 636.619 |
| 2 | 2.920 | 4.303 | 9.925 | 14.080 | 31.598 |
| 3 | 2.353 | 3.182 | 5.841 | 7.453 | 12.924 |
| 4 | 2.132 | 2.776 | 4.604 | 5.598 | 8.610 |
| 5 | 2.015 | 2.571 | 4.032 | 4.773 | 6.869 |
| 6 | 1.943 | 2.447 | 3.707 | 4.317 | 5.959 |
| 7 | 1.895 | 2.365 | 3.499 | 4.029 | 5.408 |
| 8 | 1.860 | 2.306 | 3.355 | 3.833 | 5.041 |
| 9 | 1.833 | 2.262 | 3.250 | 3.690 | 4.781 |
| 10 | 1.812 | 2.228 | 3.169 | 3.581 | 4.587 |
| 11 | 1.796 | 2.201 | 3.106 | 3.497 | 4.436 |
| 12 | 1.782 | 2.179 | 3.055 | 3.428 | 4.318 |
| 13 | 1.771 | 2.160 | 3.012 | 3.372 | 4.221 |
| 14 | 1.761 | 2.145 | 2.977 | 3.326 | 4.140 |
| 15 | 1.753 | 2.131 | 2.947 | 3.286 | 4.073 |
| 16 | 1.746 | 2.120 | 2.921 | 3.252 | 4.015 |
| 17 | 1.740 | 2.110 | 2.898 | 3.223 | 3.965 |
| 18 | 1.734 | 2.101 | 2.878 | 3.197 | 3.922 |
| 19 | 1.729 | 2.093 | 2.861 | 3.174 | 3.883 |
| 20 | 1.725 | 2.086 | 2.845 | 3.153 | 3.850 |
| 21 | 1.721 | 2.080 | 2.831 | 3.135 | 3.819 |
| 22 | 1.717 | 2.074 | 2.819 | 3.119 | 3.792 |
| 23 | 1.714 | 2.069 | 2.807 | 3.104 | 3.768 |
| 24 | 1.711 | 2.064 | 2.797 | 3.090 | 3.745 |
| 25 | 1.708 | 2.060 | 2.787 | 3.078 | 3.725 |
| 26 | 1.706 | 2.056 | 2.779 | 3.067 | 3.707 |
| 27 | 1.703 | 2.052 | 2.771 | 3.057 | 3.690 |
| 28 | 1.701 | 2.048 | 2.763 | 3.047 | 3.674 |
| 29 | 1.699 | 2.045 | 2.756 | 3.038 | 3.659 |
| 30 | 1.697 | 2.042 | 2.750 | 3.030 | 3.646 |
| 40 | 1.684 | 2.021 | 2.704 | 2.971 | 3.551 |
| 60 | 1.671 | 2.000 | 2.660 | 2.915 | 3.460 |
| 120 | 1.658 | 1.980 | 2.617 | 2.860 | 3.373 |
| ∞ | 1.645 | 1.960 | 2.576 | 2.807 | 3.291 |

[a] GIVEN ARE THE VALUES OF t FOR A CONFIDENCE LEVEL C AND NUMBER OF DEGREES OF FREEDOM ν

If $b_i$ results from the influence of M elemental error sources $(b_i)_k$, then

$$b_i^2 = \sum_{k=1}^{M} (b_i)_k^2 \qquad (2\text{-A-}10)$$

(An analogous equation holds for $S_i$ if precision uncertainties $(S_i)_k$ are estimated for elemental error sources.) There are several distributions — Gaussian, rectangular and triangular, for instance — that might logically be assumed for bias errors (Ref. 2.2). For an assumed Gaussian distribution, one might estimate the 95-percent confidence bias limit $(B_i)_k$, make the large sample assumption so that t = 2, and then

$$(b_i)_k = \frac{(B_i)_k}{2} \qquad (2\text{-A-}11)$$

If one estimates that it is equally probable for $(b_i)_k$ to lie anywhere within an interval $\pm a$ and highly unlikely that it would lie outside that range, then a rectangular error distribution of width 2a might be assumed and

$$(b_i)_k = \frac{a}{\sqrt{3}} \tag{2-A-12}$$

If one estimates that it is highly unlikely that $(b_i)_k$ would lie outside a range $\pm a$, but that values near the midpoint are more likely than near the bounds, then a distribution shaped like an isosceles triangle of base 2a might be assumed and

$$(b_i)_k = \frac{a}{\sqrt{6}} \tag{2-A-13}$$

In most practical wind tunnel tests, it seems (from an engineering perspective) that the use of the preceeding equations [(2-A-5) and (2-A-611 in this Annex would be excessively and unnecessarily complex and would tend to give a false sense of the degree of significance of the numbers computed using them. In determining what additional simplifying approximations can reasonably be made, the following factors should be considered.

The propagation equation [(Eq. (2-A-5)] is approximate — it is not an exact equation. Unavoidable uncertainties are always present in estimating the bias uncertainties $b_i$ and in estimating their associated degrees of freedom, $\nu_{bi}$. The $S_i$ are usually estimated based on previously determined information (since in most wind tunnel tests it is not possible to obtain multiple readings of an $X_i$ over an appropriate time interval), and the uncertainties associated with these $S_i$ can be surprisingly large (Ref. 2.2). For a Gaussian population, 95 out of 100 determinations of $S_i$ will scatter within a $\pm 45$ percent band about the average if the $S_i$ are determined from samples with $N = 10$ and will still scatter within approximately a $\pm 25$ percent band about the average if the $S_i$ are determined from samples with $N = 30$ (which has traditionally been considered a "large" sample).

Considering the 95-percent confidence t table (Table 2-A-1), one can see that for $\nu_r \geq 9$ the values of t are within about 13 percent of the large sample t-value of 2. This difference is relatively insignificant compared with the effects discussed in the preceeding paragraph. For most engineering applications, it is proposed that Gaussian error distributions and $\nu_r \geq 9$ be assumed so that $t = 2$ always. (This could be called the "large sample-size assumption".) This eliminates the need for evaluation of $\nu_r$ using Eq. (2-A-6) and the need to evaluate all of the $\nu_{si}$ and $\nu_{bi}$.

Consideration of Eq. (2-A-6) shows that, because of the exponent of 4 in each term, $\nu_r$ is most influenced by the number of degrees of freedom of the largest of the $\theta_i S_i$ or $\theta_i b_i$ terms. If, for example, $\theta_3 S_3$ is dominant then $\nu_r \approx \nu_{S_3} \geq 9$ for $N_3 \geq 10$ (recalling Eq. (2-A-7)). If, on the other hand, $\theta_3 b_3$ is dominant then $\nu_r \approx \nu_{b_3} \geq 9$ when the relative uncertainty in $b_i$ is about 24 percent or less (recalling Eq. (2-A-8)). Therefore, invoking the "large sample-size assumption" essentially means that if a $\theta_i S_i$ is dominant then its $N_i \geq 10$ or if a $\theta_i b_i$ is dominant then the relative uncertainty in that $b_i$ is about 24 percent or less.

If the "large sample-size assumption" is made so that $t = 2$, then from Eq. (2-A-5) the 95-percent confidence expression for U, becomes

$$U_r^2 = \sum_{i=1}^{J}\left[\theta_i^2\left(2\frac{B_i}{2}\right)^2 + \sum_{k=1}^{J}\theta_i\theta_k\rho_{b_{ik}}\left(2\frac{B_i}{2}\right)\left(2\frac{B_k}{2}\right)(1-\delta_{ik})\right]$$
$$+ \sum_{i=1}^{J}\left[\theta_i^2(2S_i)^2 + \sum_{k=1}^{J}\theta_i\theta_k\rho_{S_{ik}}(2S_i)(2S_k)(1-\delta_{ik})\right] \tag{2-A-14}$$

Remembering the definition of the precision limit $P_i$ [Eq. (2-4)], this equation can be written

$$U_r^2 = \sum_{i=1}^{J}\left(\theta_i^2 B_i^2 + \sum_{k=1}^{J} \theta_i \theta_k \rho_{b_{ik}} B_i B_k (1 - \delta_{ik})\right) + \sum_{i=1}^{J}\left[\theta_i^2 P_i^2 + \sum_{k=1}^{J} \theta_i \theta_k \rho_{S_{ik}} P_i P_k (1 - \delta_{ik})\right] \qquad (2\text{-A-15})$$

If it is additionally assumed that precision errors in different variables are uncorrelated and if the correlated bias term is approximated as discussed in (Ref. 2.1), then Eq. (2-A-15) reduces to those equations presented in the body of this chapter.

The methodology discussed in the body of this chapter is recommended for use in practical wind tunnel testing situations unless there are other overiding considerations which require the application of (the still approximate) Equations (2-A-5) and (2-A-6).

## ANNEX 2-B: IDENTIFICATION AND ELIMINATION OF OUTLIERS IN SAMPLES

All experimental endeavors can produce data points which appear to be spurious. Such points (outliers) may be caused by intermittent malfunctions of the instrumentation or a physical perturbation not connected with the experiment. For example, a calibration of a pressure measurement system was recently disturbed by random spikes in the data caused by a crane being operated in an adjacent room. Obviously, errors of this type should not be included in the uncertainty estimates, assuming that crane operation would be prohibited during a test. When such points occur, they should be removed from the data if the "best" estimate of the sample standard deviation is desired. Thus, all data should be inspected for spurious data points. Identification criteria should be based on engineering analysis of the instrumentation, the physics of the phenomena, theoretical predictions, and/or the history of similar experiments. To ease the burden of examining large amounts of data, computerized routines are available to scan data sets and flag suspected outliers. The suspected outliers should then be analyzed with respect to the data set in order to make a judgment about their quality.

The effect of outliers (if they are not rejected) is to increase the estimate of the precision limit of the variable. One of the several techniques in common usage for determining if spurious data points are outliers is Chauvenet's criterion (Ref. 2.1).

Consider a sample of N measurements of a variable X with a sample standard deviation of $S_X$. The outlier tests are performed as follows. Compute

$$\delta_k = |X_k - \bar{X}| \qquad (2\text{-B-}1)$$

Determine $\tau$ from Table 2-B-1. If

$$\delta_k \geq \tau S_X \qquad (2\text{-B-}2)$$

then $X_k$ meets the criterion and is identified as an outlier

In general, removing an outlier from the data sample will have a relatively small effect on the mean value, but can have a large effect on the sample standard deviation. There is a continuing controversy over whether the criterion should be applied only once, or more than once, to a given data set. Rejection of outliers should be documented and reported.

Table 2-B-I . Chauvenet's Criterion

| Number of Readings (N) | $\tau$ |
|---|---|
| 3 | 1.38 |
| 4 | 1.54 |
| 5 | 1.65 |
| 6 | 1.73 |
| 7 | 1.80 |
| 8 | 1.87 |
| 9 | 1.91 |
| 10 | 1.96 |
| 15 | 2.13 |
| 20 | 2.24 |
| 25 | 2.33 |
| 50 | 2.57 |
| 100 | 2.81 |
| 300 | 3.14 |
| 500 | 3.29 |
| 1,000 | 3.48 |

A curve-fit equation for $\tau$ using Chauvenet's criterion for $N < 833{,}333$ is

$$\tau = \sum_{i=1}^{5} A_i [\ln(N)]^i \qquad (2\text{-B-}3)$$

where

$A_0 = 0.720185$,
$A_1 = 0.674947$,
$A2 = -0.0771831$,
$A3 = 0.00733435$,
$A4 = -0.00040635$, and $A5 = 0.00000916028$.

# 3.0 WIND TUNNEL ERROR SOURCES

## 3.1 INTRODUCTION

The decision process for establishing a wind tunnel test is idealized in Fig. 1.3. The choice of whether or not to conduct a particular test in a certain facility should be governed by the ability of the expected test outcome to achieve the test objectives within the allowable uncertainties. **The outcome of any test will be dependent on the entire experimental process.** The process includes the design of the experiment, the techniques employed, the instrumentation selected, the flow quality of the facility, and both the reduction and presentation of data and data adjustments or corrections to convert the data to the appropriate reference condition. Under the premise that unacceptable results are worse than none at all, once the best experiment that can be conducted is found to be short of what is needed, the test should not be conducted. The usefulness in quantifying uncertainty for a test is thus to aid in designing the experiment and in formalizing the expected quality of the outcome so that the customer will know what can be expected from the test. Further evaluation and documentation of the test results, including uncertainty, will serve as a reference basis beneficial to both the subjective appraisal of test quality and the assessment of uncertainty for future tests.

As stated above, an experiment's outcome is process dependent. The purpose of this chapter is to discuss some aspects of the process of producing aerodynamic reference coefficients and the various factors that contribute to uncertainty at each step of the process. The chapter highlights considerations essential to the identification and assessment of significant error sources, both of which are key steps in the test process shown in Fig. 1.3. The definitions pertaining to uncertainty and the mathematical tools for estimating uncertainty are discussed in Chapter 2 of this report. Specific examples of the application of the methodology in Chapter 2 for the estimation of uncertainty for a variety of error sources are contained in Chapter 4.

In principle, the application of the tools of Chapter 2 is relatively simple (Fig. 2.7). But, because of the scope of the process from sensor selection to aerodynamic reference results, the application can be quite time consuming if carried out in rigorous detail. When the approach of Chapter 2 is utilized, rigor is required to assure that bias error sources are identified as being either correlated or uncorrelated to arrive at the estimate of uncertainty. The discussion in this chapter assumes that **the planned test techniques are employed faithfully and that no undetected measurement problems occur.** Subject to the considerations stated above, the approach described in Chapter 2 and Fig. 2.7 can be used to define the uncertainty.

## 3.2 PROCESS ERROR SOURCES

**Every contribution to the flow of the data stream from sensor to reported data is a source of uncertainty in the final product.** There is a choice as to what is defined as the final product. For example, the final product could be defined as merely being the coefficients that are produced without any adjustments for flow quality, support interference, or tare loads. The uncertainty could also be defined in relation to an aerodynamic reference condition. In Fig. 3.1, the progression of corrections which leads to the final corrected output from the test at the aero-reference condition is depicted. Here, the final output is assumed to be the derived parameters which can be used as the starting point in the process of extrapolating/predicting full-scale flight results. The parameters include coefficients, nondimensional quantities (Mach number, Reynolds number, etc.), fluid and

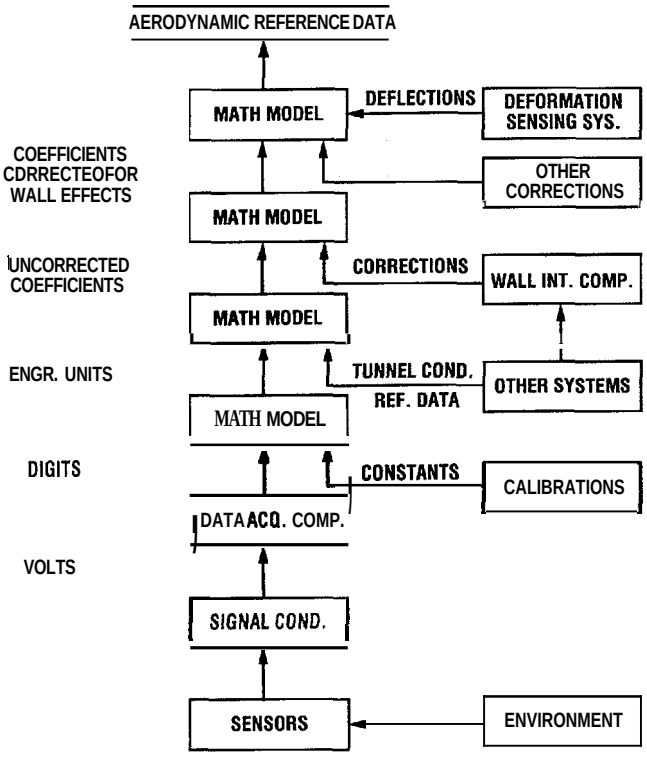


Fig. 3.1. Simplified data flow process.

stream properties (temperature, enthalpy, dynamic pressure, etc.), angles, and deflections. The process of extrapolating to flight is not considered here; this process has its own uncertainties. Depending on the test objectives, it may not be necessary to estimate the uncertainty at the aerodynamic reference condition. For example, if an increment is being sought between two conditions, corrections such as wall interference and buoyancy may, with good approximation, be the same for each condition and thus can be neglected in the assessment of uncertainty for the increment in question (see Section 2.3.3 for discussion of correlated bias error).

The first step, then, in performing an uncertainty analysis is to trace the entire data flow process from sensor output through all the conversions and adjustments to the data in arriving at the final result. Implicit in the data flow are all of the factors which serve as tributaries to the flow such as the calibrations (traceable to national standards) and all corrections applied (empirical, semiempirical, and theoretical). Further, it is assumed that sufficient significant digits are presented such that any adjustments to or manipulations of the data flow will not create additional uncertainty.

In each case, uncertainty estimates must be made to decide whether a significant contribution to either bias or precision error is produced. Uncertainty should not automatically be estimated for each potential contributor in the entire chain making up the process. Instead, it *is* recommended that opportunities for end-to-end uncertainty assessments be identified. There are two reasons for this recommendation. First, an end-to-end assessment will often produce a more realistic (usually lower) estimate of process uncertainty. Second, long-term experience may be of more value in estimating overall uncertainty than knowledge derived from expending resources to determine individual uncertainties for a series of error sources. Regardless of the method employed, it is expected that the first time an assessment of overall uncertainty is developed, it will be more involved than subsequent ones since future assessments will benefit from knowledge gained from prior work.

In Fig. 3.1, the simplified data flow process is shown as starting with the environment affecting the sensors which then respond through the signal conditioning to initiate a data flow. This data flow is processed and modified by input from various sources as it progresses through the several levels to the aerodynamic reference data level. The aerodynamic reference condition is assumed to represent the reference aerodynamic model shape in a free-air environment at wind tunnel test conditions. Departures from any of these aerodynamic reference conditions lead to corrections to the data stream.

Figure 3.2 depicts a more detailed bottom-up data flow process which begins with the environment affecting the sensors (balance, transducers, etc.). The purpose of the increased detail is to illustrate the range of the contributors to the data stream, particularly the environment. The representation is not exhaustive. For example, model motion (inertial forces) is shown coming from the envi-

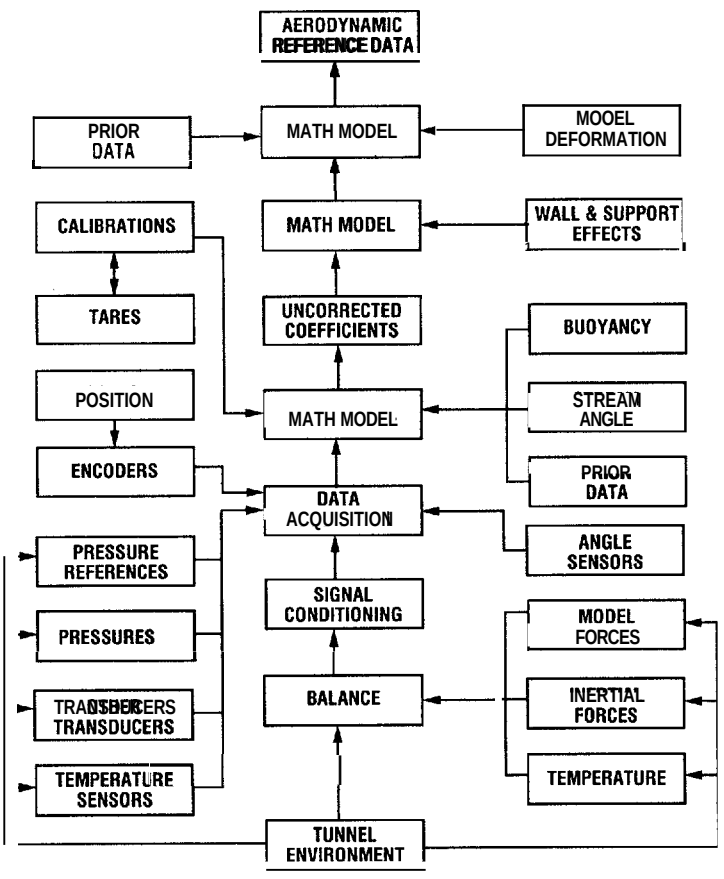


Fig. 3.2. Detailed data flow process.

ronment and feeding into the balance only and not other instrumentation such as angle sensors and transducers. In general, the sources shown in Fig. *3.2* can be classified as test technique, model, tunnel, instrumentation, and math model related, each of which will be discussed in the following sections.

### **3.2.1** Test Technique

Although a major potential source of uncertainty, test technique is not shown explicitly in Fig. *3.2.* However, it is intimately related to the design of the experiment and should be considered along with the uncertainty sources implied in Fig. *3.2.* It is essential that each step of the test technique be examined to identify and estimate uncertainty contributions to the desired result. In general, the effects of uncertainty due to test technique must be assessed on the basis of experience aided, whenever practical, by computation. Some examples of test technique-related error sources are presented below.

Model selection and mounting — The method of mounting a model and the choice of the model size are factors which lead to a variety of installation effects that may or may not be acceptable for the purpose of the test. The choice of the mounting system will compromise the test results particularly if done improperly. The choice of the size of a model may be influenced by wall interference considerations. The desire to have the model large for any number of reasons (reduce uncertainty in extrapolating for Reynolds number effects, increase model fidelity, ease of installing instrumentation, increased strength) may be significantly offset by the increased uncertainty resulting from wall interference effects. The decision to apply, or not to apply wall interference corrections should be governed by the test objectives. How one assesses both support system effects and wall interference corrections and computes their influence on the data is assumed to be part of the math model that produces data adjusted for derived wall effects. Because of the lack of definitive experiments, the uncertainty associated with these adjustments is largely a subjective estimate.

Balance selection — The choice of the capacity of the balance is part of the test technique. Frequently, a compromise in the capacity of the balance is made because the primary purpose of the test is for stability and control over a wide range of conditions and not for drag. When cruise drag is also one of the primary objectives, the proper technique is to change balances and run a drag test with the correctly sized balance. A related common occurrence, driven by schedule and economics, is to try to simultaneously obtain a massive amount of pressure data and force data. This entails crossing the balance with a host of wires and flexible tubing which generally renders the drag measurement useless for accurate determination of cruise performance. The proper technique for drag is to remove all extraneous items bridging the balance and conduct the drag portion of the test separately.

Boundary-layer simulation — Simulation of proper boundary-layer development and verifying the result is an important test technique. In principle, the techniques for sizing and application of artificial roughness are widely known. There are many techniques for application that are all effective. However, there can be secondary effects that become important in situations where accurate aerodynamic reference drag data are required. To assess these effects properly, additional testing is needed. If not verified, the roughness strips can either be partially ineffective (particularly true if the strips are not maintained) or produce too much drag of their own.

Flow angle correction — Stream angle assessment methods are widely used test techniques. An average effect is generally obtained by testing the model both upright and inverted. The choice of how to do this (roll both model and balance, or roll only model) is a part of the technique. The latter has the advantage of eliminating errors in the original positioning of the balance in the process of transferring from the balance axis to the model axis while the former maintains the same load distribution among the balance components. This approach of averaging data from upright and inverted tests is accurate if there is not spanwise variation in stream angle. In that case, drag is affected differently from lift, and a more involved computational technique is required. Similar effects in the lateral direction can lead to large errors in directional static stability assessment if the model moves off centerline and the stream angle in the lateral direction is not constant. In this event, it isn't sufficient to assume that the model is symmetrical and apply a constant correction to the lateral angle. Additional tests are required to extract the correction for each lateral position. These tests are time consuming and are frequently omitted in test planning.

The previous discussion clearly indicates that many aspects of testing significantly influence the quality of results. Detailed analyses and additional tests offer the possibility of dealing with these error sources effectively. Prior experience can also provide needed information faster and less expensively in many cases. Comprehensive evaluation of approaches to test technique can be a key to achieving data quality suitable for the purpose of the test.

### 3.2.2 Model Shape and Finish

Departure of the external lines of the as-built model from aerodynamic reference dimensions is a potential source of error which is amenable to systematic evaluation. The model is expected to be produced to the requisite dimensions, tolerances, and surface finish. For this reason, verification of critical dimensions is still required. Common error sources are airfoil contours (especially leading edge radii) and size and shape of both lifting and control surfaces. The most accurate corrections to the data for these departures require the same computational methodology used to correct for aeroelastic distortions. An additional departure from aero lines occurs on a micro-scale when the surface finish of the leading edge of the model is not maintained. This effect is generally negligible except when the prescribed test technique is for natural laminar flow development. In this case, changes in the surface roughness lead to significant changes in drag and pitching moment as the test progresses.

The effect of an improper mechanical fit between the model and the balance is an additional error source. Differences between this fit and that of the calibration body used in calibrating the balance produce other errors in the calibration constants (drag and pitching moment are usually affected the most). Assessment of this effect requires careful loading and exercise of judgment. Additionally, incorrect determination of the angle between the balance and the model reference axis, as well as moment transfer distances, introduces errors through the math model used to transfer from the balance axis to the reference axis.

### 3.2.3 Tunnel Flow Quality

Corrections required to compensate for the effects of flow quality are significant in most cases. In some situations where increments are to be obtained, flow quality influences may be neglected with confidence. Regardless, the effects of flow quality should be estimated. Estimating data corrections to account for tunnel flow quality is largely an art that can be carried out to various degrees of sophistication, depending on the computational/empirical approach taken. Estimating the uncertainty in any such corrections requires much experience which can be aided by validation experiments. The following discussion will highlight some of the issues involving flow quality that should be considered in estimating both corrections and uncertainty due to this source. The tunnel flow quality is composed of the steady and dynamic tunnel-empty flow components and the modifications to the flow field caused by the presence of the model. The model pressure field modifies the trajectory of any vortical flow components from the stilling chamber and nozzle. This affects the stream angle and curvature field. Both drag and pitching moment are particularly affected by the variation in these components over the volume occupied by the model. The model-induced flow perturbations also affect the wall boundary-layer growth which affects the buoyancy determined from prior tunnel-empty survey data. In some correction schemes this latter effect is considered as part of the wall interference correction.

In the main, tunnel-empty flow-field gradient effects on the model are not well treated. A correction methodology for taking the surveyed stream nonuniformities (flow angle, velocity, temperature) and computing their impacts as a nonlinear problem (e.g., transonic flow) has not been developed. If the upstream boundary were surveyed to establish the flow quality, and the wall boundary conditions and the model distortions (aero-elastic deflections as well as support interference) were known, a grand computation could be performed which would provide an assessment of the total effect of flow field distortions, buoyancy, wall interference, and model distortions. When that is available, one of the last two math model steps in Fig. 3.2 can be eliminated.

Corrections to account for the time-varying components of the tunnel flow (vorticity, pressure fluctuation, and temperature fluctuation), in general, are not well in hand. A turbulence sphere and

a cone are commonly used to infer an effective Reynolds number different from the Reynolds number defined on the basis of the mean flow. The use of either of these has not been definitively established as accounting for the effects of flow unsteadiness. However, they are useful in that the boundary layer of each responds to both the vorticity and pressure fluctuations and that some reference data for low disturbance conditions exist for each. The relative impact of the fluctuations on boundary-layer-sensitive phenomena has not been defined. Other measurements such as static pressures and buffeting are also affected by unsteady flow components. Some techniques have been reported in the literature for adjusting test results for unsteady flow components. However, the process is largely an art as opposed to a science, and judgment based on experience is required to determine a correction or estimate the uncertainty due to unsteady flow.

In summary, regardless of what art or science is applied to the task of estimating corrections and uncertainty due to flow quality, in the near term the final assessment will be largely dependent on experience.

### 3.2.4 Instrumentation

The instrumentation system includes the sensors as well as the signal conditioning and data acquisition system. Estimates of uncertainty can be developed for each element of the chain that contributes to a derived result from the instrumentation. Estimates can also be based on end-to-end performance. The development of end-to-end calibrations using secondary calibration standards applied in the field is preferred, whenever practical, to reduce the uncertainty of the computed result.

Calibrations are performed to ensure that correct representations of the calibration functions, traceable to a prime standard, have been derived. By applying the calibrations, some biases are reduced; but, other errors may be introduced by the method of calibration or the data acquisition system used in the calibration.

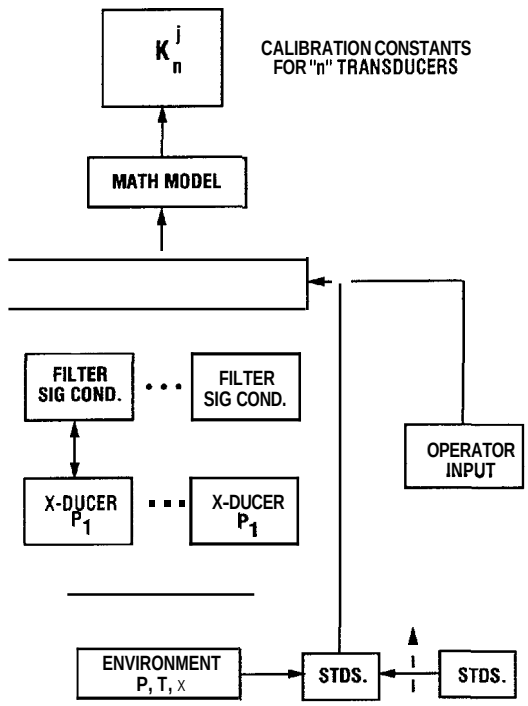


laboratory is to impose an environment on the pressure

Accelerations in continuous flow wind tunnels and many other applications normally have negligible effects and

standards of the laboratory (which have their own

The calibration process for pressure transducers depicted in Fig. 3.3 is essentially generic. In the case of a balance, F (force) and M (moment) would be substituted for ''P''. One might also add dT/dt for temperature rate in addition to T.

The possibility of signal conditioning being a significant influence should not be overlooked. In Fig. 3.4 a deviation plot for two preprogrammable amplifier filter units (PPAF) illustrates what can happen if care is not taken. The units are not perfectly linear. Two channels are shown. Channel 16 is within specifications but channel 14 could introduce a worst case error of around 0.3 percent at full-scale conditions. As an aside, there are several solutions to the problem presented by channel 14. The obvious choices are to perform an end-to-end calibration, adjust the channel, if possible, or simply not use it. The end-to-end calibration implies that the system containing the amplifier goes with the model and its instrumentation. This fidelity from the calibration process to the tunnel is not always maintained. The alternative is to introduce a data system calibration factor into the math model where appropriate. The advantage of the latter approach is that it permits interchange of amplifiers during a test without having to recalibrate, and it provides for the least bias error being introduced by the non-, linear amplifier.

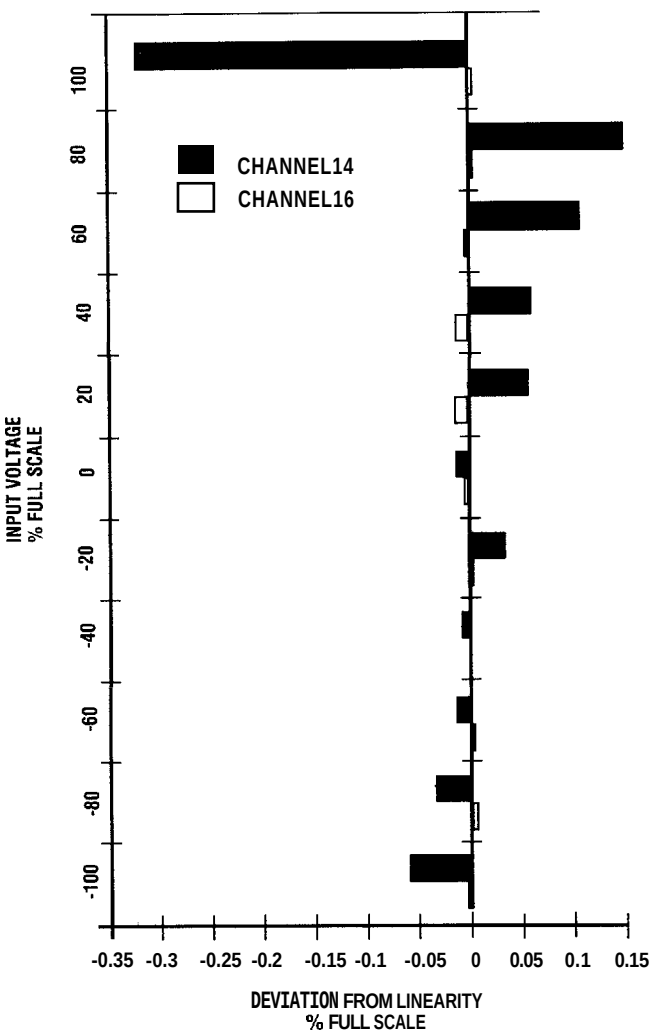


Fig. 3.4. Nonlinearity errors for two PPAF amplifer channels.

### 3.2.5 Math Models

There are numerous opportunities for math models to be sources of uncertainty. Returning to Fig. 3.1, one notes that the data flow process shows four math models. Although some portions of math models will have exact expressions, there is still opportunity for error. For example, the math model that produces uncorrected coefficients from the engineering units would appear not to be a source of error. However, items such as reference dimensions, angles, and transfer distances are inherent in the math model; thus, the model will produce inaccurate results if test article dimensions employed are in error.

The most common source of math model uncertainty is perhaps attributable to the inability of the math model to perfectly describe the true characteristics of the instrumentation. For example, hysteresis effects and secondary effects of some variables (e.g., temperature gradients, accelerations, etc.) are generally not modeled. An exception is cryogenic tunnel operations where particular care is taken to account for both mean temperature and spatial temperature gradients. Further, curve fits and interpolated values are simply approximations. For example, spline fits used in pressure integration can produce overshoot which causes considerable error. Estimation of the uncertainty due to these effects requires experienced judgment.

The math model used to apply corrections is a source of uncertainty which is apart from the uncertainty in the correction itself. For example, wall interference effects may be estimated either in advance of a test, online as the test is progressing, or after the test is over. Wall interference estimated

before the test is not subject to a precision error. The only error is bias, which is due to the assumed math model not matching reality. Since wall correction calculation methods range from classical methods using linear theory to Navier-Stokes based algorithms, a wide range of possibilities exist for bias errors to be different, depending on the model, tunnel, and test conditions. When the wall interference estimates also involve direct measurement of parameters (e.g., pressures on the tunnel walls), the estimate of wall interference is subject to both bias and precision errors. Determination of the uncertainty due to the wall correction methodology is best done through a combination of calculation and experimental verification. The application of the wall correction that has been derived can also be inexact, and consequently can be a further source of error.

Corrections to account for support interference also' have a math model element. Usually, a correction is determined experimentally (test technique). However, the experimental approach involves holding the model with at least two different support systems in and out of the presence of a nonmetric dummy system (or image). Experience shows that the two methods do not converge to the same values. If a third way of holding the model is introduced, the three methods generally don't agree. An improved estimate occurs when the experimental measurements are coupled with calculations (math model) to account for the mutual interference effects which are not eliminated in the experimental simulation. A further option exists to calculate the support interference effects directly without benefit of further tests. Regardless of the method used, the assessment of support interference is subject to significant uncertainty.

Overall, the assessment of the uncertainty due to a math model correction is best identified by tests specifically designed to determine the accuracy of the correction. Lacking such experiments, variability in any elemental values can be estimated on the basis of experience, and the math models can then be exercised to determine the components of uncertainty.

### 3.3 SIGNIFICANCE OF ERROR SOURCES

One of the most important steps in testing is determining the effect of error sources on the results. Focusing attention on the major factors controlling data quality can dramatically simplify uncertainty analyses. As part of the activity associated with developing this report, a survey was conducted to subjectively determine the importance of numerous error sources in wind tunnel testing. The survey sought to develop a list of ranked items. The survey separately treated tests conducted for absolute (reference) purposes and for comparative (incremental) purposes. Surveys are presented in Table 3.1 for absolute testing and Table 3.2 for comparative testing.

The numerical score for each source is the average of survey results. Importance was ranked according to the following numerical scale:

| | |
|---|---|
| Critical | 1 |
| Major | 2 |
| Significant | 3 |
| Minor | 4 |
| Insignificant | 5 |

Responses were based on the experience of the respondents (total of six, with some items receiving as few as four responses) for tests using conventional instrumentation systems and careful setup and monitoring practices. Significant instrumentation biases were minimized and/or corrected prior to tests. The information reported should be representative of most well-run tests.

Table 3.1 Results of error significance survey for absolute testing.

a. Error Sources Common to All Instrumentation

| RANK | ERROR SOURCE | AVERAGE RESPONSE | RESPONSE VARIANCE |
|---|---|---|---|
| 1 | Traceability to national or international standards | 1.6 | 0.3 |
| 2 | Calibration methods including setup, range, devices, etc. | 2.2 | 0.7 |
| 3 | Data reduction algorithms | 2.6 | 1.2 |
| 4 | Curve fit algorithms | 3.0 | 0.5 |
| 5 | Zeroing of readings | 3.2 | 1.4 |
| 6 | Temperature effects | 3.5 | 0.3 |
| 7 | Electrical noise | 3.5 | 0.3 |
| 8 | Vibration effects | 3.5 | 0.7 |
| 9 | Moisture effects | 3.7 | 1.0 |
| 10 | Excitation voltage | 3.8 | 0.2 |
| 11 | Electrical and mechanical deterioration | 3.8 | 0.2 |
| 12 | Data acquisition instrumentation including signal conditioners, amplifiers, filters, and analog-to-digital converters | 4.0 | 0 |

b. Error Sources in Force and Moment Measurements

| RANK | ERROR SOURCE | AVERAGE RESPONCE | RESPONSE VARIANCE |
|---|---|---|---|
| 1 | Balance calibration standard weights and/or load cells | 2.5 | 1.4 |
| 2 | Model and/or balance dynamic motion in pitch, yaw, and roll | 2.8 | 0.2 |
| 3 | Balance attachment techniques to model/calibration body | 2.8 | 1.4 |
| 4 | Mechanical and/or structural design of the balance | 3.2 | 1.4 |
| 5 | Attachment of strain gages to flexures | 3.3 | 1.4 |
| 6 | Deterioration and/or unbonding of strain gages | 3.7 | 2.0 |

c. Error Sources in Pressure Measurements made with Strain Gage Transducers

| RANK | ERROR SOURCE | AVERAGE RESPONSE | RESPONSE VARIANCE |
|---|---|---|---|
| 1 | Pressure orifice size, shape, and location | 2.7 | 0.7 |
| 2 | Time allowed for pressure to settle | 3.2 | 0.7 |
| 3 | Length and/or diameter of pressure tubing | 3.3 | 0.7 |
| 4 | Reference and calibration pressures | 3.7 | 0.3 |
| 5 | Communications and timing of microprocessors | 4.0 | 0.8 |

d. Error Sources in the Model Attitude Determined using Internal Instrumentation

| RANK | ERROR SOURCE | AVERAGE RESPONSE | RESPONSE VARIANCE |
|---|---|---|---|
| 1 | Identification of the support system angles where the model pitch, yaw, and roll angles are zero | 1.8 | 1.0 |
| 2 | Model and/or balance dynamic motion in pitch, yaw, and roll | 2.5 | 0.7 |
| 3 | Installation of the instrument(s) in the model | 2.5 | 2.0 |
| 4 | Tunnel flow angularity | 3.2 | 1.4 |

Table 3.1 Concluded

e. Error Sources in the Model Attitude Determined using Elastic Deflections

| RANK | ERROR SOURCE | AVERAGE RESPONSE | RESPONSE VARIANCE |
|---|---|---|---|
| 1 | Identification of the support system angles where the model pitch, yaw, and roll angles are zero | 1.8 | 1.0 |
| 2 | Measured model forces and moments | 2.0 | 1.2 |
| 3 | Tunnel flow angularity | 2.3 | 1.0 |
| 4 | Support system and the balance elastic deflection angles | 2.3 | 1.4 |
| 5 | Support system angles | 2.5 | 1.0 |
| 6 | Support system prebend angles (angles between the support system axes and the balance axes | 2.8 | 1.0 |
| 7 | Model static weight tares | 2.8 | 1.4 |
| 8 | Model to balance alignment angles | 2.8 | 1.4 |
| 9 | Method used to attach the balance to the model and to the sting/strut support | 2.8 | 1.7 |
| 10 | Method used to attach the sting/strut to the support system | 3.0 | 2.0 |
| 11 | Model and/or balance dynamic motion in pitch, yaw, and roll | 3.2 | 0.2 |

f. Error Sources in the Calculated Parameters

| RANK | ERROR SOURCE | AVERAGE RESPONSE | RESPONSE VARIANCE |
|---|---|---|---|
| 1 | Model aerodynamic attitude | 1.5 | 0.7 |
| 2 | Tunnel flow quality | 1.7 | 0.7 |
| 3 | Testing techniques | 1.7 | 0.7 |
| 4 | Methods used to simulate power-on conditions | 1.8 | 0.3 |
| 5 | Tunnel test conditions both steady and unsteady (Mach number, dynamic pressure, etc.) | 2.0 | 0.8 |
| 6 | Corrections for sting/strut interference | 2.0 | 0.8 |
| 7 | Accuracy of the model geometry | 2.2 | 0.7 |
| 8 | Balance-to-model transfer distances | 2.2 | 1.4 |
| 9 | Model reference dimensions and areas | 2.2 | 2.3 |
| 10 | Deterioration of model (i.e. changes in the surface roughness) | 2.3 | 0.7 |
| 11 | Corrections for wall interference | 2.3 | 0.7 |
| 12 | Method and location of boundary layer transition material | 2.3 | 1.0 |
| 13 | Interference (ie. grounding or fouling) between the balance, model, and/or sting/strut | 2.4 | 2.3 |
| 14 | Adjustments to compensate for base and/or cavity pressure | 2.5 | 0.7 |
| 15 | Adjustments to compensate for internal duct flow | 2.5 | 0.7 |
| 16 | Model aeroelasticity | 2.7 | 0.3 |
| 17 | Balance-to-model alignment angles | 2.8 | 0.7 |
| 18 | Temperature effects | 3.2 | 0.2 |
| 19 | Humidity of the tunnel flow | 3.6 | 1.2 |

Table 3.2 Results of error significance survey for comparative testing

a. Error sources common to all instrumentation

| RANK | ERROR SOURCE | AVERAGE RESPONSE | RESPONSE VARIANCE |
|---|---|---|---|
| 1 | Traceability to national or international standards | 2.4 | 0.8 |
| 2 | Calibration methods including setup, range, devices, etc. | 3.2 | 1.2 |
| 3 | Zeroing of readings | 3.2 | 1.4 |
| 4 | Curve fit algorithms | 3.4 | 0.3 |
| 5 | Data reduction algorithms | 3.4 | 0.3 |
| 6 | Temperature effects | 3.5 | 0.3 |
| 7 | Electrical noise | 3.5 | 0.3 |
| 8 | Vibration effects | 3.5 | 0.6 |
| 9 | Moisture effects | 3.7 | 1.0 |
| 10 | Excitation voltage | 3.8 | 0.2 |
| 11 | Electrical and mechanical deterioration | 3.8 | 0.2 |
| 12 | Data acquisition instrumentation including signal conditioners, amplifiers, filters, and analog-to-digital converters | 4.0 | 0 |

b. Error sources in force and moment measurements

| RANK | ERROR SOURCE | AVERAGE RESPONSE | RESPONSE VARIANCE |
|---|---|---|---|
| 1 | Model and/or balance dynamic motion in pitch, yaw, and roll | 2.8 | 0.2 |
| 2 | Balance attachment techniques to model/calibration body | 2.8 | 1.4 |
| 3 | Mechanical and/or structural design of the balance | 3.2 | 1.4 |
| 4 | Balance calibration standard weights and/or load cells | 3.3 | 0.3 |
| 5 | Attachment of strain gages to flexures | 3.3 | 1.4 |
| 6 | Deterioration and/or unbonding of strain gages | 3.7 | 2.0 |

c. Error sources in pressure measurements made with strain gage transducers

| RANK | ERROR SOURCE | AVERAGE RESPONSE | RESPONSE VARIANCE |
|---|---|---|---|
| 1 | Time allowed for pressure to settle | 3.2 | 0.7 |
| 2 | Pressure orifice size, shape, and location | 3.3 | 0.3 |
| 3 | Length and/or diameter of pressure tubing | 3.5 | 0.3 |
| 4 | Reference and calibration pressures | 3.7 | 0.3 |
| 5 | Communications and timing of microprocessors | 4.0 | 0.8 |

d. Error sources in the model attitude determined using internal instrumentation

| RANK | ERROR SOURCE | AVERAGE RESPONSE | RESPONSE VARIANCE |
|---|---|---|---|
| 1 | Identification of the support system angles where the model pitch, yaw, and roll angles are zero | 2.3 | 0.7 |
| 2 | Model and/or balance dynamic motion in pitch, yaw, and roll | 2.5 | 0.7 |
| 3 | Installation of the instrument(s) in the model | 3.0 | 1.7 |
| 4 | Tunnel flow angularity | 3.7 | 0.7 |

Table 3.2 Concluded

e. Error sources in the model attitude determined using elastic deflections

| RANK | ERROR SOURCE | AVERAGE RESPONSE | RESPONSE VARIANCE |
|---|---|---|---|
| 1 | Identification of the support system angles where the model pitch, yaw, and roll angles are zero | 2.1 | 0.8 |
| 2 | Measured model forces and moments | 2.2 | 1.0 |
| 3 | Support system angles | 2.7 | 0.7 |
| 4 | Method used to attach the balance to the model and to the sting/strut support | 2.8 | 1.7 |
| 5 | Support system and the balance elastic deflection angles | 3.0 | 0.4 |
| 6 | Method used to attach the sting/strut to the support system | 3.0 | 2.0 |
| 7 | Tunnel flow angularity | 3.3 | 0.3 |
| 8 | Model and/or balance dynamic motion in pitch, yaw, and roll | 3.3 | 0.3 |
| 9 | Model static weight tares | 3.5 | 0.3 |
| 10 | Model to balance alignment angles | 3.5 | 0.3 |
| 11 | Support system prebend angles (angles between the support system axes and the balance axes | 3.5 | 0.7 |

f. Error sources in the calculated parameters

| RANK | ERROR SOURCE | AVERAGE RESPONSE | RESPONSE VARIANCE |
|---|---|---|---|
| 1 | Testing techniques | 2.0 | 0.4 |
| 2 | Methods used to simulate power-on conditions | 2.0 | 0.7 |
| 3 | Model aerodynamic attitude | 2.0 | 0.8 |
| 4 | Accuracy of the model geometry | 2.2 | 0.7 |
| 5 | Tunnel test conditions both steady and unsteady (Mach number, dynamic pressure, etc.) | 2.2 | 0.7 |
| 6 | Interference (ie. grounding or fouling) between the balance, model, and/or sting/strut | 2.4 | 2.3 |
| 7 | Tunnel flow quality | 2.5 | 0.3 |
| 8 | Deterioration of model (i.e. changes in the surface roughness) | 2.5 | 0.7 |
| 9 | Method and location of boundary layer transition material | 3.0 | 0.4 |
| 10 | Adjustments to compensate for base and/or cavity pressure | 3.0 | 0.4 |
| 11 | Model aeroelasticity | 3.2 | 0.2 |
| 12 | Adjustments to compensate for internal duct flow | 3.2 | 0.7 |
| 13 | Balance-to-model transfer distances | 3.2 | 1.0 |
| 14 | Temperature effects | 3.3 | 0.3 |
| 15 | Corrections for sting/strut interference | 3.5 | 0.3 |
| 16 | Corrections for wall interference | 3.5 | 0.3 |
| 17 | Balance-to-model alignment angles | 3.5 | 0.7 |
| 18 | Model reference dimensions and areas | 3.5 | 1.4 |
| 19 | Humidity of the tunnel flow | 3.8 | 0.7 |

For absolute testing, model aerodynamic attitude (1.5), traceability to standards (1.6), flow quality (1.7), and testing techniques (1.7) were deemed the most critical. The variance in these rankings was 0.3 for standards and 0.7 for the others cited. The least critical was data acquisition instrumentation (4.0) with a variance of 0 and communications/timing of microprocessors (4.0) with a variance of 0.8.

For comparative testing, the average response for traceability to standards increased to 2.4. However, perhaps in recognition of the merits of incremental testing, the lowest score was 2.0 which was shared by testing techniques, power-on simulation, and model aerodynamic attitude. The least critical source (data acquisition and microprocessor) remained the same as for absolute testing.

The responses to the survey are driven by collective experience, and the variance in those responses should be recognized to mean that virtually everything on the list in the table has been a problem to someone at sometime. The tables can be used to guide comprehensive and efficient treatment of test process uncertainty.

## 3.4 CONCLUDING REMARKS

The purpose of the foregoing discussion was to illustrate the breadth and depth of the opportunities for uncertainty to exist in the test results. The treatment given is not exhaustive. The notion that the sources of uncertainty are far ranging has been put forth. Because of the scope of the sources, there may exist the temptation not to delve into the problem of identifying uncertainties. It is strongly suggested that this temptation be resisted and that time be taken to examine the process for producing wind tunnel test results that are referencable. Out of the examined process will come improved calibration and test techniques and possibly the impetus for further modification to one's facilities. It is also suggested that a database of system and elemental uncertainty estimates and related information be established. This database should prove highly beneficial in developing uncertainty estimates for other specific tests.

# 4.0 APPLICATION OF THE UNCERTAINTY METHODOLOGY TO A FORCE AND PRESSURE TEST

## 4.1 INTRODUCTION

An example is presented which illustrates how the methodologies developed in the prior chapters are applied to estimate the uncertainty for the coefficients determined during a wind tunnel test. This example focuses on the drag coefficient, but the methods illustrated can be applied to any parameter. Included in the example is a discussion of the factors involved in obtaining data to estimate the uncertainty of an instrument or instrumentation system. A sample set of evaluation data that was obtained on a system of pressure transducers is used to illustrate how the uncertainty of a pressure transducer and a system of pressure transducers is estimated. The example is then used to show how the bias and precision limits are estimated for all of the parameters required in the calculation of the drag coefficient, as well as for the drag coefficient itself. The drag coefficient is then corrected to the aerodynamic reference condition and the uncertainty is estimated. At the end of the chapter are several annexes which present supplementary equations, the consequences of determining the sensitivity coefficients (partial derivatives) with respect to dependent instead of independent parameters, the estimation of the uncertainty for a simple pressure integration, and the estimation of the uncertainty for an incremental pressure.

The uncertainty of a calculated value is dependent on the error sources, the processes used to quantify and propagate the errors, and the processes used in acquiring and reducing the measured data to the desired parameters. The estimation of the uncertainty associated with the wind tunnel testing process can be broken down into the basic tasks shown in Fig. 4.1. The outline shown in Fig. 4.1 is a compilation of some of the flow charts provided in Chapters 1 and 3, and can be used to follow the development of this example. All of the error sources listed in Chapter 3 have been considered. However, in an effort to keep the example relatively simple, some of the data reduction equations have been simplified; therefore, some error sources that would normally be included have been excluded and those instances are noted in the text. Although contributions from some of the error sources have been omitted, the example still provides a realistic application of the uncertainty methodology.

THE OUTLINE SHOWN BELOW IS A COMPILATION OF SOME OF THE FLOW CHARTS PROVIDED IN CHAPTERS 1 AND 3. THE OUTLINE IAN BE USED TO FOLLOW THE DEVELOPMENT OF CHAPTER 4. THE VALUES PROVIDED IN THE PARENTHESES INDICATE WHERE THAT PROCESS IS DESCRIBED.

TEST DESCRIPTION (4.2)
- DEFINE OBJECTIVES AND UNCERTAINTY REQUIREMENTS
- DESIGN THE TEST
  - DESIRED PARAMETER(S)
  - MODEL CONFIGURATION(S)
  - TEST TECHNIQUE(S)
  - MEASUREMENT(S) REQUIRED
  - SPECIFIC INSTRUMENTATION
  - CORRECTION(S) APPLIED

DETERMINE ERROR SOURCES AFFECTING THE RESULTS (CHAPTER 3)
- IDENTIFY SOURCES OF ERROR (CHAPTER 3)
  - EXAMINE THE CALIBRATION PROCESSES
  - EXAMINE THE DATA ACQUISITION AND REDUCTION PROCESSES
  - EXAMINE THE TEST TECHNIQUES AND PROCESS
- ASSESS RELATIVE SIGNIFICANCE OF ERROR SOURCES (CHAPTER 3)
  - REVIEW EXISTING UNCERTAINTY OATA BASE
  - DETERMINE UNCERTAINTY OF AN INSTRUMENTATION SYSTEM (4.3)
  - USE ENGINEERING JUDGMENT

ESTIMATE UNCERTAINTY (4.4 AND 4.5)
- DETERMINE SENSITIVITY COEFFICIENTS (4.4, 4.5, AND ANNEX 4-B)
- ESTIMATE BIAS AND PRECISION LIMITS FOR A RESULT (4.4 AND 4.5)
- ESTIMATE THE UNCERTAINTY OF A RESULT (4.4 AND 4.5)

DOCUMENT RESULTS
- INSTRUMENTATION SYSTEM UNCERTAINTIES (TABLE 4.2)
- MEASUREMENT RESULTS (TABLE 4.3)
- TEST DOCUMENTATION REPORT (4.6)

Fig. 41. Assessment of wind tunnel data uncertainty.

## 4.2 TEST DESCRIPTION

The tests were conducted in the Aerodynamic Wind Tunnel 4T and the Propulsion Wind Tunnel 16T at the Arnold Engineering Development Center (AEDC). The objective of the tests was to provide the data necessary to evaluate the effectiveness of a three-dimensional transonic wall interference algorithm. The tests consisted of measuring the forces, moments, and surface pressures on the generic wing/body/tail model shown in Fig. 4.2. The forces and moments were measured using an internal strain-gage balance and the surface pressures were measured using electronically scanned pressure (ESP) modules. Static pressures near the test section

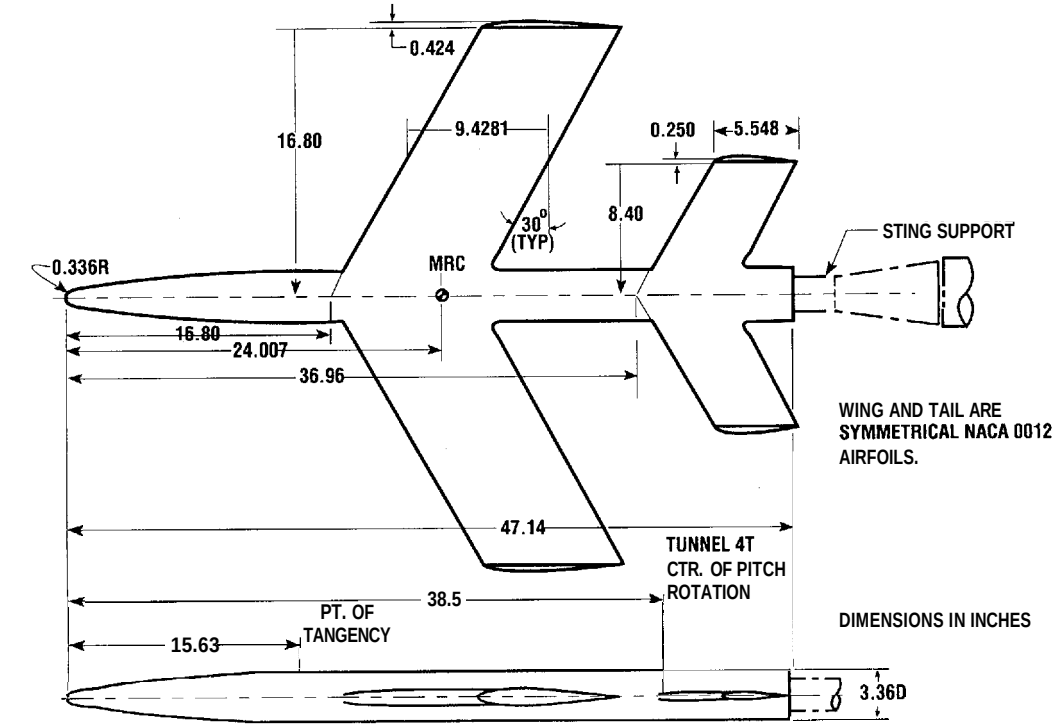


a. Model geomery

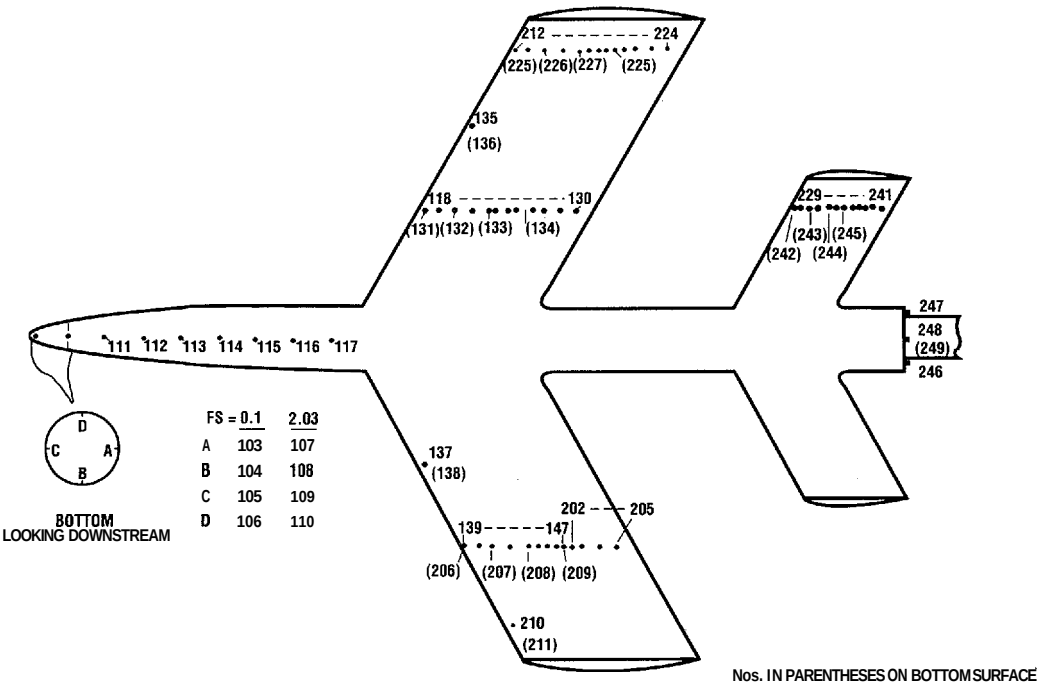


b. Identification of model pressure orifices

Figure 4.2 Model details.

walls in Tunnel 4T were measured to provide the boundary conditions for the wall interference assessments. The model was tested in Tunnel 4T with a blockage of 1.33 percent to provide data with large wall interference effects, and in Tunnel 16T for reference data assumed to be interference free, since the blockage ratio was only 0.08 percent. The aerodynamic coefficients determined in Tunnel 4T were adjusted using the wall interference algorithm for comparison with the aerodynamic coefficients in Tunnel 16T. The results are reported in AIAA paper 90-1408 entitled "Wall Interference Correction for Three-Dimensional Transonic Flows" (4.1).

In order to accomplish the objective of the tests, the aerodynamic coefficients for the model supported in the wind tunnels at various test conditions were determined. It was agreed that the drag coefficient determined in the wind tunnel would be adjusted to the aerodynamic reference conditions by making only a correction for the effects of wall interference. The wall interference correction, for this example, will be equal to the difference between the drag coefficients determined in Tunnels 4T and 16T. No correction was to be made for the support interference, since the same support was used in both tests and the aerodynamic coefficients for the unsupported model were not of interest.

Pretest discussions of the uncertainty requirements for the test resulted in the following agreements between the test personnel and the user of the data:

1. The internal strain-gage balance would have a measurement uncertainty of 0.5 percent of full scale or less for each component.

2. The ESP system would have an uncertainty for the measured differential pressure of less than 72 pascals (Pa), not including the zero drift in the ESP output produced by temperature variations.

3. Each ESP module would be monitored for temperature effects through the use of a check pressure that is measured by two pressure transducers in each ESP module and a working standard. The check pressures measured by the ESP modules would be allowed to drift ± 50 Pa, relative to the working standard, before the ESP system would be recalibrated. The ± 50 Pa would then be included as an additional bias limit in the estimation of the system uncertainty.

4. The uncertainty of the reference pressure would be less than 24 Pa.

5. The uncertainty in the model attitude would be less than 0.10 deg in angle of attack and 0.20 deg in sideslip angle.

6. The quoted uncertainties in the tunnel conditions were acceptable.

7. The uncertainty of the drag coefficient adjusted to the aerodynamic reference conditions would include an estimate of the uncertainty of the wall interference correction.

The uncertainty analysis shown in Section 4.4 should be performed prior to conducting the test using pretest estimates for the uncertainties of the error sources. The pretest uncertainty analysis performed for this example resulted in an estimated uncertainty for the drag coefficient that met the criteria requested by the user of the test data. If an unacceptable uncertainty had been estimated changes in the testing techniques or instrumentation would have been required, or the uncertainty criteria would have been relaxed before the test was conducted.

## 4.3 UNCERTAINTY OF A MEASUREMENT SYSTEM

Before the uncertainty of the data obtained during a wind tunnel test can be estimated, uncertainty estimates of the instrumentation that will be used during the test must be available. The uncertainty of an instrument can be estimated using the following four-step process:

1. Obtain the data necessary to estimate the uncertainty through an evaluation process using a working standard.
2. Evaluate any outliers for elimination from the data set.
3. Reduce the data to obtain the estimates of the bias and precision limits.
4. Document the results.

An application of the process is shown for an ESP system that consists of multiple independent channels. A discussion of the application of the methodology to systems with multiple, dependent channels is provided in Section 4.3.4.

### 4.3.1 Uncertainty Data Acquisition

The first step in the uncertainty analysis process is to obtain uncertainty evaluation data on the system. The methodology used to obtain the evaluation data can have a large effect on the magnitude and usefulness of the uncertainty estimates. The best way of obtaining the evaluation data is to perform repeated evaluations of the instrumentation against a working standard. Before acquiring the data, several important criteria must be established:

1. The range, number of increments, and cycles of data that will be obtained,

2. The extent to which the testing environment is simulated, and

3. The selection of the working standard.

The establishment of a criterion by which the evaluation data will be obtained can be developed using the following guidelines.

1. The estimated uncertainties for a system are valid only over the range for which the evaluation data are obtained. If the uncertainties are to be estimated for a system that will be used over a wide range of tests and test conditions, then evaluation data need to be obtained over the range that covers the estimated values of the measurements. However, in some instances, the magnitude of the estimated uncertainties may be smaller if they are estimated using evaluation data obtained over the range appropriate for a specific test or a small range of measurements. In this example the uncertainty analysis needs to be valid for a large range of tests and test conditions. The ESP modules in the example system contain ± 103-kPa transducers. On the basis of these conditions, the evaluation data were obtained by making repeat evaluation cycles over the ± 86 kPa range, which encompasses the expected range of measurements to be made using the system.

   The evaluation data need to be obtained at several evaluation set points over the selected range. The more set points that are used, the better the variation of the uncertainties are known over the range. However, the number of set points must be balanced against the associated cost. Based on previous experience with the ESP system, 13 set points were used which provided increments of approximately 14.3 kPa.

   The number of repeated evaluation cycles that are made will determine the degrees of freedom and the confidence level of the estimated uncertainty. An evaluation cycle is defined as a data acquisition sequence that begins at an initial evaluation set point, proceeds to slightly past one of the system limits, then proceeds to slightly past the other system limit, and back to the initial set point with data being acquired each time one of the set points is reached. This type of cycle obtains two samples at each set point (three at the initial set point) and will include any system hysteresis in the estimated uncertainty. It was recommended in Annex 2-A that for the majority of wind tunnel testing, 10 repeat samples (5 cycles) are sufficient for using a coverage factor K = 2. However, obtaining more repeated samples will increase the degrees of freedom, which increases the confidence in of the mean and standard deviation. The number of repeated samples must also be balanced against the associated cost. Since the evaluation data obtained on the ESP system are to be used to estimate an uncertainty that will be valid for many tests, an increased confidence in the mean and standard deviation was desired, so evaluation data were obtained on 14 evaluation cycles that provided up to 28 samples (up to 41 samples at the initial set point) at each set point for each channel.

2. In order for the estimated bias and precision limits to be representative of the testing process, the instrumentation system should be made to simulate the testing process and environment as closely as possible. This is normally accomplished using a two-step process:

   1. Identify the possible sources of significant errors for each device in the instrumentation system, and

   2. Allow (or force) the error sources to respond during the acquisition of the evaluation data as they would during the actual testing process. The sources of both bias and precision errors should be simulated.

   An example of forcing the inclusion of an error source is illustrated using the ESP system. As is common in many instrumentation systems, the ESP system consists of several individual devices that receive periodic calibration. The ESP system consists of ESP modules containing 48 individual pressure transducers, a working standard used to calibrate the pressure transducers, excitation supply, amplifiers, analog-to-digital converter, and computer. During testing, the pressure transducers in the ESP modules are calibrated using a 6-point calibration technique prior to their use and are recalibrated frequently during testing to compensate for zero shifts produced by temperature variations. To simulate the variations in the errors produced by the calibration of the pressure transducers, they were recalibrated between each of the evaluation cycles.

   Some error sources can be very difficult or impractical to simulate. For example, the output of the pressure transducers in the ESP modules varies with temperature. An additional bias limit and/or precision limit must be determined and included to account for the effects of the error source if the temperature and/or temperature variations cannot be simulated or eliminated. In practice, the temperature effects are quantified by using a check pressure that is applied to two transducers on each module, and a working standard. The ESP modules are recalibrated when the differences between the check pressure measured by the ESP and the working standard are greater than a small, specified value. The small, specified value is then included (root-sum-squared) into the estimated bias limit of the ESP system. The effects of some error sources can be difficult to quantify, and every effort should be made to simulate them during the acquisition of the uncertainty evaluation data.

   Error sources that were not included in the estimated uncertainty should be documented in the uncertainty analysis of the system. Listed below are error sources that are not included in the estimated uncertainty of the ESP system:

   1. Pressure lag exceeding the data acquisition delay time
   2. Undetected leaks in the pressure tubing
   3. Model orifice effects
   4. Vibration effects on the ESP module
   5. Unsteady flow effects

   Considerable effort is taken to minimize the effects of the above error sources prior to acquiring test data, and, as a result, they are deemed to be insignificant.

   When an uncertainty is estimated for a system, the experimenter must decide if data should be obtained on all of the channels in the system or only on a representative number of channels. AEDC has an inventory of approximately 70, 48-port, ± 103-kPa ESP modules, and obtaining

evaluation data on all the modules would be prohibitive in both time and cost. Through previous experience with the ESP modules, it was decided that the inventory of ESP modules would be represented by obtaining data on 5 randomly selected modules (7 percent of the inventory), which provided data on a total of 240 individual ESP pressure transducers.

3. The working standard is used to determine the reference values of the inputs to the instruments. The quality of the working standard selected should be commensurate with the uncertainty requirements for the test. For most wind tunnel tests the uncertainty of the working standard should be at least one order of magnitude less than the expected uncertainty of the instrumentation system. However, there may be occasions when the uncertainty of the working standard is not critical and therefore need not meet this criterion. However, a requirement that should not be overlooked is that the uncertainty of the working standard be traceable to a national or international standards laboratory.

### 4.3.2 Outlier Detection

Once the uncertainty evaluation data have been obtained, the data must be examined for spurious or outlier values. The process used to acquire the evaluation data may have been subjected to a temporary or intermittent malfunction which would not occur during the testing process. The errors produced by such events should not be included in the uncertainty analysis. Several methods are available for detecting outliers. Chauvenet's criterion, described in Annex 2-B, is favored because the probability of rejecting a good point decreases as the number of samples increases. An example of how the technique can be implemented is shown using the evaluation data' obtained on one of the ESP system channels. The evaluation data provided in Table 4.1 were obtained at the 86-kPa set point. The data are assumed to have normal (Gaussian) distributions, even though the data in Table 4.1 do not appear to have a normal distribution because of the small sample size. The assumption is reasonable since larger data sets previously obtained on this type of device have been shown to possess a normal distribution.

The first step in identifying the outliers is to calculate the mean and standard deviation of the sample [Eqs. (2-6) and (2-5)]. Under ideal circumstances, the evaluation set points should be accurately repeated; however, this is not often practical and, in this example, a ± 500-Pa variation in the set point was allowed. To eliminate the variation in the set points from the calculation of the sample mean and standard deviation, the individual sample errors ($E_i$) are used. The individual sample errors are the differences between the evaluation pressure as measured by the transducer being evaluated, $p_{X_i}$, and working standard, $WS_i$.

$$E_i = p_{X_i} - WS_i \tag{4-1}$$

The individual sample errors are provided in Table 4.1 and are used to calculate the mean error of the sample, $\bar{E}$,

$$\bar{E} = \frac{1}{N}\sum_{i=1}^{N} E_i = 1.26 \text{ Pa} \tag{4-2}$$

and the standard deviation of the individual sample errors, $S_E$,

$$S_E = \pm\left(\sum_{i=1}^{N}\frac{(E_i - \bar{E})^2}{N-1}\right)^{\frac{1}{2}} = \pm 20.54 \text{ Pa} \tag{4-3}$$

The outlier method determines if a value is a possible outlier by comparing the difference between the mean and each value with the outlier criteria. Most of the time it is more efficient to calculate the range or bounds within which the individual values must lie. For our example, the bounds on the maximum individual error are calculated as

Table 4.1 ESP System Calibration Data

The evaluation data were obtained on one channel (an individual pressure transducer) of the ESP system at an evaluation set point of 86 kPa. The evaluation pressure was changed between the consecutive points in a cycle and was allowed to vary ±500 Pa in magnitude from the nominal set point value.

| CYCLE | POINT | PRESSURE MEASURED BY THE WORKING STANDARD (WS, Pa) | PRESSURE MEASURED BY THE ESP THE ESP CHANNEL ($p_x$, Pa) | INDIVIDUAL SAMPLE ERRORS (E, Pa) |
|---|---|---|---|---|
| 1 | 7 | 86140.43 | 86162.66 | 22.23 |
| 1 | 8 | 86019.05 | 86036.36 | 17.31 |
| 2 | 7 | 86047.30 | 86025.45 | -21.86 |
| 2 | 8 | 86157.43 | 86134.04 | -23.39 |
| 3 | 7 | 86006.84 | 86003.81 | -3.04 |
| 3 | 8 | 86143.30 | 86143.97 | 0.67 |
| 4 | 7 | 86034.85 | 86025.13 | -9.72 |
| 4 | 8 | 86265.16 | 86276.60 | 11.44 |
| 5 | 7 | 86316.63 | 86339.57 | 22.94 |
| 5 | 8 | 86154.08 | 86166.67 | 12.60 |
| 6 | 7 | 86183.29 | 86180.38 | -2.91 |
| 6 | 8 | 86282.87 | 86292.82 | 9.95 |
| 7 | 7 | 86100.92 | 86022.69 | **-78.24 |
| 7 | 8 | 85975.24 | 85959.53 | -15.70 |
| 8 | 7 | 86081.78 | 86102.46 | 20.68 |
| 8 | 8 | 86201.96 | 86214.37 | 12.42 |
| 9 | 7 | 85949.39 | 85940.31 | -9.09 |
| 9 | 8 | 86250.55 | 86251.29 | 0.74 |
| 10 | 7 | 86267.08 | 86270.36 | 3.28 |
| 10 | 8 | 85963.51 | 85975.41 | 11.89 |
| 11 | 7 | 85765.05 | 85755.88 | -9.17 |
| 11 | 8 | 86018.34 | 86018.30 | -0.03 |
| 12 | 7 | 85957.28 | 85969.42 | 12.14 |
| 12 | 8 | 86082.97 | 86094.83 | 11.86 |
| 13 | 7 | 85795.45 | 85819.15 | 23.70 |
| 13 | 8 | 86164.13 | 86184.87 | 20.74 |
| 14 | 7 | 85847.17 | 85840.57 | -6.60 |
| 14 | 8 | 86026.47 | 86026.88 | 0.40 |

** INDICATES THE OUTLIER THAT WAS IDENTIFIED USING CHAUVENET'S OUTLIER TECHNIQUE, EXAMINED, AND ELIMINATED FROM THE DATA SET.

$$\pm E_{MAX} = \bar{E} \pm \tau S_E \tag{4-4}$$

where $\tau$ is Chauvenet's criterion.

The individual sample errors that are outside the boundaries set by $E_{MAX}$ need to be evaluated for possible elimination from the data set. The value for $\tau$ for our sample size can be determined using Eq. (2-B-3), which yields a value for $\tau$ of 2.37 and results in boundaries of:

$$+E_{MAX} = 1.26 + 2.37(20.54) = 49.94 \text{ Pa} \tag{4-5}$$

$$-E_{MAX} = 1.26 - 2.37(20.54) = -47.42 \text{ Pa} \tag{4-6}$$

Based on the boundaries set for $E_{MAX}$, the individual error for Cycle 7, Point 7 is a possible outlier and should be examined. During the evaluation of the ESP system there were occasions when the pressure applied to a given transducer did not achieve equilibrium in the allotted time because of the large pressure change. Since the rate of change in the pressure sensed by a pressure transducer is small during testing, the point is eliminated from the sample data set. Eliminating the outlier yields new values for the number of samples, sample mean, and standard deviation.

$$\bar{E} = 4.20 \text{ Pa}, \; S_E = \pm 13.64 \text{ Pa}, \text{ and } N = 27 \tag{4-7}$$

### 4.3.3 Uncertainty of an Instrumentation System Calibration

A calibration is conducted to exchange the large bias of the uncalibrated instrument with the hopefully smaller uncertainty of the working standard and the error associated with the calibration process. Once the system has been calibrated and the results implemented, the uncertainty evaluation data can be obtained. The equations developed in this section are used to estimate the uncertainty of a calibration, at a single evaluation set point, for either an instrument or a single channel of an instrumentation system. Since the calibration of the system has accounted for any large bias errors in the system, E is comprised of small known biases which are too difficult or costly to correct, and/or small unknown biases and is therefore assumed to possess an equal probability of being negative or positive valued.

The uncertainty of the working standard was determined by the AEDC metrology laboratory.

$$U_{WS} = \pm[24.42 + 0.000075|p_X|] \text{ Pa} \tag{4-8}$$

The uncertainty of the working standard is fixed for each set point and is propagated into the calibration uncertainty as a bias limit. The uncertainty of the working standard is combined with the mean of the individual sample errors, $\bar{E} = 4.20$ Pa [Eq. (4-7)], to calculate the estimated bias limit for the ESP calibration. At an evaluation set point pressure of 86 kPa this yields:

$$U_{WS} = \pm[24.42 + 0.000075|p_X|] = \pm[24.42 + 0.000075|86000.00|] = \pm 30.87 \text{ Pa} \tag{4-9}$$

$$B_{cal_{86}} = \pm\left(\bar{E}^2 + U_{WS}^2\right)^{\frac{1}{2}} = \pm\left(4.20^2 + 30.87^2\right)^{\frac{1}{2}} = \pm 31.15 \text{ Pa} \tag{4-10}$$

The uncertainty of the calibration is an estimate of the uncertainty of the mean error of the calibration. The precision limit of the mean is determined using Eqs. (2-4) and (2-7) and the values $S_E = 13.64$ and $N = 27$ [Eq. (4-7)], and $K = 2$.

$$P_{cal_{86}} = \pm K S_E = \pm 2(13.64) = \pm 27.28 \text{ Pa} \tag{4-11}$$

$$P_{\bar{E}_{86}} = \pm\frac{P_{cal_{86}}}{\sqrt{N}} = \pm\frac{27.28}{\sqrt{27}} = \pm 5.25 \text{ Pa} \tag{4-12}$$

The bias limit and the precision limit of the mean are combined [Eq. (2-9)] to calculate the estimated uncertainty of the calibration, $U_{cal}$, at an evaluation set point of 86 kPa.

$$U_{cal_{86}} = \pm\left(B_{cal_{86}}^2 + P_{\bar{E}_{86}}^2\right)^{\frac{1}{2}} = \pm\left(31.15^2 + 5.25^2\right)^{\frac{1}{2}} = \pm 31.59 \text{ Pa} \tag{4-13}$$

Now that the uncertainty of the ESP system has been estimated, the uncertainty of a value measured by the system during the testing process can be estimated. The uncertainty associated with the system calibration will be constant until the system is recalibrated. Therefore, even though the calibration uncertainty was calculated using bias and precision limits, it becomes fixed as a bias limit when it is used to estimate the uncertainty of a value measured by the system. The precision limit of the system during the testing process can be estimated from either the reproducibility [4.2] of data obtained during testing, or the precision limit of the evaluation data can be used as an estimate of the precision limit. Since the evaluation data obtained on the ESP system were a good approximation of the data that would be obtained during the testing process, the precision limit of the evaluation data is used as an estimate of the testing precision limit.

The estimated calibration uncertainty, now fixed as a bias limit, is combined [Eq. (2-3)] with the estimated testing precision limit to calculate the estimated uncertainty of a single measurement made at a pressure of *86* kPa.

$$U_{86} = \pm\left(U_{cal_{86}}^2 + P_{cal_{86}}^2\right)^{\frac{1}{2}} = \pm\left(31.59^2 + 27.282\right)^{\frac{1}{2}} = \pm 41.74 \text{ Pa} \qquad (4\text{-}14)$$

The uncertainties estimated above are valid for one particular channel of the ESP system at a pressure of *86* kPa. The same methods are applied to each set point and channel in the system. The calibration uncertainty and precision limits for each set point and channel are then represented by curve fits verses the set points which cover the entire calibration range. Using the curve fits will allow the calibration uncertainty and precision limits and thus the measurement uncertainty to be determined for measured values which fall within the calibration range. For systems with a relatively small number of channels, using and maintaining the curve fits for each channel may be feasible. However, as the number of channels in a system increases, the task of maintaining and utilizing the curve fits for each channel becomes more and more difficult. At some point it becomes more practical to estimate a calibration uncertainty and precision limit that encompass all of the channels of the system. Values for the calibration uncertainty and precision limits that are applicable for all of the channels in a system can be determined using the methodology provided in Annex 4-A. The equations in Annex 4-A are a revision of the equations reported in the AIAA paper 92-3953, "Development of an Uncertainty Methodology for Multiple-Channel Instrumentation Systems" [4.3]. Applying the equations in Annex 4-A to the ESP system and curve fitting the resulting bias and precision limits and calibration uncertainty with the set points produced the equations for the uncertainties documented in Table 4.2. The equations are provided for several values of an allowable zero drift. Based on the criteria established for the ESP system, the estimated uncertainties are valid for any test that uses any number of ESP modules selected from the inventory until such time as modifications are made which will affect the system uncertainty.

### 4.3.4 Discussion of Systems with Multiple Dependent Channels

The most common multiple, dependent channel system used in wind tunnel testing is the internal strain-gage balance. The interdependency of the channels arises from mechanical coupling because the balance design requirements do not allow sufficient flexibility to prevent one load vector from introducing stresses in another direction. Determination of the appropriate bias and precision limits that are applicable for any load combination is both difficult and expensive. Many calibration rigs cannot load multiple components simultaneously. Without combination loadings, only the primary sensitivities and the zeroth-order interactions can be determined which, for some balances, produces rather inaccurate results. One is thus forced to either ignore the interaction biases or estimate their magnitude. For calibration rigs that can be used to perform multi-component loadings, the bias terms caused by interactions can be estimated by maintaining various constant loads on the other components while varying the loads applied to one component. This results in a six-dimensional problem rather than a one-dimensional problem. For simplicity, consider a single load combination. Assume that the load combination is applied N times with N outputs for each component. The most probable output for each gage is the average of the N outputs. The bias term for each component is the difference between the average load calculated for that component using the output from each gage in the data reduction algorithm and the applied load for that channel. The precision term is determined in the usual manner by considering the outputs for each loading. The estimated uncertainties are valid only for the single load combination. With enough load combinations, two six-dimensional hypersurfaces could be constructed to represent the bias and precision terms for that balance and the load combination space. A much more practical approach, however, is to examine only the critical load combinations anticipated for the test to be conducted, or to return the balance to the calibration rig after the specific critical load combinations have been measured. Data from repeated combined-load cycles can be used to estimate the calibration uncertainty and precision limits for each balance component through the use of the differences between the applied loads and the loads calculated using the calibration matrix and data reduction program.

### 4.3.5 Uncertainty Evaluation of Other Test Systems

The other instrumentation used on the example test consisted of:

1. Standard Balance Data Acquisition System
2. Model Attitude Positioning System
3. Strain-Gage Balance
4. Standard Tunnel Condition Instrumentation

The uncertainties for the above measurement systems were estimated in a manner similar to that used for the ESP system. The estimated uncertainties for the systems are provided in Table 4.2.

### 4.3.6 Estimated Uncertainties of Various Parameters

There are many parameters that are either measured, calculated, or defined and used to reduce the measured data into the desired coefficients. A discussion of the methods used to determine the estimated uncertainties of each parameter is beyond the scope of this example. However, the uncertainties of the parameters used in the example are provided in Table 4.3. Some of the uncertainties were estimated from previous experience while others are estimated using the methods described in this example. As a rule, the more significant an error source is, the greater should be the effort spent in estimating the associated uncertainties. Note that if a parameter is assigned a value, such as a reference area and/or length, no uncertainty is introduced into the coefficients since such values have no bias or precision errors.

## 4.4 DATA REDUCTION AND ESTIMATED UNCERTAINTY OF THE FOREBODY DRAG COEFFICIENT

The objective of the tests was to acquire data with which to evaluate wall interference correction methods by differencing like parameters from the tests conducted in Tunnels 4T and 16T. This objective was attained by determining the aerodynamic coefficients for the model supported in the wind tunnel, at the various test conditions, and estimating their uncertainty. The uncertainty analysis is presented for only the test conducted in Tunnel 4T. After considering the potential error sources depicted in Fig. 1.2, the following were judged to make an insignificant contribution to the uncertainty of the wind tunnel data: flow spatial nonuniformity (spatial flow calibration of each tunnel flow showed gradients equivalent to less than 0.05 deg in flow angles), unsteadiness (raw data signal filtered and integrated to average short-term variations), humidity (flow dewpoint less than static temperature), and buoyancy (tunnel calibrations show negligible gradients at the model locations), The contributions of the significant error sources are discussed in the remainder of this example. Note that the uncertainties produced by wall and support interference are not considered until the adjustments are made to correct the data to the aerodynamic reference condition in Section 4.5.

The drag coefficient has been selected as a representative parameter to illustrate the continued application of the uncertainty methodology. The test conditions, measured forces and pressures, and model parameters for the chosen data point are:

Set point Mach number, $M = 0.95$
Total pressure, $p_T = 67690.35$ Pa
Plenum static pressure, $p_C = 38216.38$ Pa
Reference area, $A = 0.20439$ m$^2$
Base area, $A_B = 0.005723$ m$^2$
Model weight, $W_A = W_N = 111.205$ N
Alpha, $\alpha = 4.00$ deg
Beta, $\beta = 0.00$ deg

Gross axial force, $F_{AG} = 181.924$ N
Gross normal force, $F_{NG} = 1{,}666.434$ N
Measured differential base pressures, $p_{B_M}$:
$p_{B_{M_1}} = -62148.24$ Pa
$p_{B_{M_2}} = -61669.44$ Pa
$p_{B_{M_3}} = -61669.44$ Pa
$p_{B_{M_4}} = -61573.68$ Pa
Reference pressure, $p_{REF} = 98154.00$ Pa

Attitude at which the balance gage zeros were obtained: $\alpha_{s_0} = 0.00$ deg and $\phi_{s_0} = 0.0$ deg

**Table 4.2 Estimated System Calibration Uncertainties**

| DESCRIPTON | BIAS LIMIT | PRECISION LIMIT | ?, N | CALIBRATION UNCERTAINTY* | CALIBRATION RANGE | MEASURING DEVICE | CALIBRATION /ORKING STANDARI |
|---|---|---|---|---|---|---|---|
| ESP System<br>Measured Differential Pressure, $p_X$ (Pa)<br><br>No zero drift<br>±25 Pa zero drift<br>*i50* Pa zero drift<br>±100 Pa zero drift | $\pm[A0 + A1p_X + A2p_X^2]$<br><br>A0 A I A2<br>22.22 $2.20\cdot10^{-5}$ $1.2\cdot10^{-9}$<br>32.56 $1.80\cdot10^{-5}$ $9.2\cdot10^{-10}$<br>57.94 $1.28\cdot10^{-5}$ $5.4\cdot10^{-10}$<br>112.00 $5.49\cdot10^{-6}$ $2.9\cdot10^{-10}$ | $\pm[39.50 - 9.8\cdot10^{-5}p_X + 8.81\cdot10^{-10}p_X^2]$ | ?, 28 | $\pm[A0 + A1p_X + A2p_X^2]$<br><br>A0 A I A2<br>22.89 $1.60\cdot10^{-5}$ $4.3\cdot10^{-10}$<br>33.09 $1.30\cdot10^{-5}$ $8.9\cdot10^{-10}$<br>**58.22** $8.42\cdot10^{-6}$ $5.4\cdot10^{-10}$<br>112.00 $3.85\cdot10^{-6}$ $3.0\cdot10^{-10}$ | ±86.2 kPa | 'recision Systems Inc. ESP module | Sonix® and Ruska® absolute pressure transducers |
| Model Support System Pitch Angle, $\alpha_S$ (deg) | ± 0.023 | ± 0.018 | ?, 30 | ± 0.023 | -7 to 27 deg | CCC Resolver | Digital inclinometer |
| Roll Angle, $\phi_S$ (deg) | ± 0.087 | ± 0.140 | ?, 30 | ± 0.091 | ±183 deg | North Atlantic Resolver | Heidenhain angular encoder |
| Reference Pressure $p_{REF}$ (Pa) | $:[16.76 + 1.0\cdot10^{-4}\|98154 - p_{REF}\|]$ | $\pm[2.87 + 2.2\cdot10^{-5}p_{REF}]$ | ?, 34 | $[16.76 + 1.0\cdot10^{-4}\|98154 - p_{REF}\|]$ | 0 to 167.6 kPa | Sonix® absolute ressure transduce | Ruska® absolute pressure transducersi |
| Test Conditions Delta Mach Number, DM | $\pm[1.132\cdot10^{-3} - 2.533\cdot10^{-3}M + 4.166\cdot10^{-3}M^2 - 2.759\cdot10^{-3}M^3 + 7.968\cdot10^{-4}M^4]$ | $\pm[6.983\cdot10^{-4} + 6.070\cdot10^{-4}M + 7.791\cdot10^{-3}M^2 - 5.418\cdot10^{-4}M^3 + 1.287\cdot10^{-4}M^4]$ | ?, 34 | $\pm[1.313\cdot10^{-3} - 1.830\cdot10^{-3}M + 4.867\cdot10^{-3}M^2 - 3.443\cdot10^{-3}M^3 + 9.214\cdot10^{-4}M^4]$ | Mach Number 0.20 - 2.00 | Sonix® absolute ressure transduce | Ruska® absolute pressure transducers |
| Plenum Static Pressure, $p_C$ (Pa) | $\pm[16.76 + 1.0\cdot10^{-4}\|98154 - p_C\|]$ | $\pm[2.87 + 2.2\cdot10^{-5}p_C]$ | ?, 34 | $\pm[16.76 + 1.0\cdot10^{-4}\|98154 - p_C\|]$ | 0 to 167.6 kPa | Sonix® absolute ressure transduce | Ruska® absolute pressure transducers |
| Stilling Chamber Total Pressure, $p_T$ (Pa) | $\pm[16.76 + 1.0\cdot10^{-4}\|98154 - p_T\|]$ | $\pm[2.87 + 2.2\cdot10^{-5}p_T]$ | ?, 34 | $\pm[16.76 + 1.0\cdot10^{-4}\|98154 - p_T\|]$ | 0 to 167.6 kPa | Sonix® absolute ressure transduce | Ruska® absolute pressure transducers |
| Strain-gage Balance 6-1.50-1800-1.12M $F_{A_M}$ (N) | ± 0.117 | ± 2.580 | ?, 3( | ± 0.485 | ±700N | Sixcomponent nternal strain-gage balance | Dead weights |
| $F_{N_M}$ (N) | ± 0.320 | ±10.930 | ?, 3( | ± 2.619 | ±4500 N | | |

*Note that the bias limit for a value measured by a calibrated system is equal to the Calibration Uncertainty for that system. For the systems shown here, the calibration precision index can be used as an estimate of the precision limit during testing.

Table 4.3 Estimated Uncertainties of Test Parameters

| PARAMETER DESCRIPTION | BIAS LIMIT | PRECISION LIMIT | K | UNCERTAINTY | NOMINAL VALUE | TEST CONDITIONS | MODEL CONFIGURATION |
|---|---|---|---|---|---|---|---|
| Model Tare Weights (N) | | | | | | | |
| $W_A$ | 0.008 | 6.530 | 2 | 6.530 | 111.205 | NA | All Configurations |
| $W_N$ | 0 | 7.729 | 2 | 7.729 | 111.205 | NA | All Configurations |
| Base area, $A_B$ ($m^2$) | $7.07 \cdot 10^{-7}$ | — | 2 | $7.07 \cdot 10^{-7}$ | 0.005723 | NA | All Configurations |
| Reference Area. A ($m^2$) | — | — | 2 | — | 0.20439 | NA | All Configurations |
| Test Conditions | | | | | | | |
| M | 0.0019 | 0.0001 | 2 | 0.0019 | 0.95 | M=0.95, q=24 kPa | All Configurations |
| $p_T$ (Pa) | 19.81 | 4.36 | 2 | 20.28 | 67.7 kPa | | |
| $p_C$ (Pa) | 22.75 | 3.71 | 2 | 23.05 | 38.2 kPa | | |
| p (Pa) | 78.85 | 3.70 | 2 | 78.94 | 37.9 kPa | | |
| q (Pa) | 44.89 | 3.53 | 2 | 45.03 | 23.9 kPa | | |
| Model Altitude | | | | | | | |
| Angle of Attack, $\alpha$ (deg) | 0.023 | 0.018 | 2 | 0.029 | 4.0 deg | M=0.95, q=24 kPa | All Configurations |
| Sideslip Angle, $\beta$ (deg) | 0.006 | 0.010 | 2 | 0.012 | 0 deg | | |
| Base Pressure | | | | | | | |
| $p_B$ (Pa) | 61.38 | 37.20 | 2 | 71.77 | 36.4 kPa | M=0.95, q=24 kPa | All Configurations |
| $\bar{p}_B$ (Pa) | 32.56 | 18.48 | 2 | 37.44 | 36.4 kPa | | |
| Forebody Drag Coefficient, $C_D$ | | | | | | | |
| Wind Tunnel | 0.00016 | 0.00056 | 2 | 0.00058 | 0.0592 | M=0.95, q=24 kPa | All Configurations |
| Wall Interference Correction | 0.00002 | 0.00079 | 2 | 0.00079 | 0.0098 | " | " |
| Aerodynamic Reference | 0.00081 | 0.00056 | 2 | 0.00099 | 0.0690 | " | " |

A recommendation made in Chapter 2 stated that unless there are overriding circumstances a coverage factor, K, of 2 should be used in estimating uncertainty. Consistant with that recommendation, each of the bias limits, B, and precision limits, P, shown in this example has been estimated using K = 2. In the following sections most of the equations for the sensitivity coefficients (partial derivatives) are quite complex and are therefore shown in symbolic form. The actual equations and calculations of the sensitivity coefficients are contained in Annex 4-B.

### 4.4.1 Tunnel Conditions

Before the estimated uncertainty of the drag coefficient can be calculated, the uncertainties of the test conditions must be estimated. In Tunnel 4T the free-stream Mach number, static pressure, and dynamic pressure are calculated using measurements of the stilling chamber total pressure and the static pressure in the plenum chamber surrounding the test section. This method requires that delta Mach numbers, DM, be determined for each Mach number during the tunnel calibration. The delta Mach number corresponding to the set point Mach number is then added to the Mach number calculated using the stilling chamber total pressure and the static pressure in the plenum to determine the test section free-stream Mach number.

$$M = \left(5.0\left[\left(\frac{p_T}{p_C}\right)^{\frac{2}{7}} - 1.0\right]\right)^{\frac{1}{2}} + DM = \left(5.0\left[\left(\frac{67690.35}{38216.38}\right)^{\frac{2}{7}} - 1.0\right]\right)^{\frac{1}{2}} + 0.0081 = \mathbf{0.950} \qquad (4\text{-}15)$$

The free-stream Mach number is then used to calculate the free-stream static and dynamic pressures using the standard equations for isentropic flow with a perfect gas.

Static pressure,

$$p = p_T(1.0 + 0.2M^2)^{-3.5} = 67690.35(1.0 + 0.2[0.950]^2)^{-3.5} = \mathbf{37870.04 Pa} \qquad (4\text{-}16)$$

Dynamic pressure,

$$q = 0.70p(M^2) = 0.70(37870.04)(0.950)^2 = 23924.40 \text{ Pa} \tag{4-17}$$

The uncertainties of the Mach number and dynamic pressure are determined using the partial derivatives of the above equations with respect to the independent parameters $p_T$, $p_C$, and DM [Eqs. (2-16) and (2-13)]. The uncertainties for $p_T$, $p_C$, and DM are found in Table 4.2. Because the values for $p_T$ and $p_C$ were measured using calibrated systems, the calibration uncertainty is now fixed and is propagated as a bias limit for measured values. The evaluation data were acquired in a manner that simulated the testing process; therefore, the precision limit estimated for the uncertainty evaluation is used as an estimate of the precision limit for the testing process. The calibration uncertainty for DM is also propagated as a bias limit in calculating the bias limits for M, p, and q, and since DM is a constant, there is no associated precision limit. The statements concerning the bias and precision limits for $p_T$, $p_C$, and DM will apply throughout the remainder of this chapter.

The pressure transducers used to measure the stilling chamber total pressure and the plenum static pressure were calibrated against the same working standard, which results in a correlated bias effect [Eq. (2-16)] which will need to be considered when determining the bias limits for M, p, and q. The correlated bias limits for $p_T$ and $p_C$ are limited to the uncertainty of the working standard they were calibrated against. The uncertainty of the working standard as estimated by the AEDC metrology lab is

$$U_{WS} \approx \pm[4.79 + 0.00003(p_X)], \text{ where } p_X \text{ is an absolute pressure.} \tag{4-18}$$

Therefore, the correlated bias limits for $p_T$ and $p_C$ are

$$B'_{pT} = \pm[4.79 + 0.00003(p_T)] = \pm[4.79 + 0.00003(67690.35)] = k6.82 \text{ Pa} \tag{4-19}$$

$$B'_{pC} = \pm[4.79 + 0.00003(p_C)] = \pm[4.79 + 0.00003(38216.38)] = \pm 5.94 \text{ Pa} \tag{4-20}$$

$$B_M = \pm\left(\left[\frac{\partial M}{\partial p_T} B_{pT}\right]^2 + \left[\frac{\partial M}{\partial p_C} B_{pC}\right]^2 + \left[\frac{\partial M}{\partial DM} B_{DM}\right]^2 + 2\frac{\partial M}{\partial p_T}\frac{\partial M}{\partial p_C} B'_{pT} B'_{pC}\right)^{\frac{1}{2}}$$

$$= \pm\left(\left[1.319*10^{-5}(19.81)\right]^2 + \left[-2.337*10^{-5}(22.75)\right]^2 + \left[1(0.00177)\right]^2 + 2\left[1.319*10^{-5}\right]\left[-2.337*10^{-5}\right][6.82][5.94]\right)^{\frac{1}{2}} = \pm 0.0019 \tag{4-21}$$

$$P_M = \pm\left(\left[\frac{\partial M}{\partial p_T} P_{PT}\right]^2 + \left[\frac{\partial M}{\partial p_C} P_{PC}\right]^2\right)^{\frac{1}{2}}$$

$$= \pm\left(\left[1.319*10^{-5}(4.36)\right]^2 + \left[-2.337*10^{-5}(3.71)\right]^2\right)^{\frac{1}{2}} = \pm 0.0001 \tag{4-22}$$

$$B_p = \pm\left(\left[\frac{\partial p}{\partial p_T} B_{pT}\right]^2 + \left[\frac{\partial p}{\partial p_C} B_{pC}\right]^2 + \left[\frac{\partial p}{\partial DM} B_{DM}\right]^2 + 2\frac{\partial p}{\partial p_T}\frac{\partial p}{\partial p_C} B'_{pT} B'_{pC}\right)^{\frac{1}{2}}$$

$$= \pm\left(\left[-0.003344(19.81)\right]^2 + \left[0.9969(22.75)\right]^2 + \left[-42665.95(0.00177)\right]^2 + 2\left[-0.003344\right]\left[0.9969\right][6.82][5.94]\right)^{\frac{1}{2}} = k78.85 \text{ Pa} \tag{4-23}$$

$$P_p = \pm\left(\left[\frac{\partial p}{\partial p_T} P_{pT}\right]^2 + \left[\frac{\partial p}{\partial p_C} P_{pC}\right]^2\right)^{\frac{1}{2}}$$

$$= \pm\left(\left[-0.003344(4.36)\right]^2 + \left[0.9969(3.71)\right]^2\right)^{\frac{1}{2}} = \pm 3.70 \text{ Pa} \tag{4-24}$$

$$B_q = \pm\left(\left[\frac{\partial q}{\partial p_T} B_{p_T}\right]^2 + \left[\frac{\partial q}{\partial p_C} B_{p_C}\right]^2 + \left[\frac{\partial q}{\partial DM} B_{DM}\right]^2 + 2\frac{\partial q}{\partial p_T}\frac{\partial q}{\partial p_C} B'_{p_T} B'_{p_C}\right)^{\frac{1}{2}}$$

$$= \pm\left([0.6623(19.81)]^2 + [-0.5470(22.75)]^2 + [23412.94(0.00177)]^2 + 2[0.6623][-0.5470][6.82][5.94]\right)^{\frac{1}{2}} = \pm 44.89 \text{ Pa} \quad (4\text{-}25)$$

$$P_q = \pm\left(\left[\frac{\partial q}{\partial p_T} P_{p_T}\right]^2 + \left[\frac{\partial q}{\partial p_C} P_{p_C}\right]^2\right)^{\frac{1}{2}}$$

$$= \pm\left([0.6623(4.36)]^2 + [-0.5470(3.71)]^2\right)^{\frac{1}{2}} = \pm 3.53 \text{ Pa} \quad (4\text{-}26)$$

The estimated bias and precision limits are then combined [Eq. (2-9)] to estimate the uncertainty of **M**, p, and q.

$$U_M = \pm\left(B_M^2 + P_M^2\right)^{\frac{1}{2}} = \pm\left(0.0019^2 + 0.0001^2\right)^{\frac{1}{2}} = \pm 0.0019 \quad (4\text{-}27)$$

$$U_p = \pm\left(B_p^2 + P_p^2\right)^{\frac{1}{2}} = \pm\left(78.85^2 + 3.70^2\right)^{\frac{1}{2}} = \pm 78.94 \text{ Pa} \quad (4\text{-}28)$$

$$U_q = \pm\left(B_q^2 + P_q^2\right)^{\frac{1}{2}} = \pm\left(44.89^2 + 3.53^2\right)^{\frac{1}{2}} = \pm 45.03 \text{ Pa} \quad (4\text{-}29)$$

After seeing the complexity of the equations used to estimate the uncertainties for the Mach number, static pressure, and dynamic pressure, it would be very tempting to determine the partial derivatives with respect to the parameters that are used to calculate them. However, that can result in incorrect values for the estimated uncertainty. Examples of how this practice affects the uncertainty of q and $C_{D_F}$ are presented in Annex 4-C.

### 4.4.2 Model Attitude

The model/balance was supported by a sting which entered through the aft end of the generic fuselage. The sting was supported by the standard model attitude positioning system which consists of pitch and roll mechanisms. The model attitude is set by pitching and rolling the model to an orientation which corresponds to the desired attitude. For this test the model attitude was determined in the stability axis system (Alpha and Beta). The following angles must be considered in the order in which they physically occur to correctly calculate the model attitude:

a. Tunnel flow angles in pitch and yaw.
b. Support system pitch ($\alpha_s$) angle.
c. Deflection of the support mechanism in pitch, yaw, and roll produced by the gross forces and moments.
d. Deflection of the balance in pitch due to the weight of the sting and balance.
e. Support system roll ($\phi_s$) angle.
f. Gravity axis-to-balance axis incidence angles in pitch, yaw, and roll.
g. Sting and balance elastic deflection angles in pitch, yaw, and roll produced by the gross forces and moments.
h. Balance axis-to-model axis incidence angles in pitch, yaw, and roll.

To simplify this example, only the support system angles are considered. For an actual test all of the error sources associated with all of the above angles are considered. The methods demonstrated here should be applied to the actual equations used to determine the model attitude in the desired axis system.

For this simplified example the following equations are used to calculate the model attitude in the stability axis system.

$$\text{Alpha, } a = \text{ArcTan}\left[\text{Tan}(\alpha_s)\text{Cos}(\phi_s)\right] \tag{4-30}$$

$$\text{Beta, } \beta = \text{ArcSin}\left[\text{Sin}(\alpha_s)\text{Sin}(\phi_s)\right] \tag{4-31}$$

Solving these equations for $a = 4.00$ and $\beta = 0.00$ results in the support system pitch, $a,$, and roll, $\phi_s$, angles.

$$a, = 4.00 \text{ deg and } \phi_s = 0.0 \text{ deg} \tag{4-32}$$

The estimated uncertainties of $a$ and $\beta$ are determined using the estimated uncertainties of $\alpha_s$ and $\phi_s$ and the partial derivatives of Eqs. (4-30) and (4-31) with respect to $\alpha_s$ and **4,** [Eqs. (2-16) and (2-13)]. The uncertainties for $\alpha_s$ and $\phi_s$ can be found in Table 4.2. The pitch and roll angles were measured using calibrated systems and therefore, calibration uncertainty is propagated as a bias limit for measured values. Also, the system performs virtually identically during both the evaluation and testing processes; therefore the precision limit estimated for the uncertainty evaluation should be a very good estimate of the precision limit during testing. Note that the bias and precision limits for angles must be in radians when used in calculations. The statements concerning the bias and precision limits for $\alpha_s$ and $\phi_s$ will apply throughout the remainder of this chapter.

$$B_\alpha = \pm\left(\left[\frac{\partial\alpha}{\partial\alpha_s}B_{\alpha_s}\right]^2 + \left[\frac{\partial\alpha}{\partial\phi_s}B_{\phi_s}\right]^2\right)^{\frac{1}{2}}$$

$$= \pm\left(\left[(1)0.00040\right]^2 + \left[(0)0.00159\right]^2\right)^{\frac{1}{2}} = \pm 0.00040 \text{ radians } (0.023 \text{deg}) \tag{4-33}$$

$$P_\alpha = \pm\left(\left[\frac{\partial\alpha}{\partial\alpha_s}P_{\alpha_s}\right]^2 + \left[\frac{\partial\alpha}{\partial\phi_s}P_{\phi_s}\right]^2\right)^{\frac{1}{2}}$$

$$= \pm\left(\left[(1)0.00031\right]^2 + \left[(0)0.00244\right]^2\right)^{\frac{1}{2}} = \pm 0.00031 \text{ radians } (0.018 \text{deg}) \tag{4-34}$$

$$B_\beta = \pm\left(\left[\frac{\partial\beta}{\partial\alpha_s}B_{\alpha_s}\right]^2 + \left[\frac{\partial\beta}{\partial\phi_s}B_{\phi_s}\right]^2\right)^{\frac{1}{2}}$$

$$= \pm\left(\left[(0)0.00040\right]^2 + \left[(0.06959)0.00159\right]^2\right)^{\frac{1}{2}} = \pm 0.00011 \text{ radians } (0.006 \text{ deg}) \tag{4-35}$$

$$P_\beta = \pm\left(\left[\frac{\partial\beta}{\partial\alpha_s}P_{\alpha_s}\right]^2 + \left[\frac{\partial\beta}{\partial\phi_s}P_{\phi_s}\right]^2\right)^{\frac{1}{2}}$$

$$= \pm\left(\left[(0)0.00031\right]^2 + \left[(0.06959)0.00244\right]^2\right)^{\frac{1}{2}} = \pm 0.00017 \text{ radians } (0.010 \text{ deg}) \tag{4-36}$$

The estimated bias and precision limits for the model attitude angles are then combined [Eq. (2-9)] to calculate the estimated uncertainty in $a$ and $\beta$.

$$U_\alpha = \pm\left(B_\alpha^2 + P_\alpha^2\right)^{\frac{1}{2}} = \pm\left(0.00040^2 + 0.00031^2\right)^{\frac{1}{2}} = \pm 0.00051 \text{ radians } (0.029 \text{deg}) \tag{4-37}$$

$$U_\beta = \pm\left(B_\beta^2 + P_\beta^2\right)^{\frac{1}{2}} = \pm\left(0.00011^2 + 0.00017^2\right)^{\frac{1}{2}} = \pm 0.00020 \text{ radians } (0.011 \text{ deg}) \tag{4-38}$$

### 4.4.3 Measured Gross Axial and Normal Forces

The loads acting on the balance are a combination of the aerodynamic loads and the weight of the model (and a part of the balance). The balance calibration matrix used at AEDC is determined using a non-linear math model with the origin defined by gage voltages of zero and an unloaded balance. Experimental techniques vary, but at AEDC the balance is loaded with the weight of the model (initial loads) when the balance gage readings are zeroed (wind-off zeros). Therefore, the zero balance gage voltages do not correspond to an unloaded balance but to a balance that is loaded by the initial loads. To calculate the gross loads acting on the balance, the measured balance loads need to be adjusted for the initial loads which have been zeroed out. The technique used at AEDC to ensure that balance loads are determined by starting with an unloaded balance is to determine balance gage voltages (unloading constants) that represent the initial loads acting on the balance at the attitude the wind-off zeros were obtained ($\alpha_{s_0}$ and $\phi_{s_0}$). The gage voltages produced by the total loads acting on the balance are measured relative to the wind-off zeros and then corrected by the unloading constants, which effectively shifts the wind-off zeros to correspond to the unloaded balance condition. The corrected gage voltages are then multiplied by the balance calibration matrix to obtain the gage forces and/or moments. The gage forces and/or moments are then used to determine the forces and moments in the balance axis system.

However, for the purposes of this example, the forces in the balance axis system are used in place of the balance gage voltages. The axial-force tare weight, $W_A$, is determined using the balance axial force gage and the normal-force tare weight, $W_N$, is determined using the normal-force gage(s). The balance gross forces are determined by modifying the forces measured by the balance, $F_{A_M}$ and $F_{N_M}$, by the initial loads that were zeroed out when the wind-off zeros were obtained.

Gross axial force, $$F_{A_G} = F_{A_M} + W_A \sin(\alpha_{s_0}) \tag{4-39}$$

Gross normal force, $$F_{N_G} = F_{N_M} - W_N \cos(\alpha_{s_0}) \cos(\phi_{s_0}) \tag{4-40}$$

The uncertainties of the gross forces are estimated by using the partial derivatives of the above equations with respect to $F_{A_M}$, $F_{N_M}$, $W_A$, $W_N$, $\alpha_{s_0}$, and $\phi_{s_0}$. The uncertainties of the sting attitude and measured forces can be found in Table 4.2, and the uncertainty of the model tare weights can be found in Table 4.3. The forces were measured using a calibrated system; therefore, the calibration uncertainty becomes the bias limit for values measured by the system. Because, the system performs virtually identically during both the evaluation and testing processes, the precision limit for the uncertainty evaluation should be a very good estimate of the precision limit during testing. Since the model weight is constant over the timeframe of this example, its uncertainty is included only as a bias limit. The measured forces and model tare weights were determined using the same balance and calibration, which introduces a correlated bias, There are also correlated bias effects produced by the interaction one balance component on another; however, these biases are included in the uncertainty of balance calibration. The statements concerning the bias and precision limits for $F_{A_M}$, $F_{N_M}$, $W_A$, and $W_N$ will apply throughout the remainder of this chapter.

$$B_{F_{A_G}} = \pm\left(\left[\frac{\partial F_{A_G}}{\partial F_{A_M}} B_{F_{A_M}}\right]^2 + \left[\frac{\partial F_{A_G}}{\partial W_A} B_{W_A}\right]^2 + \left[\frac{\partial F_{A_G}}{\partial \alpha_{s_0}} B_{\alpha_s}\right]^2 + 2\frac{\partial F_{A_G}}{\partial F_{A_M}}\frac{\partial F_{A_G}}{\partial W_A} B'_{F_{A_M}} B'_{W_A}\right)^{\frac{1}{2}}$$

$$= \pm\left([(1)0.485]^2 + [(0)6.530]^2 + [(111.205)0.00040]^2 + 2(1)(0)(0.485)6.530\right)^{\frac{1}{2}} = \pm 0.487 \text{ N} \tag{4-41}$$

$$P_{F_{A_G}} = \pm\left(\left[\frac{\partial F_{A_G}}{\partial F_{A_M}} P_{F_{A_M}}\right]^2 + \left[\frac{\partial F_{A_G}}{\partial \alpha_{s_0}} P_{\alpha_s}\right]^2\right)^{\frac{1}{2}}$$

$$= \pm\left([(1)2.580]^2 + [(111.205)0.00031]^2\right)^{\frac{1}{2}} = \pm 2.580 \text{ N} \tag{4-42}$$

$$B_{F_{N_G}} = \pm\left(\left[\frac{\partial F_{N_G}}{\partial F_{N_M}} B_{F_{N_M}}\right]^2 + \left[\frac{\partial F_{N_G}}{\partial W_N} B_{W_N}\right]^2 + \left[\frac{\partial F_{N_G}}{\partial \alpha_{s_0}} B_{\alpha_s}\right]^2 + \left[\frac{\partial F_{N_G}}{\partial \phi_{s_0}} B_{\phi_s}\right]^2 + 2\frac{\partial F_{N_G}}{\partial F_{N_M}}\frac{\partial F_{N_G}}{\partial W_N} B'_{F_{N_M}} B'_{W_N}\right)^{\frac{1}{2}}$$

$$= \pm\left([(1)2.019]^2 + [(-1)7.729]^2 + [(0)0.00040]^2 + [(0)0.00159]^2 + 2(1)(-1)(2.019)7.729\right)^{\frac{1}{2}} = \pm 5.710 \text{ N} \tag{4-43}$$

$$P_{F_{N_G}} = \pm\left(\left[\frac{\partial F_{N_G}}{\partial F_{N_M}} P_{F_{N_M}}\right]^2 + \left[\frac{\partial F_{N_G}}{\partial \alpha_{s_0}} P_{\alpha_s}\right]^2 + \left[\frac{\partial F_{N_G}}{\partial \phi_{s_0}} P_{\phi_s}\right]^2\right)^{\frac{1}{2}}$$

$$= \pm\left(\left[(1)10.930\right]^2 + \left[(0)0.00031\right]^2 + \left[(0)0.00244\right]^2\right)^{\frac{1}{2}} = \pm 10.930 \text{ N} \quad (4\text{-}44)$$

The estimated bias and precision limits are then combined [Eq. (2-9)] to calculate the estimated uncertainty in the measured gross forces.

$$U_{F_{A_G}} = \pm\left(B_{F_{A_G}}^2 + P_{F_{A_G}}^2\right)^{\frac{1}{2}} = \pm\left(0.487^2 + 2.580^2\right)^{\frac{1}{2}} = \pm 2.626 \text{ N} \quad (4\text{-}45)$$

$$U_{F_{N_G}} = \pm\left(B_{F_{N_G}}^2 + P_{F_{N_G}}^2\right)^{\frac{1}{2}} = \pm\left(5.710^2 + 10.930^2\right)^{\frac{1}{2}} = \pm 12.332 \text{ N} \quad (4\text{-}46)$$

In using the bias limit (calibration uncertainty) and the evaluation precision limit to estimate the uncertainty of the measured forces, it was assumed that the uncertainty of the balance data acquisition system used during testing was the same as that used during the balance calibration. If that were not true, an additional bias limit and/or precision limit would be required to account for the uncertainties of the system used during testing. In this example it is also assumed that the output of the balance at the wind-off zero attitude has not shifted from pre-run to post-run (commonly termed balance wind-off zero shifts). If balance wind-off zero shifts that are significant with respect to the balance measurement uncertainty occur, then an additional bias term is required to estimate the bias limit for the associated balance components.

### 4.4.4 Model Aerodynamic Axial and Normal Forces

The forces measured by the balance $F_{A_M}$ and $F_{N_M}$, are combinations of the aerodynamic loads and fractions of the model weight (that result from changing the model attitude). Therefore, the gross axial and normal forces must be corrected to remove the effects of the model weight in order to determine the aerodynamic loads (net forces) on the model. The weight adjustments are termed static weight tare corrections and are calculated using the following equations:

$$\text{Axial force tare correction, } F_{A_{ST}} = W_A \text{Sin}(\alpha_s) = 111.205\text{Sin}(4.00) = 7.757 \text{ N} \quad (4\text{-}47)$$

$$\text{Normal force tare correction, } F_{N_{ST}} = -W_N \text{Cos}(\alpha_s)\text{Cos}(\phi_s) = -111.205\text{Cos}(4.00)\text{Cos}(0.0) = -110.934 \text{ N} \quad (4\text{-}48)$$

The equations for calculating estimates of the bias and precision limits for the static weight tare corrections are obtained by taking the partial derivatives of the above equations with respect to $W_A$, $W_N$, $\alpha_s$, and $\phi_s$. Note that the attitude of the balance is normally used in the calculation of the weight tare corrections; however, in this example the balance attitude is determined only by $\alpha_s$ and $\phi_s$, which greatly simplifies this example. The bias and precision limits for $\alpha_s$ and $\phi_s$ are provided in Table 4.2, and the uncertainty of the model tare weights can be found in Table 4.3.

$$B_{F_{A_{ST}}} = \pm\left(\left[\frac{\partial F_{A_{ST}}}{\partial W_A} B_{W_A}\right]^2 + \left[\frac{\partial F_{A_{ST}}}{\partial \alpha_s} B_{\alpha_s}\right]^2\right)^{\frac{1}{2}} = \pm\left(\left[(0.06976)6.530\right]^2 + \left[(110.934)0.00040\right]^2\right)^{\frac{1}{2}} = \pm 0.458 \text{N} \quad (4\text{-}49)$$

$$P_{F_{A_{ST}}} = \pm\left(\left[\frac{\partial F_{A_{ST}}}{\partial \alpha_s} P_{\alpha_s}\right]^2\right)^{\frac{1}{2}} = \pm\left(\left[(110.934)0.00031\right]^2\right)^{\frac{1}{2}} = \pm 0.034 \text{ N} \quad (4\text{-}50)$$

$$B_{F_{N_{ST}}} = \pm\left(\left[\frac{\partial F_{N_{ST}}}{\partial W_N} B_{W_N}\right]^2 + \left[\frac{\partial F_{N_{ST}}}{\partial \alpha_s} B_{\alpha_s}\right]^2 + \left[\frac{\partial F_{N_{ST}}}{\partial \phi_s} B_{\phi_s}\right]^2\right)^{\frac{1}{2}}$$

$$= \pm\left(\left[(-0.9976)7.729\right]^2 + \left[(7.757)0.00040\right]^2 + \left[(0)0.00159\right]^2\right)^{\frac{1}{2}} = \pm 7.710 \text{ N} \quad (4\text{-}51)$$

$$P_{F_{N_{ST}}} = \pm\left(\left[\frac{\partial F_{N_{ST}}}{\partial \alpha_s} P_{\alpha_s}\right]^2 + \left[\frac{\partial F_{N_{ST}}}{\partial \phi_s} P_{\phi_s}\right]^2\right)^{\frac{1}{2}}$$

$$= \pm\left([(7.757)0.00031]^2 + [(0)0.00244]^2\right)^{\frac{1}{2}} = \pm 0.002 \text{ N} \qquad (4\text{-}52)$$

The estimated bias and precision limits are then combined [Eq. (2-9)] to calculate the estimated uncertainty in the static weight tare corrections.

$$U_{F_{A_{ST}}} = \pm\left(B_{F_{A_{ST}}}^2 + P_{F_{A_{ST}}}^2\right)^{\frac{1}{2}} = \pm\left(0.458^2 + 0.034^2\right)^{\frac{1}{2}} = \pm 0.459 \text{ N} \qquad (4\text{-}53)$$

$$U_{F_{N_{ST}}} = \pm\left(B_{F_{N_{ST}}}^2 + P_{F_{N_{ST}}}^2\right)^{\frac{1}{2}} = \pm\left(7.710^2 + 0.002^2\right)^{\frac{1}{2}} = \pm 7.710 \text{ N} \qquad (4\text{-}54)$$

The weight tare corrections are subtracted from the gross forces to yield the aerodynamic forces acting on the model.

**Axial force,** $F_A = F_{A_G} - F_{A_{ST}} = 181.924 - 7.757 = 174.167$ **N** (4-55)

**Normal force,** $F_N = F_{N_G} - F_{N_{ST}} = 1666.434 + 110.934 = 1777.368$ N (4-56)

The equations for calculating estimates of the bias and precision limits for the aerodynamic forces are obtained by taking the partial derivatives of the above equations with respect to the gross forces, tare weights, and pitch and roll angles. The uncertainties of the gross forces and pitch and roll angles are found in Table 4.2, and the uncertainty of the tare weights are found in Table 4.3.

$$B_{F_A} = \pm\left(\left[\frac{\partial F_A}{\partial F_{A_M}} B_{F_{A_M}}\right]^2 + \left[\frac{\partial F_A}{\partial W_A} B_{W_A}\right]^2 + \left[\frac{\partial F_A}{\partial \alpha_s} B_{\alpha_s}\right]^2 + \left[\frac{\partial F_A}{\partial \alpha_{s_0}} B_{\alpha_s}\right]^2 + 2\frac{\partial F_A}{\partial F_{A_M}}\frac{\partial F_A}{\partial W_A} B'_{F_{A_M}} B'_{W_A}\right.$$

$$\left. + 2\frac{\partial F_A}{\partial \alpha_s}\frac{\partial F_A}{\partial \alpha_{s_0}} B'_{\alpha_s} B'_{\alpha_s}\right)^{\frac{1}{2}}$$

$$= \pm\left([(1)0.485]^2 + [(-0.06976)6.530]^2 + [(-110.934)0.00040]^2 + [(111.205)0.00040]^2\right.$$

$$\left. + 2(1)(-0.06976)(0.485)6.530 + 2(-110.934)(111.205)(0.00040)0.00040\right)^{\frac{1}{2}} = \pm 0.029 \text{ N} \qquad (4\text{-}57)$$

$$P_{F_A} = \pm\left(\left[\frac{\partial F_A}{\partial F_{A_M}} P_{F_{A_M}}\right]^2 + \left[\frac{\partial F_A}{\partial \alpha_s} P_{\alpha_s}\right]^2 + \left[\frac{\partial F_A}{\partial \alpha_{s_0}} P_{\alpha_s}\right]^2\right)^{\frac{1}{2}}$$

$$= \pm\left([(1)2.580]^2 + [(-110.934)0.00031]^2 + [(111.205)0.00031]^2\right)^{\frac{1}{2}} = \pm 2.580 \text{ N} \qquad (4\text{-}58)$$

$$B_{F_N} = \pm\left(\left[\frac{\partial F_N}{\partial F_{N_M}} B_{F_{N_M}}\right]^2 + \left[\frac{\partial F_N}{\partial W_N} B_{W_N}\right]^2 + \left[\frac{\partial F_N}{\partial \alpha_s} B_{\alpha_s}\right]^2 + \left[\frac{\partial F_N}{\partial \phi_s} B_{\phi_s}\right]^2 + \left[\frac{\partial F_N}{\partial \alpha_{s_0}} B_{\alpha_s}\right]^2 + \left[\frac{\partial F_N}{\partial \phi_{s_0}} B_{\phi_s}\right]^2\right.$$

$$\left. + 2\frac{\partial F_N}{\partial F_{N_M}}\frac{\partial F_N}{\partial W_N} B'_{F_{N_M}} B'_{W_N} + 2\frac{\partial F_N}{\partial \alpha_s}\frac{\partial F_N}{\partial \alpha_{s_0}} B'_{\alpha_s} B'_{\alpha_s} + 2\frac{\partial F_N}{\partial \phi_s}\frac{\partial F_N}{\partial \phi_{s_0}} B'_{\phi_s} B'_{\phi_s}\right)^{\frac{1}{2}}$$

$$= \pm\left([(1)2.019]^2 + [(-0.002436)7.729]^2 + [(-7.757)0.00040]^2 + [(0)0.00159]^2 + [(0)0.00040]^2\right.$$

$$+ [(0)0.00159]^2 + 2(1)(-0.002436)(2.019)(7.729) + 2(-7.757)(0)(0.00040)(0.00040)$$

$$\left. + 2(0)(0)(0.00159)(0.00159)\right)^{\frac{1}{2}} = \pm 2.000 \text{ N} \qquad (4\text{-}59)$$

$$P_{F_N} = \pm\left(\left[\frac{\partial F_N}{\partial F_{N_M}} P_{F_{N_M}}\right]^2 + \left[\frac{\partial F_N}{\partial \alpha_s} P_{\alpha_s}\right]^2 + \left[\frac{\partial F_N}{\partial \phi_s} P_{\phi_s}\right]^2 + \left[\frac{\partial F_N}{\partial \alpha_{s_0}} P_{\alpha_s}\right]^2 + \left[\frac{\partial F_N}{\partial \phi_{s_0}} P_{\phi_s}\right]^2\right)^{\frac{1}{2}}$$

$$= \pm\left([(1)10.934]^2 + [(-7.757)0.00031]^2 + [(0)0.00244]^2 + [(0)0.00031]^2 + [(0)0.00244]^2\right)^{\frac{1}{2}}$$

$$= \pm 10.934 \text{ N} \qquad (4\text{-}60)$$

The estimated bias and precision limits for the aerodynamic forces are then combined [Eq. (2-9)] to calculate the estimated uncertainty in $F_A$ and $F_N$.

$$U_{F_A} = \pm\left(B_{F_A}^2 + P_{F_A}^2\right)^{\frac{1}{2}} = \pm\left(0.029^2 + 2.580^2\right)^{\frac{1}{2}} = \pm 2.580 \text{ N} \qquad (4\text{-}61)$$

$$U_{F_N} = \pm\left(B_{F_N}^2 + P_{F_N}^2\right)^{\frac{1}{2}} = \pm\left(2.000^2 + 10.934^2\right)^{\frac{1}{2}} = \pm 11.115 \text{ N} \qquad (4\text{-}62)$$

### 4.4.5 Model Base Axial Force

The measured axial force includes the force produced by the pressure on the model base/cavity area. A typical data reduction requirement is to subtract the base axial force from the measured axial force. The base axial force is calculated using the following equations and the four base pressures that were measured on the model.

Base pressures:

$$p_{B_1} = p_{B_{M_1}} + p_{REF} = -62148.24 + 98154.00 = 36005.76 \text{ Pa} \qquad (4\text{-}63)$$

$$p_{B_2} = p_{B_{M_2}} + p_{REF} = -61669.44 + 98154.00 = 36484.56 \text{ Pa} \qquad (4\text{-}64)$$

$$p_{B_3} = p_{B_{M_3}} + p_{REF} = -61669.44 + 98154.00 = 36484.56 \text{ Pa} \qquad (4\text{-}65)$$

$$p_{B_4} = p_{B^{M_4}} + p_{REF} = -61573.68 + 98154.00 = 36580.32 \text{ Pa} \qquad (4\text{-}66)$$

$$\text{Average base pressure, } \bar{p}_B = \frac{1}{4}\sum_{i=1}^{4} p_{B_i} = 36388.80 \text{ Pa} \qquad (4\text{-}67)$$

$$\text{Base axial force, } F_{A_B} = (p - \bar{p}_B)A_B = (37870.04 - 36388.80)0.005723 = 8.477 \text{ N} \qquad (4\text{-}68)$$

The forebody axial force is determined by subtracting the base axial force from the axial force.

$$\text{Forebody axial force, } F_{A_F} = F_A - F_{A_B} = 174.167 - 8.477 = 165.690 \text{ N} \qquad (4\text{-}69)$$

The equations used to estimate the bias and precision limits of the base pressure are obtained by taking the partial derivatives of Eqs. (4-63) - (4-66) with respect to $p_{B_M}$ and $p_{REF}$ (note that the partial derivatives are equal to 1). The uncertainties of $p_{B_M}$ and $p_{REF}$ can be found in Table 4.2. The bias limit for the measured pressures was determined using the ESP calibration uncertainty for a zero drift of 50 Pa. The pressures were measured using a calibrated system; therefore, the calibration uncertainty becomes the bias limit for the measured value. The evaluation data were acquired in a manner that simulated the testing process, which allows the precision limit estimated for the uncertainty evaluation to be used as an estimate of the precision limit for the testing process. Since the values for all of the measured pressures are nearly the same, the average of the measured pressures (−61765.20 Pa) are used in the calculations. The statements concerning the bias and precision limits for the pressures and using the average measured pressure will apply throughout the remainder of this chapter.

$$B_{p_B} = \pm\left(B_{p_{B_M}}^2 + B_{p_{REF}}^2\right)^{\frac{1}{2}} = \pm\left(59.76^2 + 16.76^2\right)^{\frac{1}{2}} = k62.07 \text{ Pa} \tag{4-70}$$

$$P_{p_B} = \pm\left(P_{p_{B_M}}^2 + P_{p_{REF}}^2\right)^{\frac{1}{2}} = \pm\left(48.91^2 + 5.03^2\right)^{\frac{1}{2}} = \pm 49.17 \text{ Pa} \tag{4-71}$$

$$U_{p_B} = \pm\left(B_{p_B}^2 + P_{p_B}^2\right)^{\frac{1}{2}} = \pm\left(62.07^2 + 49.17^2\right)^{\frac{1}{2}} = i79.19 \text{ Pa} \tag{4-72}$$

The equations for calculating the estimated bias and precision limits for the average base pressure and the base axial force are obtained by taking the partial derivatives of Eq. (4-67) with respected to $p_{B_{Mi}}$ and $p_{REF}$ and Eq. (4-68) with respect to $p_T$, $p_C$, DM, $p_{B_{Mi}}$, $p_{REF}$, and $A_B$. The bias and precision limits for $p_T$ and $p_C$ are shown in Eq. (4-19) and (4-20). There is a correlated bias effect in the measured base pressures since the individual transducers were calibrated against the same working standard (Sonic@ transducer). The four measured pressures, taken in combinations of two, produce six correlated bias terms [Eq. (2-A-211. The correlated bias limits in the measured base pressures are equal to the uncertainty of the working standard. The uncertainty of the Sonic@ transducer is the same as used for $p_T$, $p_C$, and $p_{REF}$, which can be found in Table 4.2. Note that the equation for the bias limit of the Sonic® transducer requires the pressure to be an absolute, not a differential pressure.

$$\begin{aligned} B'_{p_{B_M}} &= \pm\left[16.76 + 0.0001\,|98154.00 - (p_{B_{Mi}} + p_{REF})|\right] \\ &= \pm\left[16.76 + 0.0001\,|98154.00 - (-61765.20 + 98154.00)|\right] = 122.94 \text{ Pa} \end{aligned} \tag{4-73}$$

Note that the bias/precision limits for the measured base pressures have been grouped together, as have the correlated bias limits. The partial derivatives, bias/precision limits, and the correlated bias limits have the same values for each of the measured pressures since they were calculated using the average measured base pressure (-61765.20 Pa). Since the base area is a constant there is no associated precision error. This procedure will be used through the remainder of the example.

$$B_{\bar{p}_B} = \pm\left(\sum_{i=1}^{N_{p_B}}\left\{\left[\frac{\partial \bar{p}_B}{\partial p_{B_{Mi}}} B_{p_{B_{Mi}}}\right]^2 + \left[\frac{\partial \bar{p}_B}{\partial p_{REF}} B_{p_{REF}}\right]^2\right\} + \left[\sum_{j=1}^{N_{p_B}-1} j\right] 2\left[\frac{\partial \bar{p}_B}{\partial p_{B_{Mi}}} B'_{p_{B_{Mi}}}\right]^2\right)^{\frac{1}{2}}$$

$$= \pm\left(4\left\{\left[(0.25)\,59.76\right]^2 + \left[(0.25)16.76\right]^2\right\} + 6(2)\left[(0.25)(22.94)\right]^2\right)^{\frac{1}{2}} = k36.85 \text{ Pa} \tag{4-74}$$

$$P_{\bar{p}_B} = \pm\left(\sum_{i=1}^{N_{p_B}}\left\{\left[\frac{\partial \bar{p}_B}{\partial p_{B_{Mi}}} P_{p_{B_{Mi}}}\right]^2 + \left[\frac{\partial \bar{p}_B}{\partial p_{REF}} P_{p_{REF}}\right]^2\right\}\right)^{\frac{1}{2}}$$

$$= \pm\left(4\left\{\left[(0.25)\,48.91\right]^2 + \left[(0.25)5.03\right]^2\right\}\right)^{\frac{1}{2}} = k24.58 \text{ Pa} \tag{4-75}$$

$$B_{F_{A_B}} = \pm\left(\left[\frac{\partial F_{A_B}}{\partial p_T} B_{p_T}\right]^2 + \left[\frac{\partial F_{A_B}}{\partial p_C} B_{p_C}\right]^2 + \left[\frac{\partial F_{A_B}}{\partial DM} B_{DM}\right]^2 + \left[\frac{\partial F_{A_B}}{\partial A_B} B_{A_B}\right]^2 + \sum_{i=1}^{N_{p_B}}\left\{\left[\frac{\partial F_{A_B}}{\partial p_{B_{Mi}}} B_{p_{B_{Mi}}}\right]^2\right.\right.$$

$$\left.\left. + \left[\frac{\partial F_{A_B}}{\partial p_{REF}} B_{p_{REF}}\right]^2\right\} + \left[\sum_{j=1}^{N_{p_B}-1} j\right] 2\left[\frac{\partial F_{A_B}}{\partial p_{B_{Mi}}} B'_{p_{B_{Mi}}}\right]^2 + 2\frac{\partial F_{A_B}}{\partial p_T}\frac{\partial F_{A_B}}{\partial p_C} B'_{p_T} B'_{p_C}\right)^{\frac{1}{2}}$$

$$= \pm\left(\left[(-1.914*10^{-5})19.81\right]^2 + \left[(0.005705)22.75\right]^2 + \left[(-244.18)0.00177\right]^2 + \left[(1481.24)7.07*10^{-7}\right]^2\right.$$

$$+ 4\left\{\left[(-0.00143)\,59.76\right]^2 + \left[(-0.00143)16.76\right]^2\right\} + 6(2)\left[(-0.00143)(22.94)\right]^2$$

$$\left. + 2(-1.914*10^{-5})(0.005705)\,(6.82)\,(5.94)\right)^{\frac{1}{2}} = k0.498 \text{ N} \tag{4-76}$$

$$P_{F_{A_B}} = \pm\left( \left[\frac{\partial F_{A_B}}{\partial p_T} P_{p_T}\right]^2 + \left[\frac{\partial F_{A_B}}{\partial p_C} P_{p_C}\right]^2 + \sum_{i=1}^{N_{pB}} \left\{ \left[\frac{\partial F_{A_B}}{\partial p_{B_{Mi}}} P_{p_{B_{Mi}}}\right]^2 + \left[\frac{\partial F_{A_B}}{\partial p_{REF}} P_{p_{REF}}\right]^2 \right\} \right)^{\frac{1}{2}}$$

$$= \pm\Big( \left[(-1.914*10^{-5})4.36\right]^2 + \left[(0.005705)3.71\right]^2 + 4\left\{\left[(-0.00143)48.91\right]^2 + \left[(-0.00143)5.03\right]^2\right\} \Big)^{\frac{1}{2}} = \pm 0.142 \text{ N} \quad (4\text{-}77)$$

The equations to calculate the estimated bias and precision limits of the forebody axial force are derived by taking the partial derivatives of Eq. (4-69) with respect to $p_T$, $p_C$, DM, $p_{B_{Mi}}$, $p_{REF}$, $\alpha_s$, $A_B$, W, $\alpha_{s_0}$, and $F_{A_M}$. The bias and precision limits of $p_T$, $p_C$, DM, $p_{B_{Mi}}$, $p_{REF}$, $\alpha_s$, $A_B$, W, and $F_{A_M}$ can be found in Tables 4.2 and 4.3.

$$B_{F_{A_F}} = \pm\Bigg( \left[\frac{\partial F_{A_F}}{\partial p_T} B_{p_T}\right]^2 + \left[\frac{\partial F_{A_F}}{\partial p_C} B_{p_C}\right]^2 + \left[\frac{\partial F_{A_F}}{\partial DM} B_{DM}\right]^2 + \left[\frac{\partial F_{A_F}}{\partial A_B} B_{A_B}\right]^2 + \left[\frac{\partial F_{A_F}}{\partial F_{A_M}} B_{F_{A_M}}\right]^2$$
$$+ \sum_{i=1}^{N_{pB}} \left\{ \left[\frac{\partial F_{A_F}}{\partial p_{B_{Mi}}} B_{p_{B_{Mi}}}\right]^2 + \left[\frac{\partial F_{A_F}}{\partial p_{REF}} B_{p_{REF}}\right]^2 \right\} + \left[\frac{\partial F_{A_F}}{\partial W_A} B_{W_A}\right]^2 + \left[\frac{\partial F_{A_F}}{\partial \alpha_s} B_{\alpha_s}\right]^2 + \left[\frac{\partial F_{A_F}}{\partial \alpha_{s_0}} B_{\alpha_s}\right]^2$$
$$+ 2\frac{\partial F_{A_F}}{\partial p_T}\frac{\partial F_{A_F}}{\partial p_C} B'_{p_T} B'_{p_C} + \left[\sum_{j=1}^{N_{pB}-1}\right] 2\left[\frac{\partial F_{A_B}}{\partial p_{B_{Mi}}} B'_{p_{B_{Mi}}}\right]^2 + 2\frac{\partial F_{A_F}}{\partial F_{A_M}}\frac{\partial F_{A_F}}{\partial W_A} B'_{F_{A_M}} B'_{W_A}$$
$$+ 2\frac{\partial F_{A_F}}{\partial \alpha_s}\frac{\partial F_{A_F}}{\partial \alpha_{s_0}} B'_{\alpha_s} B'_{\alpha_s} \Bigg)^{\frac{1}{2}}$$

$$= \pm\Big( \left[(1.914*10^{-5})19.81\right]^2 + \left[(-0.005705)22.75\right]^2 + \left[(244.18)0.00177\right]^2 + \left[(-1481.24)7.07*10^{-7}\right]^2$$
$$+ \left[(1)0.485\right]^2 + 4\left\{\left[(0.00143)59.76\right]^2 + \left[(0.00143)16.76\right]^2\right\} + \left[(-0.06976)6.530\right]^2$$
$$+ \left[(-110.934)0.00040\right]^2 + \left[(111.205)0.00040\right]^2 + 2(1.914*10^{-5})(-0.005705)(6.82)(5.94)$$
$$+ 6(2)\left[(0.00143)22.94\right]^2 + 2(1)(-0.06976)(0.485)(6.530)$$
$$+ 2(-110.934)(111.205)(0.00040)(0.00040)\Big)^{\frac{1}{2}} = \pm 0.499 \text{ N} \quad (4\text{-}78)$$

$$P_{F_{A_F}} = \pm\Bigg( \left[\frac{\partial F_{A_F}}{\partial p_T} P_{p_T}\right]^2 + \left[\frac{\partial F_{A_F}}{\partial p_C} P_{p_C}\right]^2 + \left[\frac{\partial F_{A_F}}{\partial F_{A_M}} P_{F_{A_M}}\right]^2 + \sum_{i=1}^{N_{pB}} \left\{ \left[\frac{\partial F_{A_F}}{\partial p_{B_{Mi}}} P_{p_{B_{Mi}}}\right]^2 + \left[\frac{\partial F_{A_F}}{\partial p_{REF}} P_{p_{REF}}\right]^2 \right\}$$
$$+ \left[\frac{\partial F_{A_F}}{\partial \alpha_s} P_{\alpha_s}\right]^2 + \left[\frac{\partial F_{A_F}}{\partial \alpha_{s_0}} P_{\alpha_s}\right]^2 \Bigg)^{\frac{1}{2}}$$

$$= \pm\Big( \left[(1.914*10^{-5})4.36\right]^2 + \left[(-0.005705)3.71\right]^2 + \left[(1)2.580\right]^2 + 4\left\{\left[(0.00143)48.91\right]^2 + \left[(0.00143)5.03\right]^2\right\}$$
$$+ \left[(-110.934)0.00031\right]^2 + \left[(111.205)0.00031\right]^2 \Big)^{\frac{1}{2}} = \pm 2.584 \text{ N} \quad (4\text{-}79)$$

The bias and precision limits determined for the base pressure, base axial force, and forebody axial force are combined [Eq. (2-9)] to calculate estimated uncertainty in $p_B$, $\bar{p}_B$, $F_{A_B}$, and $F_{A_F}$.

$$U_{p_B} = \pm\left(B_{p_B}^2 + P_{p_B}^2\right)^{\frac{1}{2}} = \pm\left(62.07^2 + 49.17^2\right)^{\frac{1}{2}} = \pm 79.19 \text{ Pa} \quad (4\text{-}80)$$

$$U_{\bar{p}_B} = \pm\left(B_{\bar{p}_B}^2 + P_{\bar{p}_B}^2\right)^{\frac{1}{2}} = \pm\left(36.85^2 + 24.58^2\right)^{\frac{1}{2}} = \pm 44.30 \text{ Pa} \tag{4-81}$$

$$U_{F_{A_B}} = \pm\left(B_{F_{A_B}}^2 + P_{F_{A_B}}^2\right)^{\frac{1}{2}} = \pm\left(0.498^2 + 0.142^2\right)^{\frac{1}{2}} = \pm 0.518 \text{ N} \tag{4-82}$$

$$U_{F_{A_F}} = \pm\left(B_{F_{A_F}}^2 + P_{F_{A_F}}^2\right)^{\frac{1}{2}} = \pm\left(0.499^2 + 2.584^2\right)^{\frac{1}{2}} = \pm 2.632 \text{ N} \tag{4-83}$$

### 4.4.6 Wind Tunnel Aerodynamic Drag Coefficient

The calculated aerodynamic normal and forebody axial forces are combined using an industry standard equation to calculate the wind tunnel forebody drag coefficient in the stability axis system.

$$C_{D_F} = \frac{\left[F_{A_F}\text{Cos}(\alpha) + F_N\text{Sin}(\alpha)\right]}{qA} = \frac{\left[165.690\text{Cos}(4.00) + 1777.368\text{Sin}(4.00)\right]}{23924.40(0.20439)} = 0.0592 \tag{4-84}$$

The partial derivatives of the above equation with respect to $p_T$, $p_C$, DM, $\alpha_s$, $\phi_s$, $\alpha_{s_0}$, $\phi_{s_0}$, $W_A$, $W_N$, $F_{A_M}$, $F_{N_M}$, $p_{B_{Mi}}$, $p_{REF}$, and $A_B$ are used to produce the equations for the bias and precision limits. The bias and precision limits of these parameters are found in Tables 4.2 and 4.3. The bias and precision limits for the model reference area, A, are assumed to be zero since the reference area was a defined value for this example. The correlated bias limits for $p_T$ and $p_C$ can be found in Eqs. (4-19) and (4-20), and the correlated bias limit for the measured base pressures can be found in Eq. (4-73). The correlated bias effect between $F_{A_M}$ and $F_{N_M}$ due to the uncertainty of the dead weights used in the calibration of the balance has been determined to be insignificant.

$$\begin{aligned}
B_{C_{D_F}} = \pm\Bigg( & \left[\frac{\partial C_{D_F}}{\partial p_T} B_{p_T}\right]^2 + \left[\frac{\partial C_{D_F}}{\partial p_C} B_{p_C}\right]^2 + \left[\frac{\partial C_{D_F}}{\partial DM} B_{DM}\right]^2 + \left[\frac{\partial C_{D_F}}{\partial A_B} B_{A_B}\right]^2 + \left[\frac{\partial C_{D_F}}{\partial F_{A_M}} B_{F_{A_M}}\right]^2 \\
& + \left[\frac{\partial C_{D_F}}{\partial F_{N_M}} B_{F_{N_M}}\right]^2 + \sum_{i=1}^{N_{pB}} \left\{\left[\frac{\partial C_{D_F}}{\partial p_{B_{Mi}}} B_{p_{B_{Mi}}}\right]^2 + \left[\frac{\partial C_{D_F}}{\partial p_{REF}} B_{p_{REF}}\right]^2\right\} + \left[\frac{\partial C_{D_F}}{\partial W_A} B_{W_A}\right]^2 + \left[\frac{\partial C_{D_F}}{\partial W_N} B_{W_N}\right]^2 \\
& + \left[\frac{\partial C_{D_F}}{\partial \alpha_s} B_{\alpha_s}\right]^2 + \left[\frac{\partial C_{D_F}}{\partial \phi_s} B_{\phi_s}\right]^2 + \left[\frac{\partial C_{D_F}}{\partial \alpha_{s_0}} B_{\alpha_s}\right]^2 + \left[\frac{\partial C_{D_F}}{\partial \phi_{s_0}} B_{\phi_s}\right]^2 + 2\frac{\partial C_{D_F}}{\partial p_T}\frac{\partial C_{D_F}}{\partial p_C} B'_{p_T} B'_{p_C} \\
& + \left[\sum_{j=1}^{N_{pB}-1} j\right] 2\left[\frac{\partial C_{D_F}}{\partial p_{B_M}} B'_{p_{B_M}}\right]^2 + 2\frac{\partial C_{D_F}}{\partial F_{A_M}}\frac{\partial C_{D_F}}{\partial W_A} B'_{F_{A_M}} B'_{W_A} + 2\frac{\partial C_{D_F}}{\partial F_{N_M}}\frac{\partial C_{D_F}}{\partial W_N} B'_{F_{N_M}} B'_{W_N} \\
& + 2\frac{\partial C_{D_F}}{\partial \alpha_s}\frac{\partial C_{D_F}}{\partial \alpha_{s_0}} B'_{\alpha_s} B'_{\alpha_s} + 2\frac{\partial C_{D_F}}{\partial \phi_s}\frac{\partial C_{D_F}}{\partial \phi_{s_0}} B'_{\phi_s} B'_{\phi_s}\Bigg)^{\frac{1}{2}}
\end{aligned}$$

$$\begin{aligned}
= \pm\Big( & \left[(-1.635*10^{-6})19.81\right]^2 + \left[(1.897*10^{-7})22.75\right]^2 + \left[(-0.008121)0.00177\right]^2 + \left[(-0.3022)7.07*10^{-7}\right]^2 \\
& + \left[(2.040*10^{-4})0.485\right]^2 + \left[(1.427*10^{-5})2.019\right]^2 + 4\left\{\left[(2.919*10^{-7})59.76\right]^2 + \left[(2.919*10^{-7})16.76\right]^2\right\} \\
& + \left[(-1.423*10^{-5})6.530\right]^2 + \left[(-3.475*10^{-8})7.729\right]^2 + \left[(0.3375)0.00040\right]^2 + \left[(0)0.00159\right]^2 \\
& + \left[(0.02269)0.00040\right]^2 + \left[(0)0.00159\right]^2 + 2(-1.635*10^{-6})(1.897*10^{-7})(6.82)(5.94) \\
& + 6(2)\left[(2.919*10^{-7})(22.94)\right]^2 + 2(2.040*10^{-4})(-1.423*10^{-5})(0.485)(6.530) \\
& + 2(1.427*10^{-5})(-3.475*10^{-8})(2.019)(7.729) + 2(0.3375)(0.02269)(0.00040)(0.00040) \\
& + 2(0)(0)(0.00159)(0.00159)\Big)^{\frac{1}{2}} = \pm 0.00016
\end{aligned} \tag{4-85}$$

$$P_{C_{D_F}} = \pm\left(\left[\frac{\partial C_{D_F}}{\partial p_T} P_{p_T}\right]^2 + \left[\frac{\partial C_{D_F}}{\partial p_C} P_{p_C}\right]^2 + \left[\frac{\partial C_{D_F}}{\partial F_{A_M}} P_{F_{A_M}}\right]^2 + \left[\frac{\partial C_{D_F}}{\partial F_{N_M}} P_{F_{N_M}}\right]^2\right.$$

$$+ \sum_{i=1}^{N_{p_B}} \left\{\left[\frac{\partial C_{D_F}}{\partial p_{B_{M_i}}} P_{p_{B_{M_i}}}\right]^2 + \left[\frac{\partial C_{D_F}}{\partial p_{REF}} P_{p_{REF}}\right]^2\right\} + \left[\frac{\partial C_{D_F}}{\partial \alpha_s} P_{\alpha_s}\right]^2 + \left[\frac{\partial C_{D_F}}{\partial \phi_s} P_{\phi_s}\right]^2$$

$$\left. + \left[\frac{\partial C_{D_F}}{\partial \alpha_{s_0}} P_{\alpha_s}\right]^2 + \left[\frac{\partial C_{D_F}}{\partial \phi_{s_0}} P_{\phi_s}\right]^2\right)^{\frac{1}{2}}$$

$$= \pm\left(\left[(-1.635*10^{-6})4.36\right]^2 + \left[(1.897*10^{-7})3.71\right]^2 + \left[(2.040*10^{-4})2.580\right]^2 + \left[(1.427*10^{-5})10.934\right]^2\right.$$

$$+ 4\left\{\left[(2.919*10^{-7})48.91\right]^2 + \left[(2.919*10^{-7})5.03\right]^2\right\} + \left[(0.3375)0.00031\right]^2$$

$$\left. + \left[(0)0.00244\right]^2 + \left[(0.02269)0.00031\right]^2 + \left[(0)0.00244\right]2\right)^{\frac{1}{2}} = \pm 0.00056 \qquad (4\text{-}86)$$

$$U_{C_{D_F}} = \pm\left(B_{C_{D_F}}^2 + P_{C_{D_F}}^2\right)^{\frac{1}{2}} = (0.00016^2 + 0.00056^2)^{\frac{1}{2}} = \pm 0.00058 \qquad (4\text{-}87)$$

The precision limit for the drag coefficient can also be estimated by using an alternate method. The drag coefficient can be determined at the same test conditions repeatedly during the test, and an average drag coefficient can be calculated. The precision limit for the average drag coefficient can then be determined using the standard deviation of the repeated data multiplied by the coverage factor, K, corresponding to the number of repeated data points. Every effort must be taken to assure that all of the individual sources of precision error have been exercised between each of the repeated data points. The precision limit determined using this method will include the variation in the drag coefficient produced by the variation in setting the test conditions. The precision limit will only be valid for the test conditions, model attitude, and configuration for which the repeated data points were obtained and averaged. However, it should also be a good indicator of the precision limit at other conditions.

The choice of which method to use in estimating the precision limit will depend on many factors such as type of test, test budget, experience, and the test facility. Using the precision limits estimated from the uncertainty evaluation data, when they are reasonable estimates of the precision limits for the testing process, allows the calculation of a precision limit for each data point. Using a precision limit determined during the test will provide a value only for an averaged coefficient and, for almost all test programs, enough repeat data can only be obtained on a limited number of test conditions, model attitudes, and configurations. A combination of both methods can be used, although it must be remembered that one of the precision limits is for an individual data point whereas the other is estimated for an averaged coefficient. Regardless of the method used, the precision limit should be documented along with how it was determined and applied.

## 4.5 ADJUSTMENT TO THE AERODYNAMIC REFERENCE CONDITION

The next step in attaining the test objective is to adjust the aerodynamic coefficients determined for the model supported in the wind tunnel to the aerodynamic reference conditions. Referring to Fig. 1.2 and the discussion in Section 4.4, the only remaining adjustments are for wall and support interference. In this example only the application of the wall interference adjustment is illustrated. For other tests all of the necessary adjustments should be made to the data and the associated uncertainties applied and reported in the test documentation. To make the adjustment, a method of determining the magnitude of the wall interference is needed. In this example, the wall interference correction is the difference between the drag coefficient determined in Tunnels 4T and 16T since the drag coefficient determined in Tunnel 16T is assumed to be a wall interference-free reference.

$$C_{D_{WI}} = C_{D_{F_{16T}}} - C_{D_F} = 0.0690 - 0.0592 = 0.0098 \tag{4-88}$$

Having interference-free reference data is a rare luxury, and the correction usually has to be determined using an algorithm developed for the particular correction and, possibly, even the particular wind tunnel. If an algorithm is used to determine the correction, a method to estimate its uncertainty must be devised and documented. To estimate the uncertainty of the wall interference correction used here, the error sources shown in Fig. 1.2 must again be considered. The statements made in Section 4.4 concerning the error sources involved also apply. Additional sources of error that were considered and judged to provide an insignificant contribution to the estimated uncertainty are: model fidelity (same model used in both tests), support interference (same support used in both tests), and boundary-layer treatment (transition fixed at the same location using the same method in both tests). The uncertainty of the wall interference correction can be estimated by using the methods illustrated in this chapter. The forces and pressures acting on the model during each test were measured using the same balance (and balance calibration) and ESP system which results in correlated bias effects which will need to be included. This yields an uncertainty for the wall interference correction of

$$U_{C_{D_{WI}}} = \pm 0.00079 \tag{4-89}$$

Note that the correction is a fixed value and, as such, its uncertainty will be propagated as a bias limit into the bias limit for the aerodynamic drag coefficient at the aerodynamic reference condition.

Now that the wall interference correction has been determined, the drag coefficient can be adjusted to the aerodynamic reference conditions, and the uncertainty can be estimated.

$$C_{D_{F,AR}} = C_{D_F} + C_{D_{WI}} = 0.0592 + 0.0098 = 0.0690 \tag{4-90}$$

$$B_{C_{D_{F,AR}}} = \pm\left(B^2_{C_{D_F}} + U^2_{C_{D_{WI}}}\right)^{\frac{1}{2}} = \pm\left(0.00016^2 + 0.00079^2\right)^{\frac{1}{2}} = \pm 0.00081 \tag{4-91}$$

$$P_{C_{D_{F,AR}}} = P_{C_D} = \pm 0.00056 \tag{4-92}$$

$$U_{C_{D_{F,AR}}} = \pm\left(B^2_{C_{D_{FA,R}}} + P^2_{C_{D_{FA,R}}}\right)^{\frac{1}{2}} = \pm\left(0.00081^2 + 0.00056^2\right)^{\frac{1}{2}} = \pm 0.00099 \tag{4-93}$$

The adjustment made to the drag coefficient has been limited to wall interference in this example. The techniques shown for wall interference should be applied to all the corrections which need to be made to adjust the wind tunnel drag coefficient to the aerodynamic reference condition.

## 4.6 REPORTING UNCERTAITNY

The reporting of the uncertainty for a wind tunnel test is not limited to just documenting the uncertainties of the test conditions and aerodynamic coefficients. A complete report of the uncertainty for a test project should include the following:

1. A table similar to Table 4.2 containing the calibration uncertainties for the systems used during the test.

2. A table similar to Table 4.3 containing the uncertainties for the coefficients as well as the measured values used in reducing the aerodynamic forces, moments, and pressures to coefficient form.

3. A general discussion of the methods used to estimate the uncertainties.

4. A discussion on what adjustments have been made to the coefficients and how the uncertainties of the adjustments were estimated.

5. A discussion on what has been included in estimating the uncertainty of the coefficients.

The following paragraph contains an example of the uncertainty analysis discussion that would be included in the documentation of this example test. Remember that the uncertainty of any adjustment made to any parameter needs to be included in uncertainty analysis discussion.

> "The uncertainties for the systems used during the test are provided in Table 4.2 and were estimated using the methodology contained in AGARD-AR-304. The uncertainties of the wind tunnel test conditions were estimated from the tunnel calibration data and the uncertainty of the tunnel pressure instrumentation. The uncertainty of the Mach number calibration constant, DM, is provided in Table 4.2. The uncertainty evaluations for the instrumentation systems used on this test are available upon request. The uncertainties of the calculated parameters of interest are provided in Table 4.3 and were also estimated using the methodology contained in AGARD-AR-304. The uncertainty of the forebody drag coefficient for the model supported in the wind tunnel, $C_{D_F}$, includes the uncertainties of parameters contained in Tables 4.2 and 4.3. The uncertainty of the drag coefficient for the model at the aerodynamic reference conditions, $C_{D_{F,AR}}$, includes the uncertainty of the wall interference correction. The wall interference correction was determined by subtracting the drag coefficients determined in Tunnels 4T and 16T since the 16T data were assumed to be a wall interference free reference. The uncertainty of the wall interference correction is provided in Table 4.3 and was estimated by combining the uncertainties of the wind tunnel data determined in Tunnels 16T and 4T according to the methods contained in AGARD-AR-304."

Another topic to be addressed is the number of significant digits that should be quoted for a value and its uncertainty. The number of significant digits for the uncertainties is dependent on the uncertainty of the working standard and the quality of the instrumentation itself. One important thought to keep in mind when quoting uncertainties is that they are estimated values, and quoting uncertainties to 3 or more significant digits hardly seems like an estimate. The resolution of a device has no effect on the uncertainty except that the uncertainty can be no smaller than the resolution, however the uncertainty may be much larger than the resolution. In general, the number of significant digits quoted for a parameter should be approximately one order of magnitude less than the uncertainty of the parameter. For example, the forebody drag coefficient calculated in Eq. (4-84) is 0.059156390.... However, the uncertainty of $C_{D_F}$ is 0.00058 [Eq.(4-87)], and therefore the value quoted for $C_{D_F}$ is rounded to 0.0592. Note that values should be rounded to the appropriate significant digits only for quoted values and not for the value's use in calculations.

## REFERENCES

4.1 Sickles, W. and Erickson, J.C. "Wall Interference Correction for Three-Dimensional Transonic Flows." AIAA Paper No. 90-1408, AIAA 16th Aerodynamic Ground Testing Conference, Seattle, WA, June 18-20, 1990.

4.2 ISO/TAG/WG3 "Guide to the Expression of Uncertainty in Measurement." Draft dated June 1992

4.3 Cahill, D.M. "Development of an Uncertainty Methodology for Multiple-Channel Instrumentation Systems." AIAA Paper No. 92-3953, AIAA 17th Aerodynamic Ground Testing Conference, Nashville, TN, July 6-8, 1992.

## ANNEX 4-A

## UNCERTAINTY METHODOLOGY FOR MULTIPLE CHANNEL INSTRUMENTATION SYSTEMS

For systems with a relatively small number of channels, using and maintaining curve fits for the calibration uncertainty and precision limits for each channel is feasible. However, as the number of channels in a system increases, the task of maintaining and utilizing the curve fits for each channel becomes more and more difficult. At some point it becomes more practical to estimate a calibration uncertainty and precision limit that encompasses all of the channels of the system. Values for the calibration uncertainty and precision limits that are applicable for an entire system at each evaluation set point can be determined using the equations provided in this Annex. The development of the methodology is documented in [4.3]. The values determined for the system calibration uncertainty and precision limit at each set point provide an approximate 95-percent coverage of the values determined for each channel and set point. The methodology uses the distribution of the averages and standard deviations of the precision limits and the calibration uncertainties determined using Eqs. (4-11) and (4-13). The equations are used to calculate the calibration uncertainties and precision limits for the system which can then be used to determine the estimated uncertainty for a single measurement made using the system.

Subscripts i and j are defined as: i = individual channels
j = evaluation set points

The first step is to calculate an intermediate value for the calibration uncertainty by removing the uncertainty of the working standard.

$$I U_{cal_{ij}} = \left( U^2_{cal_{ij}} - U^2_{WS_j} \right)^{\frac{1}{2}} \tag{4-A-1}$$

The averages and standard deviations of the precision limits and intermediate calibration uncertainties for the individual channels are then calculated.

Averages for the precision limits and intermediate calibration uncertainties:

$$\bar{P}_{cal_j} = \pm \sum_{i=1}^{N} \frac{P_{cal_{ij}}}{N} \tag{4-A-2}$$

$$\overline{IU}_{cal_j} = \pm \sum_{i=1}^{N} \frac{I U_{cal_{ij}}}{N} \tag{4-A-3}$$

Standard deviations for the precision limits and intermediate calibration uncertainties:

$$S_{P_{cal_j}} = \pm \left( \sum_{i=1}^{N} \frac{\left( P_{cal_{ij}} - \bar{P}_{cal_j} \right)^2}{N-1} \right)^{\frac{1}{2}} \tag{4-A-4}$$

$$S_{IU_{cal_j}} = \pm \left( \sum_{i=1}^{N} \frac{\left( IU_{cal_{ij}} - \overline{IU}_{cal_j} \right)^2}{N-1} \right)^{\frac{1}{2}} \tag{4-A-5}$$

The above values were calculated assuming a normal distribution; however, in most instances the distribution is better represented by a log-normal distribution. Therefore, the following equations are used to convert the mean and standard deviations for a normal distribution to those for a log-normal distribution.

Log-normal standard deviations for the precision limits and intermediate calibration uncertainties:

$$Sln_{P_{cal_j}} = \pm \left( \ln \left( \frac{S^2_{P_{cal_j}}}{\overline{P}^2_{cal_j}} + 1 \right) \right)^{\frac{1}{2}} \tag{4-A-6}$$

$$Sln_{IU_{cal_j}} = \pm \left( \ln \left( \frac{S^2_{IU_{cal_j}}}{\overline{IU}^2_{cal_j}} + 1 \right) \right)^{\frac{1}{2}} \tag{4-A-7}$$

Log-normal mean values for the precision limits and intermediate calibration uncertainties:

$$T_{P_{cal_j}} = \pm \frac{\overline{P}_{cal_j}}{\exp\left( Sln^2_{P_{cal_j}}/2 \right)} \tag{4-A-8}$$

$$T_{IU_{cal_j}} = \pm \frac{\overline{IU}_{cal_j}}{\exp\left( Sln^2_{IU_{cal_j}}/2 \right)} \tag{4-A-9}$$

The log-normal mean values and standard deviations are then used to calculate the precision limit and intermediate calibration uncertainty for the system at each evaluation set point.

$$P_{cal_j} = \pm T_{P_{cal_j}} \left( \exp\left[ t_s \left( Sln_{P_{cal_j}} \right) \right] \right) \tag{4-A-10}$$

$$IU_{cal_j} = \pm T_{IU_{cal_j}} \left( \exp\left[ t_s \left( Sln_{IU_{cal_j}} \right) \right] \right) \tag{4-A-11}$$

The system intermediate calibration uncertainties are then combined with the uncertainty of the working standard to determine the estimates of the system calibration uncertainty at each evaluation set point.

$$U_{cal_j} = \pm \left( IU^2_{cal_j} + U^2_{WS_j} \right)^{\frac{1}{2}} \tag{4-A-12}$$

Note that the parameter $t_s$ in Eqs. (4-A-10) and (4-A-11) is the single-tailed Student's t distribution for a 95-percent confidence level. The value for $t_s$ can be determined using the following equation where **N** is the number of channels:

$$t_s = 1.645 + 1.525v^{-1} + 1.381v^{-2} + 1.090v^{-3} + 2.019v^{-4} + 0.210v^{-5} \text{ ; where } v = N - 1 \tag{4-A-13}$$

The system precision limits and calibration uncertainties can be combined to estimate the uncertainty of single measurements made using the system.

$$U_j = \pm \left( U^2_{cal_j} + P^2_{cal_j} \right)^{\frac{1}{2}} \tag{4-A-14}$$

Curve fitting values of $P_{cal_j}$ and $U_{cal_j}$ against the evaluation set points, j, will then allow the system precision limit and calibration uncertainty (measurement bias limit) to be determined for any value measured by the system.

## ANNEX 4-B

## DETERMINATION AND EVALUATION OF THE PARTIAL DERIVATIVES USED IN THE TEXT

This appendix contains the partial derivatives that are presented in the equations used in the text. Note that the partial derivatives must be taken with respect to the independent parameters. For example, the free-stream dynamic pressure, q, is calculated using the free-stream values of the static pressure, p, and Mach number, M. However, p and M are dependent since both are functions of the measured values of $p_T$ and $p_C$ and the appropriate Mach number calibration constant **DM,** which are independent parameters. Note that the tunnel conditions M, p, and q are calculated using equations that were derived assuming isentropic flow in a perfect gas. For the derivatives shown below, the specific heat ratio constant, y ($\gamma = 1.4$), was assumed to have insignificant error; therefore, derivatives were not taken with respect to $\gamma$.

The partial derivatives shown here are in some cases very complex. The partial derivatives shown were determined using a symbolic mathematics program on a personal computer and once determined, they will not change unless the data reduction equations are changed. The partial derivatives can be determined numerically by using finite increments of the independent parameters. The numerical partial derivatives are normally determined using the data reduction algorithm and incrementing each of the independent parameters individually and recording the changes in the dependent parameters. The magnitude of the increments should be sufficiently small such that the correct magnitude of the partial derivatives will be estimated.

### Mach Number, M

The free-stream Mach number, M [Eq. (4-15)], is a function of the measured values of $p_T$ and $p_C$ and the Mach number calibration constants DM. Taking the partial derivatives of M with respect to these parameters and substituting for the values of the parameters produces the values of the partial derivatives used in this example.

$$\frac{\partial M}{\partial p_T} = \left( \frac{0.31944}{p_C \left[\frac{p_T}{p_C}\right]^{\frac{5}{7}} \left[ \left(\frac{p_T}{p_C}\right)^{\frac{2}{7}} - 1 \right]^{\frac{1}{2}}} \right) = \left( \frac{0.31944}{38216.38 \left[\frac{67690.35}{38216.38}\right]^{\frac{5}{7}} \left[ \left(\frac{67690.35}{38216.38}\right)^{\frac{2}{7}} - 1 \right]^{\frac{1}{2}}} \right) = 1.319 * 10^{-5} \qquad (4\text{-B-1})$$

$$\frac{\partial M}{\partial p_C} = \left| \frac{-0.31944 p_T}{p_C^2 \left[\frac{p_T}{p_C}\right]^{\frac{5}{7}} \left[ \left(\frac{p_T}{p_C}\right)^{\frac{2}{7}} - 1 \right]^{\frac{1}{2}}} \right| = \left( 38216.38^2 \left[\frac{67690.35}{38216.38}\right]^{\frac{5}{7}} \left[ \left(\frac{67690.35}{38216.38}\right)^{\frac{2}{7}} - 1 \right]^{\frac{1}{2}} \right) = -2.337 * 10^{-5} \qquad (4\text{-B-2})$$

$$\frac{\partial M}{\partial DM} = 1 \qquad (4\text{-B-3})$$

### Static pressure, p

The free-stream static pressure, p [Eq. (4-16)], is a function of the measured values of $p_T$ and $p_C$ and the Mach number calibration constants DM. Taking the partial derivatives of p with respect to these parameters and substituting for the values of the parameters produces the values of the partial derivatives used in this example.

$$\frac{\partial p}{\partial p_T} = \left( \frac{-0.44721 p(M)}{p_C \left[\frac{p_T}{p_C}\right]^{\frac{5}{7}} \left[ \left(\frac{p_T}{p_C}\right)^{\frac{2}{7}} - 1 \right]^{\frac{1}{2}} \left[1 + 0.20M^2\right]} + \frac{p}{p_T} \right)$$

$$= \left( \frac{-0.44721(37870.04)(0.95)}{38216.38 \left[\frac{67690.35}{38216.38}\right]^{\frac{5}{7}} \left[ \left(\frac{67690.35}{38216.38}\right)^{\frac{2}{7}} - 1 \right]^{\frac{1}{2}} \left[1 + 0.20(0.95)^2\right]} + \frac{37870.04}{67690.35} \right) = -0.003344 \qquad (4\text{-B-4})$$

$$\frac{\partial p}{\partial p_C} = \left( \frac{0.44721 p_T (p)(M)}{p_C^2 \left[\frac{p_T}{p_C}\right]^{\frac{5}{7}} \left[ \left(\frac{p_T}{p_C}\right)^{\frac{2}{7}} - 1 \right]^{\frac{1}{2}} [1 + 0.20M^2]} \right)$$

$$= \left( \frac{0.44721(67690.35)(37870.04)(0.95)}{38216.38^2 \left[\frac{67690.35}{38216.38}\right]^{\frac{5}{7}} \left[ \left(\frac{67690.35}{38216.38}\right)^{\frac{2}{7}} - 1 \right]^{\frac{1}{2}} [1 + 0.20(0.95)^2]} \right) = 0.9969 \qquad (4\text{-B-}5)$$

$$\frac{\partial p}{\partial DM} = \left( \frac{-1.40 p(M)}{[1 + 0.20M^2]} \right) = \left( \frac{-1.40(37870.04)(0.95)}{[1 + 0.20(0.95)^2]} \right) = -42665.95 \qquad (4\text{-B-}6)$$

**Dynamic pressure, q**

The free-stream dynamic pressure, q [Eq. (4-17)], is a function of the measured values of $p_T$ and $p_C$ and the Mach number calibration constants DM. Taking the partial derivatives of q with respect to these parameters and substituting for the values of the parameters produces the values of the partial derivatives used in this example.

$$\frac{\partial q}{\partial p_T} = \left( \frac{p(M)(0.44721 - 0.22361M^2)}{p_C \left[\frac{p_T}{p_C}\right]^{\frac{5}{7}} \left[ \left(\frac{p_T}{p_C}\right)^{\frac{2}{7}} - 1 \right]^{\frac{1}{2}} [1 + 0.20M^2]} + \frac{q}{p_T} \right)$$

$$= \left( \frac{37870.04(0.95)(0.44721 - 0.22361(0.95)^2)}{38216.38 \left[\frac{67690.35}{38216.38}\right]^{\frac{5}{7}} \left[ \left(\frac{67690.35}{38216.38}\right)^{\frac{2}{7}} - 1 \right]^{\frac{1}{2}} [1 + 0.20(0.95)^2]} + \frac{23924.40}{67690.35} \right) = 0.6623 \qquad (4\text{-B-}7)$$

$$\frac{\partial q}{\partial p_C} = \left( \frac{-p_T (p)(M)(0.44721 - 0.22361M^2)}{p_C^2 \left[\frac{p_T}{p_C}\right]^{\frac{5}{7}} \left[ \left(\frac{p_T}{p_C}\right)^{\frac{2}{7}} - 1 \right]^{\frac{1}{2}} [1 + 0.20M^2]} \right)$$

$$= \left( \frac{-67690.35(37870.04)(0.95)(0.44721 - 0.22361(0.95)^2)}{38216.38^2 \left[\frac{67690.35}{38216.38}\right]^{\frac{5}{7}} \left[ \left(\frac{67690.35}{38216.38}\right)^{\frac{2}{7}} - 1 \right]^{\frac{1}{2}} [1 + 0.20(0.95)^2]} \right) = -0.5470 \qquad (4\text{-B-}8)$$

$$\frac{\partial q}{\partial DM} = \left( \frac{p(M)(-0.98M^2 + 1.40[1 + 0.20M^2])}{[1 + 0.20M^2]} \right)$$

$$= \left( \frac{37870.04(0.95)(-0.98[0.95]^2 + 1.40[1 + 0.20(0.95)^2])}{[1 + 0.20(0.95)^2]} \right) = 23412.94 \qquad (4\text{-B-}9)$$

**Model Attitude, $\alpha$ and $\beta$**

The model attitude, $\alpha$ and $\beta$ [Eqs. (4-30) and (4-31)], are functions of the measured values of $\alpha_s$ and $\phi_s$. Taking the partial derivatives of $\alpha$ and $\beta$ with respect to these parameters and substituting for the values of the parameters produces the values of the partial derivatives used in this example.

$$\frac{\partial \alpha}{\partial \alpha_s} = \frac{\text{Cos}(\phi_s)}{\text{Cos}^2(\alpha_s) + \text{Cos}^2(\phi_s)\,\text{Sin}^2(\alpha_s)} = \frac{\text{Cos}(0)}{\text{Cos}^2(4.00) + \text{Cos}^2(0)\,\text{Sin}^2(4.00)} = \qquad (4\text{-B-}10)$$

$$\frac{\partial \alpha}{\partial \phi_s} = \frac{-\text{Sin}(\phi_s)\text{Tan}(\alpha_s)}{1+\text{Cos}^2(\phi_s)\,\text{Tan}^2(\alpha_s)} = \frac{-\text{Sin}(0)\text{Tan}(4.00)}{1+\text{Cos}^2(0)\,\text{Tan}^2(4.00)} = 0 \qquad (4\text{-B-}11)$$

$$\frac{\partial \beta}{\partial \alpha_s} = \frac{\text{Sin}(\phi_s)\text{Cos}(\alpha_s)}{\sqrt{1+\text{Sin}^2(\phi_s)\,\text{Sin}^2(\alpha_s)}} = \frac{\text{Sin}(0)\text{Cos}(4.00)}{\sqrt{1+\text{Sin}^2(0)\,\text{Sin}^2(4.00)}} = 0 \qquad (4\text{-B-}12)$$

$$\frac{\partial \beta}{\partial \phi_s} = \frac{\text{Sin}(\alpha_s)\text{Cos}(\phi_s)}{\sqrt{1+\text{Sin}^2(\phi_s)\,\text{Sin}^2(\alpha_s)}} = \frac{\text{Sin}(4.00)\text{Cos}(0)}{\sqrt{1+\text{Sin}^2(0)\,\text{Sin}^2(4.00)}} = 0.06959 \qquad (4\text{-B-}13)$$

**Measured Gross Axial and Normal Forces, $F_{A_G}$ and $F_{N_G}$**

The measured gross axial and normal forces, $F_{A_G}$ and $F_{N_G}$ [Eqs. (4-39) and (4-40))], are functions of the measured values of $F_{A_M}$ or $F_{N_M}$, $\alpha_{s_o}$, $\phi_{s_o}$, and the constant $W_A$ or $W_N$. Taking the partial derivatives of $F_{A_G}$ and $F_{N_G}$ with respect to these parameters and substituting for the values of the parameters produces the values of the partial derivatives used in this example.

$$\frac{\partial F_{A_G}}{\partial F_{A_M}} = 1 \qquad (4\text{-B-}14)$$

$$\frac{\partial F_{A_G}}{\partial W_A} = \text{Sin}(\alpha_{s_0}) = \text{Sin}(0.00) = 0 \qquad (4\text{-B-}15)$$

$$\frac{\partial F_{A_G}}{\partial \alpha_{s_0}} = W_A\text{Cos}(\alpha_{s_0}) = 111.205\text{Cos}(0.00) = 111.205 \qquad (4\text{-B-}16)$$

$$\frac{\partial F_{N_G}}{\partial F_{N_M}} = 1 \qquad (4\text{-B-}17)$$

$$\frac{\partial F_{N_G}}{\partial W_N} = -\text{Cos}(\alpha_{s_0})\text{Cos}(\phi_{s_0}) = -\text{Cos}(0.00)\text{Cos}(0.0) = -1 \qquad (4\text{-B-}18)$$

$$\frac{\partial F_{N_G}}{\partial \alpha_{s_0}} = W_N\text{Sin}(\alpha_{s_0})\text{Cos}(\phi_{s_0}) = 111.205\text{Sin}(0.00)\text{Cos}(0.0) = 0 \qquad (4\text{-B-}19)$$

$$\frac{\partial F_{N_G}}{\partial \phi_{s_0}} = W_N\text{Cos}(\alpha_{s_0})\text{Sin}(\phi_{s_0}) = 111.205\text{Cos}(0.00)\text{Sin}(0.0) = 0 \qquad (4\text{-B-}20)$$

**Model Tare Weights, $F_{A_{ST}}$ and $F_{N_{ST}}$**

The model tare weights corrections, $F_{A_{ST}}$ and $F_{N_{ST}}$ [Eqs. (4-47) and (4-48)], are functions of the measured values of $\alpha_s$ and $\phi_s$ and the constants $W_A$ or $W_N$. Taking the partial derivatives of $F_{A_{ST}}$ and $F_{N_{ST}}$ with respect to these parameters and substituting for the values of the parameters produces the values of the partial derivatives used in this example.

$$\frac{\partial F_{A_{ST}}}{\partial W_A} = \text{Sin}(\alpha_s) = \text{Sin}(4.00) = 0.06976 \qquad (4\text{-B-}21)$$

$$\frac{\partial F_{A_{ST}}}{\partial \alpha_s} = W_A\text{Cos}(\alpha_s) = 111.205\text{Cos}(4.00) = 110.934 \qquad (4\text{-B-}22)$$

$$\frac{\partial F_{N_{ST}}}{\partial W_N} = -\text{Cos}(\alpha_s)\text{Cos}(\phi_s) = -\text{Cos}(4.00)\text{Cos}(0.0) = -0.9976 \qquad (4\text{-B-}23)$$

$$\frac{\partial F_{N_{ST}}}{\partial \alpha_s} = W_N\text{Sin}(\alpha_s)\text{Cos}(\phi_s) = 111.205\text{Sin}(4.00)\text{Cos}(0.0) = 7.757 \qquad (4\text{-B-}24)$$

$$\frac{\partial F_{N_{ST}}}{\partial \phi_s} = W_N \text{Cos}(\alpha_s)\text{Sin}(\phi_s) = 111.205\text{Cos}(4.00)\text{Sin}(0.0) = 0 \quad (4\text{-B-}25)$$

Model Aerodynamic Normal and Axial Forces, $F_A$ and $F_N$

The model aerodynamic normal and axial forces, $F_A$ and $F_N$ [Eqs. (4-55) and (4-56)], are functions of the measured values of $\alpha_{s_0}$, $\phi_{s_0}$, $\alpha_s$, $\phi_s$, $F_{A_M}$ or $F_{N_M}$, and the constant $W_A$ or $W_N$. Taking the partial derivatives of $F_A$ and $F_N$ with respect to these parameters and substituting for the values of the parameters produces the values of the partial derivatives used in this example.

$$\frac{\partial F_A}{\partial F_{A_M}} = 1 \quad (4\text{-B-}26)$$

$$\frac{\partial F_A}{\partial W_A} = \text{Sin}(\alpha_{s_0}) - \text{Sin}(\%) = \text{Sin}(0.00) - \text{Sin}(4.00) = -0.06976 \quad (4\text{-B-}27)$$

$$\frac{\partial F_A}{\partial \alpha_s} = -W_A \text{Cos}(\alpha_s) = -111.205\text{Cos}(4.00) = -110.934 \quad (4\text{-B-}28)$$

$$\frac{\partial F_A}{\partial \alpha_{s_0}} = W_A \text{Cos}(\alpha_{s_0}) = 111.205\text{Cos}(0.00) = 111.205 \quad (4\text{-B-}29)$$

$$\frac{\partial F_N}{\partial F_{N_M}} = 1 \quad (4\text{-B-}30)$$

$$\frac{\partial F_N}{\partial W_N} = \text{Cos}(\alpha_s)\text{Cos}(\phi_s) - \text{Cos}(\alpha_{s_0})\text{Cos}(\phi_{s_0}) = \text{Cos}(4.00)\text{Cos}(0.0) - \text{Cos}(0.00)\text{Cos}(0.0) = -0.002436 \quad (4\text{-B-}31)$$

$$\frac{\partial F_N}{\partial \alpha_s} = -W_N \text{Sin}(\alpha_s)\text{Cos}(\phi_s) = -111.205\text{Sin}(4.00)\text{Cos}(0.0) = -7.757 \quad (4\text{-B-}32)$$

$$\frac{\partial F_N}{\partial \phi_s} = -W_N \text{Cos}(\alpha_s)\text{Sin}(\phi_s) = -111.205\text{Cos}(4.00)\text{Sin}(0.0) = 0 \quad (4\text{-B-}33)$$

$$\frac{\partial F_N}{\partial \alpha_{s_0}} = W_N \text{Sin}(\alpha_{s_0})\text{Cos}(\phi_{s_0}) = 111.205\text{Sin}(0.00)\text{Cos}(0.0) = 0 \quad (4\text{-B-}34)$$

$$\frac{\partial F_N}{\partial \phi_{s_0}} = W_N \text{Cos}(\alpha_{s_0})\text{Sin}(\phi_{s_0}) = 111.205\text{Cos}(0.00)\text{Sin}(0.0) = 0 \quad (4\text{-B-}35)$$

Model Average Base Pressure, $\bar{p}_B$

The average base pressure, $\bar{p}_B$ [Eq. (4-67)], is a function of the measured values of $p_{B_{Mi}}$ and $p_{REF}$. Taking the partial derivatives of $\bar{p}_B$ with respect to these parameters and substituting for the values of the parameters produces the values of the partial derivatives used in this example.

$$\frac{\partial \bar{p}_B}{\partial p_{B_{Mi}}} = \frac{1}{4} \quad (4\text{-B-}36)$$

$$\frac{\partial \bar{p}_B}{\partial p_{REF}} = \frac{1}{4} \quad (4\text{-B-}37)$$

Model Base Axial Force, $F_{A_B}$

The model base axial force, $F_{A_B}$, [Eq. (4-68)], is a function of the measured values of $p_T$, $p_C$, $A_B$, $p_{B_{Mi}}$, and $p_{REF}$ and the Mach number calibration constants DM. Taking the partial derivatives of $F_{A_B}$

with respect to these parameters and substituting for the values of the parameters produces the values of the partial derivatives used in this example.

$$\frac{\partial F_{A_B}}{\partial p_T} = A_B \left( \frac{-0.44721 p(M)}{p_C \left[\frac{p_T}{p_C}\right]^{\frac{5}{7}} \left[ \left(\frac{p_T}{p_C}\right)^{\frac{2}{7}} - 1 \right]^{\frac{1}{2}} \left[1 + 0.20M^2\right]} + \frac{p}{p_T} \right)$$

$$= 0.005723 \left( \frac{-0.44721(37870.04)(0.95)}{38216.38 \left[\frac{67690.35}{38216.38}\right]^{\frac{5}{7}} \left[ \left(\frac{67690.35}{38216.38}\right)^{\frac{2}{7}} - 1 \right]^{\frac{1}{2}} \left[1 + 0.20(0.95)^2\right]} + \frac{37870.04}{67690.35} \right)$$

$$= -1.914 * 10^{-5} \qquad \text{(4-B-38)}$$

$$\frac{\partial F_{A_B}}{\partial p_C} = \left( \frac{0.44721 p_T(p)(M)(A_B)}{p_C^2 \left[\frac{p_T}{p_C}\right]^{\frac{5}{7}} \left[ \left(\frac{p_T}{p_C}\right)^{\frac{2}{7}} - 1 \right]^{\frac{1}{2}} \left[1 + 0.20M^2\right]} \right)$$

$$= \left( \frac{(0.95)(0.005723)}{38216.38^2 \left[\frac{67690.35}{38216.38}\right]^{\frac{5}{7}} \left[ \left(\frac{67690.35}{38216.38}\right)^{\frac{2}{7}} - 1 \right]^{\frac{1}{2}} \left[1 + 0.20(0.95)^2\right]} \right) = 0.005705 \qquad \text{(4-B-39)}$$

$$\frac{\partial F_{A_B}}{\partial DM} = \frac{-1.40 A_B(p)(M)}{1 + 0.20M^2} = \frac{-1.40(0.005723)(37870.04)(0.95)}{1 + 0.20(0.95)^2} = -244.18 \qquad \text{(4-B-40)}$$

$$\frac{\partial F_{A_B}}{\partial A_B} = p - \bar{p}_B = 37870.04 - 36388.80 = 1481.24 \qquad \text{(4-B-41)}$$

$$\frac{\partial F_{A_B}}{\partial p_{B_{Mi}}} = \frac{-A_B}{4} = \frac{-0.005723}{4} = -0.00143 \qquad \text{(4-B-42)}$$

$$\frac{\partial F_{A_B}}{\partial p_{REF}} = \frac{-A_B}{4} = \frac{-0.005723}{4} = -0.00143 \qquad \text{(4-B-43)}$$

**Model Forebody Axial Force, $F_{A_F}$**

The model forebody axial force, $F_{A_F}$ [Eq. (4-69)], is a function of the measured values of $p_T$, $p_C$, $A_B$, $p_{B_{Mi}}$, $p_{REF}$, $F_{A_M}$, $\alpha_s$, and $\alpha_{s_0}$ and the constants $W_A$ and DM. Taking the partial derivatives of $F_{A_F}$ with respect to these parameters and substituting for the values of the parameters produces the values of the partial derivatives used in this example.

$$\frac{\partial F_{A_F}}{\partial p_T} = -A_B \left( \frac{-0.44721 p(M)}{p_C \left[\frac{p_T}{p_C}\right]^{\frac{5}{7}} \left[ \left(\frac{p_T}{p_C}\right)^{\frac{2}{7}} - 1 \right]^{\frac{1}{2}} \left[1 + 0.20M^2\right]} + \frac{P}{p_T} \right|$$

$$= -0.005723 \left( \frac{-0.44721(37870.04)(0.95)}{38216.38 \left[\frac{67690.35}{38216.38}\right]^{\frac{5}{7}} \left[ \left(\frac{67690.35}{38216.38}\right)^{\frac{2}{7}} - \right]^{\frac{1}{2}} \left[1 + 0.20(0.95)^2\right]} + \frac{37870.04}{67690.35} \right)$$

$$= 1.914 * 10^{-5} \qquad \text{(4-B-44)}$$

$$\frac{\partial F_{A_F}}{\partial p_C} = \left( \frac{-0.44721 p_T (p)(M)(A_B)}{p_C^2 \left[\frac{p_T}{p_C}\right]^{\frac{5}{7}} \left[ \left(\frac{p_T}{p_C}\right)^{\frac{2}{7}} - 1 \right]^{\frac{1}{2}} \left[1 + 0.20M^2\right]} \right)$$

$$= \left( \frac{-0.44721(67690.35)(37870.04)(0.95)(0.005723)}{38216.38^2 \left[\frac{67690.35}{38216.38}\right]^{\frac{5}{7}} \left[ \left(\frac{67690.35}{38216.38}\right)^{\frac{2}{7}} - 1 \right]^{\frac{1}{2}} \left[1 + 0.20(0.95)^2\right]} \right) = -0.005705 \qquad (4\text{-B-}45)$$

$$\frac{\partial F_{A_F}}{\partial DM} = \frac{1.40 A_B (p)(M)}{1 + 0.20M^2} = \frac{140(0.005723)(37870.04)(0.95)}{1 + 0.20(0.95)^2} = 244.18 \qquad (4\text{-B-}46)$$

$$\frac{\partial F_{A_F}}{\partial A_B} = \bar{p}_B - p = 36388.80 - 37870.04 = -1481.24 \qquad (4\text{-B-}47)$$

$$\frac{\partial F_{A_F}}{\partial F_{A_M}} = I \qquad (4\text{-B-}48)$$

$$\frac{\partial F_{A_F}}{\partial p_{B_{Mi}}} = \frac{A_B}{4} = \frac{0.005723}{4} = 0.00143 \qquad (4\text{-B-}49)$$

$$\frac{\partial F_{A_F}}{\partial p_{REF}} = \frac{A_B}{4} = \frac{0.005723}{4} = 0.00143 \qquad (4\text{-B-}50)$$

$$\frac{\partial F_{A_F}}{\partial W_A} = \mathrm{Sin}(\alpha_{s_0}) - \mathrm{Sin}(\alpha_s) = \mathrm{Sin}(0.00) - \mathrm{Sin}(4.00) = -0.06976 \qquad (4\text{-6-}51)$$

$$\frac{\partial F_{A_F}}{\partial \alpha_s} = -W_A \mathrm{Cos}(\alpha_s) = -111.205\mathrm{Cos}(4.00) = -110.934 \qquad (4\text{-6-}52)$$

$$\frac{\partial F_{A_F}}{\partial \alpha_{s_0}} = W_A \mathrm{Cos}(\alpha_{s_0}) = 111.205\mathrm{Cos}(0.00) = 111.205 \qquad (4\text{-B-}53)$$

**Model Forebody Drag Coefficient, $C_{D_F}$**

The model forebody drag coefficient, $C_{D_F}$ [Eq. (4-84)], is a function of the measured values of $p_T$, $p_C$, $A_B$, $p_{B_{Mi}}$, $p_{REF}$, $F_{A_M}$, $F_{N_M}$, $\alpha_s$, $\phi_s$, $\alpha_{s_0}$, and $\phi_{s_r}$ and the constants $W_A$, $W_N$, and DM. Taking the partial derivatives of $C_{D_F}$ with respect to these parameters and substituting for the values of the parameters produces the values of the partial derivatives used in this example.

$$\frac{\partial C_{D_F}}{\partial p_T} = \left[ \left( \frac{-1.42857 A_B \mathrm{Cos}(\alpha)}{A(p_C)(M)^2} \left( \frac{-0.44721 M \left[1 + 0.20M^2\right]^{-1}}{\left[\frac{p_T}{p_C}\right]^{\frac{5}{7}} \left[ \left(\frac{p_T}{p_C}\right)^{\frac{2}{7}} - 1 \right]^{\frac{1}{2}}} + \frac{p_C}{p_T} \right) \right) \right.$$

$$\left. + \left( \frac{0.638877 C_{D_F} \left[ q(1 + 0.20M^2)^{2.5} - p_T \right]}{p_C (p_T)(M) \left[\frac{p_T}{p_C}\right]^{\frac{5}{7}} \left[ \left(\frac{p_T}{p_C}\right)^{\frac{2}{7}} - 1 \right]^{\frac{1}{2}}} \right) - \frac{C_{D_F}}{p_T} \right]$$

$$- \left[ \left( \frac{-1.42857(0.005723)\mathrm{Cos}(4.00)}{0.20439(38216.38)(0.95)^2} \left( \frac{-0.44721(0.95)\left[1 + 0.20(0.95)^2\right]^{-1}}{\left[\frac{67690.35}{38216.38}\right]^{\frac{5}{7}} \left[ \left(\frac{67690.35}{38216.38}\right)^{\frac{2}{7}} - 1 \right]^{\frac{1}{2}}} + \frac{38216.38}{67690.35} \right) \right) \right.$$

$$\left. + \left( \frac{0.638877(0.0592)\left[23924.40(1 + 0.20[0.95]^2)^{2.5} - 67690.35\right]}{38216.38(67690.35)(0.95)\left[\frac{67690.35}{38216.38}\right]^{\frac{5}{7}} \left[ \left(\frac{67690.35}{38216.38}\right)^{\frac{2}{7}} - 1 \right]^{\frac{1}{2}}} - \frac{0.0592}{67690.35} \right) \right] = -1.635 * 10^{-6} \qquad (4\text{-B-}54)$$

$$\frac{\partial C_{D_F}}{\partial p_C} = \left[\left(\frac{C_{D_F}(q)(1+0.20M^2)^{2.5}\left[0.912681(1+0.20M^2) - 0.638877M^2\right]}{p_C^2(M)^3\left[\frac{p_T}{p_C}\right]^{\frac{5}{7}}\left[\left(\frac{p_T}{p_C}\right)^{\frac{2}{7}} - 1\right]^{\frac{1}{2}}}\right)\right.$$

$$\left. + \left(\frac{-0.638877A_B(p_T)\mathrm{Cos}(a)}{p_C^2(M)(A)\left[\frac{p_T}{p_C}\right]^{\frac{5}{7}}\left[\left(\frac{p_T}{p_C}\right)^{\frac{2}{7}} - 1\right]^{\frac{1}{2}}\left[1 + 0.20M^2\right]}\right)\right]$$

$$= \left[\left(\frac{0.0592(23924.40)\left[1+0.20(0.95)^2\right]^{2.5}\left[0.912681\left(1+0.20[0.95]^2\right) - 0.638877(0.95)^2\right]}{38216.38^2(0.95)^3\left[\frac{67690.35}{38216.38}\right]^{\frac{5}{7}}\left[\left(\frac{67690.35}{38216.38}\right)^{\frac{2}{7}} - 1\right]^{\frac{1}{2}}}\right)\right.$$

$$\left. + \left(\frac{-0.638877(0.005723)(67690.35)\mathrm{Cos}(4.00)\left[1 + 0.20(0.95)^2\right]^{-1}}{38216.38^2(0.95)(0.20439)\left[\frac{67690.35}{38216.38}\right]^{\frac{5}{7}}\left[\left(\frac{67690.35}{38216.38}\right)^{\frac{2}{7}} - 1\right]^{\frac{1}{2}}}\right)\right] = 1.897*10^{-7} \quad (4\text{-B-}55)$$

$$\frac{\partial C_{D_F}}{\partial DM} = \left[\frac{2C_{D_F}}{M}\left(\frac{0.7M^2}{1+0.20M^2} - 1\right) + \left(\frac{2A_B\mathrm{Cos}(\alpha)}{M(A)\left[1+0.20M^2\right]}\right)\right]$$

$$= \left[\frac{(0.0592)}{0.95}\left(\frac{0.7(0.95)^2}{1+0.20(0.95)^2} - 1\right) + \left(\frac{2(0.005723)\mathrm{Cos}(4.00)}{0.95(0.20439)\left[1+0.20(0.95)^2\right]}\right)\right] = -0.008121 \quad (4\text{-B-}56)$$

$$\frac{\partial C_{D_F}}{\partial A_B} = \frac{1.42857\mathrm{Cos}(\alpha)\left(\bar{p}_B - p\right)}{p(M)^2(A)} = \frac{1.42857\mathrm{Cos}(4.00)\ (36388.80 - 37870.04)}{37870.04(0.95)^2(0.20439)} = -0.3022 \quad (4\text{-B-}57)$$

$$\frac{\partial C_{D_F}}{\partial F_{A_M}} = \frac{1.42857\mathrm{Cos}(\alpha)}{p(M)^2(A)} = \frac{1.42857\mathrm{Cos}(4.00)}{37870.04(0.95)^2(0.20439)} = 2.040*10^{-4} \quad (4\text{-B-}58)$$

$$\frac{\partial C_{D_F}}{\partial F_{N_M}} = \frac{1.42857\mathrm{Sin}(\alpha)}{p(M)^2(A)} = \frac{1.42857\mathrm{Sin}(4.00)}{37870.04(0.95)^2(0.20439)} = 1.427*10^{-5} \quad (4\text{-B-}59)$$

$$\frac{\partial C_{D_F}}{\partial p_{B_{Mi}}} = -\frac{0.357143A_B\mathrm{Cos}(\alpha)}{p(M)^2(A)} = \frac{0.357143(0.005723)\mathrm{Cos}(4.00)}{37870.04(0.95)^2(0.20439)} = 2.919*10^{-7} \quad (4\text{-B-}60)$$

$$\frac{\partial C_{D_F}}{\partial p_{REF}} = -\frac{0.357143A_B\mathrm{Cos}(\alpha)}{p(M)^2(A)} = \frac{0.357143(0.005723)\mathrm{Cos}(4.00)}{37870.04(0.95)^2(0.20439)} = 2.919*10^{-7} \quad (4\text{-B-}61)$$

$$\frac{\partial C_{D_F}}{\partial W_A} = \frac{\mathrm{Cos}(\alpha)\left[\mathrm{Sin}(\alpha_{s_0}) - \mathrm{Sin}(\alpha_s)\right]}{Aq} = \frac{\mathrm{Cos}(4.00)\left[\mathrm{Sin}(0.00) - \mathrm{Sin}(4.00)\right]}{0.20439\ (23924.40)} = -1.423*10^{-5} \quad (4\text{-B-}62)$$

$$\frac{\partial C_{D_F}}{\partial W_N} = \frac{\mathrm{Sin}(\alpha)\left[\mathrm{Cos}(\alpha_s)\mathrm{Cos}(\phi_s) - \mathrm{Cos}(\alpha_{s_0})\mathrm{Cos}(\phi_{s_0})\right]}{Aq}$$

$$- \frac{\mathrm{Sin}(4.00)\left[\mathrm{Cos}(4.00)\mathrm{Cos}(0.0) - \mathrm{Cos}(0.00)\mathrm{Cos}(0.0)\right]}{0.20439\ (23924.40)} = -3.475*10^{-8} \quad (4\text{-B-}63)$$

$$\frac{\partial C_{D_F}}{\partial \alpha_s} = \frac{1}{Aq}\left[-W_N \text{Cos}(\phi_s)\text{Sin}(\alpha_s)\text{Sin}(\alpha) - W_A \text{Cos}(\alpha_s)\text{Cos}(\alpha) + \frac{\text{Cos}(\phi_s)[F_N \text{Cos}(\alpha) - F_{A_F}\text{Sin}(\alpha)]}{\text{Cos}^2(\alpha_s)[1 + \text{Cos}^2(\phi_s)\text{Tan}^2(\alpha_s)]}\right]$$

$$-\frac{1}{0.20439(23924.40)}\left[-111.205\text{Cos}(0.0)\text{Sin}(4.00)\text{Sin}(4.00) - 111.205\text{Cos}(4.00)\text{Cos}(4.00)\right.$$

$$\left.+\frac{\text{Cos}(0.0)[1777.368\text{Cos}(4.00) - 165.690\text{Sin}(4.00)]}{\text{Cos}^2(4.00)[1 + \text{Cos}^2(0.0)\text{Tan}^2(4.00)]}\right] = 0.3375 \qquad (4\text{-B-64})$$

$$\frac{\partial C_{D_F}}{\partial \phi_s} = \frac{-1}{Aq}\left[W_N \text{Cos}(\alpha_s)\text{Sin}(\phi_s)\text{Sin}(\alpha) + \frac{\text{Sin}(\phi_s)\text{Tan}(\alpha_s)[F_N \text{Cos}(\alpha) + F_{A_F}\text{Sin}(\alpha)]}{1 + \text{Cos}^2(\phi_s)\text{Tan}^2(\alpha_s)}\right]$$

$$-\frac{-1}{0.20439\,(23924.40)}\left[111.205\text{Cos}(4.00)\text{Sin}(0.0)\text{Sin}(4.00)\right.$$

$$\left.+\frac{\text{Sin}(0.0)\text{Tan}(4.00)[1777.368\text{Cos}(4.00) + 165.690\text{Sin}(4.00)]}{1 + \text{Cos}^2(0.0)\text{Tan}^2(4.00)}\right] = 0.000 \qquad (4\text{B-65})$$

$$\frac{\partial C_{D_F}}{\partial \alpha_{s_0}} = -\frac{W_A \text{Cos}(\alpha_{s_0})\text{Cos}(\alpha) + W_N \text{Sin}(\alpha_{s_0})\text{Cos}(\phi_{s_0})\text{Sin}(\alpha)}{Aq}$$

$$-\frac{111.205\text{Cos}(0.00)\text{Cos}(4.00) + 111.205\text{Sin}(0.00)\text{Cos}(0.0)\text{Sin}(4.00)}{0.20439\,(23924.40)} = 0.02269 \qquad (4\text{-B-66})$$

$$\frac{\partial C_{D_F}}{\partial \phi_{s_0}} = -\frac{W_N \text{Cos}(\alpha_{s_0})\text{Sin}(\phi_{s_0})\text{Sin}(\alpha)}{Aq} - \frac{111.205\text{Cos}(0.00)\text{Sin}(0.0)\text{Sin}(4.00)}{0.20439\,(23924.40)} = 0.0 \qquad (4\text{-B-67})$$

## ANNEX 4-C

## THE EFFECT OF DETERMINING THE PARTIAL DERIVATIVES WITH RESPECT TO DEPENDENT PARAMETERS

This Annex contains two illustrations of what can happen if the partial derivatives are not taken with respect to the independent parameters. Taking the partial derivatives with respect to the independent parameters is simple in concept but can be very complex and deceptive in practice. The illustrations provide some insight into the errors that can be produced by taking the partial derivatives with respect to dependent parameters. The first example is for the dynamic pressure and the second is for the forebody drag coefficient. The dynamic pressure and forebody drag were chosen because they illustrate common errors that are made when taking the partial derivatives.

### Dynamic pressure. q

The dynamic pressure, q, is determined by combining the calculated values of Mach number, M, and static pressure, p according to the following equation:

$$q = 0.70p(M^2) \tag{4-C-1}$$

In the text, the partial derivatives of q were taken with respect to the independent variables $p_T$, $p_C$, and DM, since both M and p are functions of these parameters. As shown in Eqs. (4-B-7)- (4-B-9), the equations for the partial derivatives are very complex. However, much simpler equations result by taking the partial derivatives of q with respect to M and p.

$$\frac{\partial q}{\partial M} = 1.40p(M) = [1.40(37870.04)(0.95)] = 50367.15 \tag{4-C-2}$$

$$\frac{\partial q}{\partial p} = 0.70M^2 = [0.70(0.95)^2] = 0.6318 \tag{4-c-3}$$

These partial derivatives are then used to develop equations for the bias and precision limits of q. Note that the bias and precision limits for p used in Eqs. (4-C-4) and (4-C-5) are the values as calculated in Eqs. (4-23) and (4-24).The bias and precision limits for p would be larger if they were also determined incorrectly by using the partial derivatives with respect to $p_T$ and M. Note that correlated bias effects are not included in the bias limit equation.

$$B_q = \pm\left(\left[\frac{\partial q}{\partial M}B_M\right]^2 + \left[\frac{\partial q}{\partial p}B_p\right]^2\right)^{\frac{1}{2}} = \pm\left([(50367.15)0.0019]^2 + [(0.6318)78.85]^2\right)^{\frac{1}{2}} = \pm 107.89\ \text{Pa} \tag{4-C-4}$$

$$P_q = \pm\left(\left[\frac{\partial q}{\partial M}P_M\right]^2 + \left[\frac{\partial q}{\partial p}P_p\right]^2\right)^{\frac{1}{2}} = \pm\left([(50367.15)0.00010]^2 + [(0.6318)3.70]^2\right)^{\frac{1}{2}} = \pm 5.55\ \text{Pa} \tag{4-c-5}$$

$$U_q = \pm\left(B_q^2 + P_q^2\right)^{\frac{1}{2}} = \pm\left(107.89^2 + 5.55^2\right)^{\frac{1}{2}} = \pm 108.03 \tag{4-C-6}$$

The uncertainties determined in Eqs. (4-25), (4-26), and (4-29) (excludingthe correlated bias limits for $p_T$ and $p_C$) are:

$$B_q = k45.21\ \textbf{Pa} \qquad P_q = \pm 3.53\ \text{Pa} \qquad U_q = 145.35\ \text{Pa} \tag{4-c-7}$$

Comparison of the correct values with those determined in this example shows that using the incorrect partial derivatives produces results that are about twice those determined using the partial derivatives with respect to the independent variables $p_T$, $p_C$, and DM. The reason for the difference is that p and M are dependent as p is a function of M. In order to correctly estimate the uncertainty for q the partial derivatives must be taken with respect to the independent parameters $p_T$, $p_C$, and DM.

A comparison of the results obtained by applying Eqs. (4-C-4)- (4-C-6) and Eqs. (4-25), (4-26), and (4-29) (excluding the correlated bias limits for $p_T$ and $p_C$) over the Mach number range is shown in the following graph.

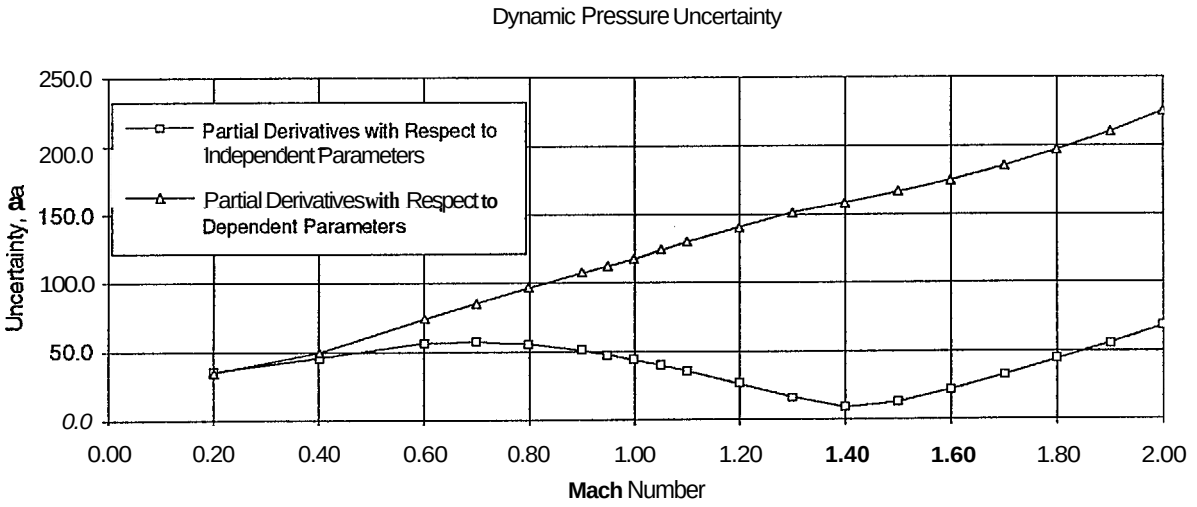


**Forebody Drag Coefficient, $C_{D_F}$**

This example illustrates the effects of using the partial derivatives of the forebody drag coefficient with respect *to* dependent parameters instead *of* independent parameters in estimating the uncertainty of the drag coefficient. The example shows only the effects on the uncertainty produced by the test conditions and ignores the uncertainty produced by the other parameters. The forebody drag coefficient is calculated from Eq. (4-84)

$$C_{D_F} = \frac{[F_{A_F}\mathrm{Cos}(\alpha) + F_N \mathrm{Sin}(\alpha)]}{qA} \tag{4-C-8}$$

As shown in the text the partial derivatives of $C_{D_F}$ with respect to q involves taking the partial derivatives with respect to $p_T$, $p_C$, and DM. However, taking the partial derivative with respect to q results in a very simple equation.

$$\frac{\partial C_{D_F}}{\partial q} = \frac{-C_{D_F}}{q} = \frac{-0.0592}{23924.40} = -2.474*10^{-6} \tag{4-c-9}$$

Using the above result to determine the contribution of the uncertainty of q to the uncertainty of the drag coefficient results in:

$$B_{C_{D_F}} = \pm\left(\left[\frac{\partial C_{D_F}}{\partial q} B_q\right]^2\right)^{\frac{1}{2}} = \left([-2.474*10^{-6}\,(44.89)]^2\right)^{\frac{1}{2}} = 0.000111 \tag{4-C-10}$$

$$P_{C_{D_F}} = \pm\left(\left[\frac{\partial C_{D_F}}{\partial q} P_q\right]^2\right)^{\frac{1}{2}} = \left([-2.474*10^{-6}\,(3.53)]^2\right)^{\frac{1}{2}} = 0.0000087 \tag{4-C-11}$$

$$U_{C_{D_F}} = \pm\left(B^2_{C_{D_F}} + P^2_{C_{D_F}}\right)^{\frac{1}{2}} = (0.0001\,11^2 + 0.0000087^2)^{\frac{1}{2}} = \pm 0.00011 \tag{4-C-12}$$

These same uncertainties determined using $p_T$, $p_C$, and DM [Eqs. (4-85) - (4-87)] are (remember the DM term is a constant and therefore has no precision term):

$$B_{C_{D_F}} = \pm\left(\left[\frac{\partial C_{D_F}}{\partial p_T} B_{p_T}\right]^2 + \left[\frac{\partial C_{D_F}}{\partial p_C} B_{p_C}\right]^2 + \left[\frac{\partial C_{D_F}}{\partial DM} B_{DM}\right]^2\right)^{\frac{1}{2}} \tag{4-C-13}$$

$$= \pm\left([(-1.635*10^{-6})19.81]^2 + [(1.897*10^{-7})22.75]^2 + [(-0.008121)0.00177]^2\right)^{\frac{1}{2}} = \pm 0.0000357$$

$$P_{C_{D_F}} = \pm\left(\left[\frac{\partial C_{D_F}}{\partial p_T} P_{p_T}\right]^2 + \left[\frac{\partial C_{D_F}}{\partial p_C} P_{p_C}\right]^2\right)^{\frac{1}{2}}$$

$$= \pm\left(\left[(-1.635*10^{-6})4.36\right]^2 + \left[(1.897*10^{-7})3.71\right]^2\right)^{\frac{1}{2}} = \sim 0.00000716 \qquad (4\text{-}C\text{-}14)$$

$$U_{C_{D_F}} = \pm\left(B_{C_{D_F}}^2 + P_{C_{D_F}}^2\right)^{\frac{1}{2}} = (0.0000357^2 + 0.00000716^2)^{\frac{1}{2}} = k0.0000364 \qquad (4\text{-}C\text{-}15)$$

Comparing the values determined by the different methods shows that using the partial derivatives with respect to $p_T$, $p_C$, and DM reduces the contribution of the uncertainties in the tunnel conditions to the uncertainty of the forebody drag coefficient by almost a factor of 3. The estimated uncertainty of the drag coefficient would not be significantly affected, for this example, because the contributions from the balance and model attitude overshadow those due to the static tunnel conditions. The reason that the partial derivative with respect to q gives the wrong result is that the terms $F_{A_F}$ and q are functions of p; therefore, q is not an independent parameter. However, for the drag coefficient without the forebody drag correction, taking the partial derivative with respect to q will provide the correct result since q and the parameters that compose q are not found in any of the other terms in the drag coefficient equation. This example illustrates how easy it is to unknowingly take a partial derivative with respect to a dependent parameter, instead of an independent parameter. To avoid this error the partial derivatives should always be determined (mathematically or numerically) with respect to measured parameters or constants. This will sometimes result in more complex partial derivatives but will ensure that they were determined with respect to independent parameters.

## ANNEX 4-D

## PRESSURE INTEGRATION EXAMPLE

The surface pressures measured during a typical pressure test are often used to determine the forces acting on the surface. This example is used to illustrate how the uncertainty methodology should be applied to a pressure integration problem. In most instances, the uncertainties in the measured and reference pressures, length and width of the surface, and the orientation of the surface to the direction of desired force would be considered in estimating the uncertainty of the integrated force. To simplify this example, a flat plate with a constant pressure acting over the entire surface is used. However, all of the correlated bias effects that will be present because the transducers were all calibrated against the same standard at the same time are included.

This example is based on the following:

A flat plate 1 m long and 0.15 m wide is at atmospheric pressure (98154.00 Pa), and the differential pressures on the plate are measured by an ESP module(s) which is referenced to atmospheric pressure. Therefore, the measured pressures will have a theoretical value of zero. The equation in Table 4.2 can be used, allowing for a ± 50-Pa drift before the ESP modules are recalibrated, to produce bias and precision limits for the pressure measurements. Note that the pressures were measured using a calibrated system; therefore, calibration uncertainty becomes the bias limit for the measured values. Also, the evaluation data were acquired in a manner that simulated the testing process as *a* result the precision limit estimated for the uncertainty evaluation is used as an estimate of the precision limit for the testing process.

$$P_{X_i} = 0 \tag{4-D-1}$$

$$B_{pX_i} = \pm 58.22 \text{ Pa and } P_{pX_i} = \pm 39.50 \text{ Pa} \tag{4-D-2}$$

$$U_{pX_i} = \pm\left(B_{pX_i}^2 + P_{pX_i}^2\right)^{\frac{1}{2}} = \left(58.22^2 + 39.50^2\right)^{\frac{1}{2}} = \pm 70.35 \text{ Pa} \tag{4-D-3}$$

There are correlated bias limits for the pressure measurements which result from calibrating all of the transducers against the same standard (Sonix® transducer) at the same time. The correlated bias limits are equal to the uncertainty of the Sonix® transducer (see Table 4.2 i.e., $p_{REF}$, $p_C$, etc.) at the measured pressure (note that the uncertainty equation for the Sonix® transducer requires an absolute pressure).

$$B'_{pX_i} = \pm\left[16.76 + 0.0001\left|98154 - (p_{X_i} + 98154)\right|\right] \tag{4-D-4}$$

$$= \pm\left[16.76 + 0.0001\left|98154 - (0 + 98154)\right|\right] = \pm 16.76 \text{ Pa}$$

Equations for the bias and precision limits for the reference pressure can be found in Table 4.2.

$$B_{pREF} = \pm\left[16.76 + 0.0001\left|98154 - p_{REF}\right|\right] = \pm\left[16.76 + 0.0001\left|0\right|\right] = \pm 16.76 \text{ Pa} \tag{4-D-5}$$

$$P_{pREF} = \pm\left[2.87 + 0.000022 p_{REF}\right] = \pm\left[2.87 + 0.000022(98154)\right] = \pm 5.03 \text{ Pa} \tag{4-D-6}$$

The bias and precision limits *for* the device used to measure the length and width of the plate are ± 0.000025 m and ± 0.000013 m, respectively. Therefore, the bias and precision limits for the width and length of the plate are:

$$B_W = B_L = \pm 0.000025 \text{ m} \tag{4-D-7}$$

$$P_W = P_L = \pm 0.000013 \text{ m} \tag{4-D-8}$$

The pressure orifices are located in a single column longitudinally down the center of the plate and are spaced in equal increments. The pressures are integrated using the trapezoidal rule (assumes

constant pressure acts over each area) with each pressure acting over equal areas. Examples are shown for 4, 10, and 40 pressure orifices.

The integrated force is determined by the following generic equation:

$$F = \sum_{i=1}^{N_{ps}} p_{S_i} L_i W_i \tag{4-D-9}$$

Where $p_{S_i}$ = Surface pressure = $p_{X_i} + p_{REF}$
$L_i$ = Length of the plate associated with each surface pressure
$W_i$ = Width of the plate associated with each surface pressure
$N_{ps}$ = Number of surface pressures

The generic equations for the bias and precision limits of the integrated force are developed by taking the partial derivatives with respect to $p_{X_i}$, $p_{REF}$, $L_i$, and $W_i$.

$$B_F = \pm\left[\sum_{i=1}^{N_{ps}}\left(\left[\frac{\partial F}{\partial p_{X_i}} B_{p_{X_1}}\right]^2 + \left[\frac{\partial F}{\partial p_{REF}} B_{p_{REF}}\right]^2 + \left[\frac{\partial F}{\partial L_i} B_{L_i}\right]^2 + \left[\frac{\partial F}{\partial W_i} B_{W_i}\right]^2\right) + \sum_{i=1}^{N_{ps}-1}\sum_{j=i+1}^{N_{ps}}\left(2\frac{\partial F}{\partial p_{X_i}}\frac{\partial F}{\partial p_{X_j}} B'_{p_{X_i}} B'_{p_{X_j}}\right) + B_{IT}^2\right]^{\frac{1}{2}} \tag{4-D-10}$$

$$P_F = \pm\left[\sum_{i=1}^{N_{ps}}\left(\left[\frac{\partial F}{\partial p_{X_i}} P_{p_{X_1}}\right]^2 + \left[\frac{\partial F}{\partial p_{REF}} P_{p_{REF}}\right]^2 + \left[\frac{\partial F}{\partial L_i} P_{L_i}\right]^2 + \left[\frac{\partial F}{\partial W_i} P_{W_i}\right]^2\right)\right]^{\frac{1}{2}} \tag{4-D-11}$$

Notice that a bias limit for the integration technique, $B_{IT}$, *has* been included in the equation for the estimation of the bias limit of the calculated force. The magnitude of this bias limit depends on the accuracy of the representation of the pressure distribution on the surface (i.e., the number of surface pressures) and the integration technique.

Equations (4-D-10) and (4-D-11) can be rewritten by applying the assumptions made for this example and the equations determined for the partial derivatives. The integration technique models this example perfectly; therefore, $B_{IT}$ will have a value of zero.

$$\frac{\partial F}{\partial p_{X_i}} = \frac{\partial F}{\partial p_{REF}} = L_i W_i\,;\ \frac{\partial F}{\partial L_i} = p_{S_i} W_i\,;\ \frac{\partial F}{\partial W_i} = p_{S_i} L_i \tag{4-D-12}$$

$$B_F = \pm\left[N_{ps}\left(\left[L_i W_i B_{p_{X_i}}\right]^2 + \left[L_i W_i B_{p_{REF}}\right]^2 + \left[p_{S_i} W_i B_{L_i}\right]^2 + \left[p_{S_i} L_i B_{W_i}\right]^2\right) + \left(\left[\sum_{i=1}^{N_{ps}-1} i\right]\left(2\left[L_i W_i B'_{p_{X_i}}\right]^2\right)\right)\right]^{\frac{1}{2}} \tag{4-D-13}$$

$$P_F = \pm\sqrt{N_{ps}}\left(\left[L_i W_i P_{p_{X_i}}\right]^2 + \left[L_i W_i P_{p_{REF}}\right]^2 + \left[p_{S_i} W_i P_{L_i}\right]^2 + \left[p_{S_i} L_i P_{W_i}\right]^2\right)^{\frac{1}{2}} \tag{4-D-14}$$

$$U_F = \pm\left(B_F^2 + P_F^2\right)^{\frac{1}{2}} \tag{4-D-15}$$

The bias and precision limits for the length of each segment, $L_i$, can be estimated by determining a bias and precision limit for each $L_i$ such that their root-sum-squared value will be equal to the bias and precision limit for the overall length measurement. This method results in the following equations which are used to estimate the bias and precision limits for each $L_i$.

$$B_L = \pm\sqrt{N_{ps}}\left(B_{L_i}^2\right)^{\frac{1}{2}} \Rightarrow B_{L_i} = \pm\frac{B_L}{\sqrt{N_{ps}}} \tag{4-D-16}$$

$$P_L = \pm\sqrt{N_{ps}}\left(P_{L_i}^2\right)^{\frac{1}{2}} \Rightarrow P_{L_i} = \pm\frac{P_L}{\sqrt{N_{ps}}} \tag{4-D-17}$$

The bias limits shown in this example have been divided into the bias errors from the measurements and the correlated bias errors to illustrate their relationship. The first part **of** the bias limit equations contains the bias errors from the measurements, and the second part **of** the equations contains the correlated bias errors.

**Example A. Four surface pressures**

$$N_{ps} = 4;\ L_i = L/4 = 1/4 = 0.25\text{m} \tag{4-D-18}$$

$$B_{L_i} = \pm\frac{B_L}{\sqrt{N_{ps}}} = \pm\frac{0.000025}{\sqrt{4}} = \sim 0.0000125 \tag{4-D-19}$$

$$P_{L_i} = \pm\frac{P_L}{\sqrt{N_{ps}}} = \pm\frac{0.000013}{\sqrt{4}} = \pm 0.0000065\ \text{m} \tag{4-D-20}$$

$$B_F = \pm\Big[4\Big([(0.25)(0.15)58.22]^2 + [(0.25)(0.15)16.76]^2 + [(98154)(0.15)0.0000125]^2 + [(98154)(0.25)0.000025]^2\Big) + \big(6(2)[(0.25)(0.15)16.76]^2\big)\Big]^{\frac{1}{2}} = \pm[22.29 + 4.74]^{\frac{1}{2}} = \pm 5.20\ \text{N} \tag{4-D-21}$$

$$P_F = \pm\sqrt{4}\Big([(0.25)(0.15)39.50]^2 + [(0.25)(0.15)5.03]^2 + [(98154)(0.15)0.0000065]^2 + [(98154)(0.25)0.000013]^2\Big)^{\frac{1}{2}} = \pm 3.06\ \text{N} \tag{4-D-22}$$

$$U_F = \pm\left(5.20^2 + 3.06^2\right)^{\frac{1}{2}} = \pm 6.03\ \text{N} \tag{4-D-23}$$

$$\therefore\ F = \sum_{i=1}^{N_{ps}} p_{S_i} L_i W_i = 4[98154.00(0.25)(0.15)] = 14723.10 \pm 6.03\text{N} \tag{4-D-24}$$

**Example B. Ten surface pressures**

$$N_{ps} = 10;\ L_i = L/10 = 1/10 = 0.1\text{m} \tag{4-D-25}$$

$$B_{L_i} = \pm\frac{B_L}{\sqrt{N_{ps}}} = \pm\frac{0.000025}{\sqrt{10}} = \pm 0.0000079\text{m} \tag{4-D-26}$$

$$P_{L_i} = \pm\frac{P_L}{\sqrt{N_{ps}}} = \pm\frac{0.000013}{\sqrt{10}} = \sim 0.0000041\text{m} \tag{4-D-27}$$

$$B_F = \pm\Big[10\Big([(0.10)(0.15)58.22]^2 + [(0.10)(0.15)16.76]^2 + [(98154)(0.15)0.0000079]^2 + [(98154)(0.10)0.000025]^2\Big) + \big(45(2)[(0.10)(0.15)16.76]^2\big)\Big]^{\frac{1}{2}} = \pm[9.00 + 5.69]^{\frac{1}{2}} = \pm 3.83\ \text{N} \tag{4-D-28}$$

$$P_F = \pm\sqrt{10}\Big([(0.10)(0.15)39.50]^2 + [(0.10)(0.15)5.03]^2 + [(98154)(0.15)0.0000041]^2 + [(98154)(0.10)0.000013]^2\Big)^{\frac{1}{2}} = \pm 1.94\text{N} \tag{4-D-29}$$

$$U_F = \pm\left(3.83^2 + 1.94^2\right)^{\frac{1}{2}} = \pm 4.29\ \text{N} \tag{4-D-30}$$

$$\therefore\ F = \sum_{i=1}^{N_{ps}} p_{S_i} L_i W_i = 10[98154.00(0.10)(0.15)] = 14723.10 \pm 4.29\ \text{N} \tag{4-D-31}$$

**Example C. Forty surface pressures**

$$N_{ps} = 40;\ L_i = L/40 = 1/40 = 0.025\ \text{m} \tag{4-D-32}$$

$$B_{L_i} = \pm\frac{B_L}{\sqrt{N_{ps}}} = \pm\frac{0.000025}{\sqrt{40}} = \pm 0.0000040\text{m} \tag{4-D-33}$$

$$P_{L_i} = \pm\frac{P_L}{\sqrt{N_{ps}}} = \pm\frac{0.000013}{\sqrt{40}} = \pm 0.0000021\text{m} \tag{4-D-34}$$

$$B_F = \pm\Big[40\Big([(0.025)(0.15)58.22]^2 + [(0.025)(0.15)16.76]^2 + [(98154)(0.15)0.0000040]^2 + [(98154)(0.025)0.000025]^2\Big) + \big(780(2)[(0.025)(0.15)16.76]^2\big)\Big]^{\frac{1}{2}} = \pm\big[2.35 + 6.16\big]^{\frac{1}{2}} = \pm 2.92 \text{ N} \quad (4\text{-D-}35)$$

$$P_F = \pm\sqrt{40}\,\Big([(0.025)(0.15)39.50]^2 + [(0.025)(0.15)5.03]^2 + [(98154)(0.15)0.0000021]^2 + [(98154)(0.025)0.000013]^2\Big)^{\frac{1}{2}} = \pm 0.99 \text{ N} \quad (4\text{-D-}36)$$

$$U_F = \pm\big(2.92^2 + 0.99^2\big)^{\frac{1}{2}} = \pm 3.08 \text{ N} \quad (4\text{-D-}37)$$

$$\therefore F = \sum_{i=1}^{N_{PS}} p_{S_i} L_i W_i = 40[98154.00(0.025)(0.15)] = 14723.10 \pm 3.08 \text{ N} \quad (4\text{-D-}38)$$

The estimated uncertainties determined in the example are shown along with the uncertainty estimates for 100, 1,000 and 10,000 surface pressures in Fig. 4-D-l . Note that in the figure the estimated bias limit has been shown along with the components of the bias limit produced by the bias errors of the measurements and the correlated bias errors. The results show that increasing the number of surface pressures decreases the estimated uncertainties asymptotically, with the exception of the correlated bias effects, which increase asymptotically. Developing this type of graph provides the information necessary for determing if the uncertainty criteria can be met and the number of surface pressures needed. In this example, using 10000 surface pressures would result in an estimated uncertainty for the integrated force of 2.6 N, which is only 0.6 N less than the uncertainty estimated using 40 surface pressures. However, the bias error associated with the pressure distribution and integration technique may also be dependent on the number of pressures used and may be significantly decreased by using more pressures.

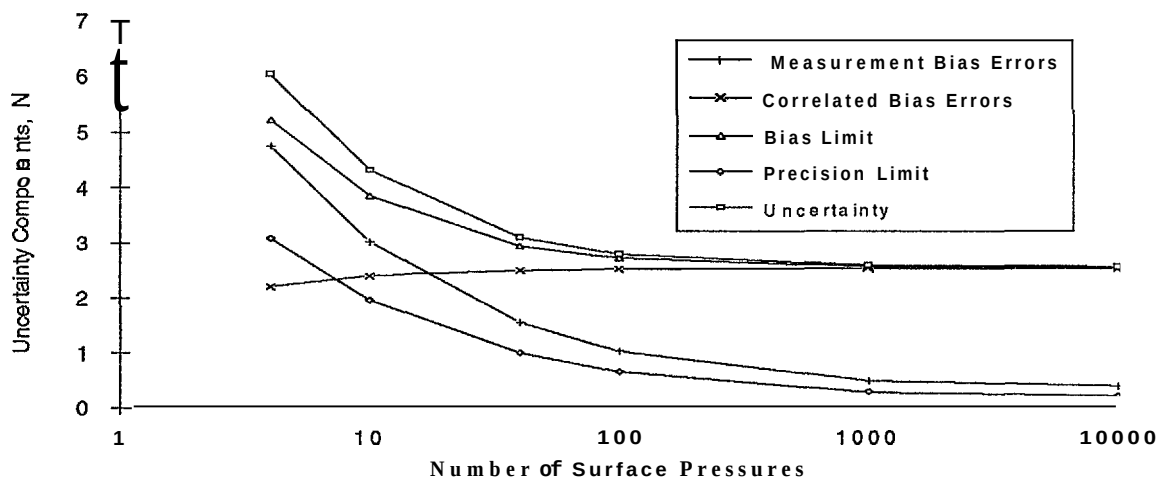


Figure 4-D-1. Effects of increasing the number of surface pressures on the uncertainty of the integrated force.

This example illustrates the importance of performing a pretest uncertainty analysis. In this instance, the uncertainty analysis would be used to determine the number of surface pressures that would be needed to provide the required uncertainty in the integrated force. Failure to perform the uncertainty analysis may result in added expense by fabricating a model with more surface pressures than are necessary. One might also discover that the uncertainty requirement cannot be met with the existing model, resulting in a requirement to either modify the existing model, fabricate a new model, relax the uncertainty requirements, or cancel the test.

## ANNEX 4-E

## UNCERTAINTY OF AN INCREMENTAL VALUE

Frequently the difference *between* measured values (incremental value), not the magnitude of measured values, is of primary importance. The bias limit for an incremental value is reduced as a result of the correlated bias effects produced by the subtraction of measured values which have common sources of bias errors. When determining the correlated bias effects, care must be taken to ensure that they are included properly. For the example of the forebody drag coefficient discussed in the text, correlated bias effects are present in the measured forces, pressures, model attitude, and tunnel conditions. The bias limits produced by these sources would be nearly eliminated for an incremental forebody drag coefficient using the assumptions made in the example. However, as shown by the results obtained in Section 4.4.6, the precision limit for the forebody drag coefficient is much larger than the bias limit; completely eliminating the bias limit would reduce the estimated uncertainty of the incremental forebody drag coefficient by one drag count (0.0001). This result may not be typical and each case should be evaluated to determine if a reduction in the bias limit will have the desired effect on the overall uncertainty.

An example of an incremental pressure is used to illustrate how the correlated bias effects are included for an incremental value. Pressure measurements $p_{X_1}$ and $p_{X_2}$ have been made at the same orifice and test conditions for model configurations 1 and 2, respectively. The surface pressures and incremental surface pressure are calculated using the following equations.

$$p_{S_1} = p_{X_1} + p_{REF} = -74214.00 + 98154.00 = 23940.0 \text{ Pa} \tag{4-E-1}$$

$$p_{S_2} = p_{X_2} + p_{REF} = 2394.00 + 98154.00 = 100548.0 \text{ Pa} \tag{4-E-2}$$

$$\Delta p_S = p_{S_2} - p_{S_1} = (p_{X_2} + p_{REF}) - (p_{X_1} + p_{REF}) = p_{X_2} - p_{X_1} = 2394.00 + 74214.00 = 76608.0 \text{ Pa} \tag{4-E-3}$$

Taking the partial derivatives of the above equation with respect to the measured pressures and including the correlated bias effects found in Eq. (2-16) yields the following equation for the bias limit of the incremental pressure.

$$B_{\Delta p_S} = \pm\left[\left(\frac{\partial \Delta p_S}{\partial p_{X_2}} B_{p_{X_2}}\right)^2 + \left(\frac{\partial \Delta p_S}{\partial p_{X_1}} B_{p_{X_1}}\right)^2 + 2\left(\frac{\partial \Delta p_S}{\partial p_{X_2}}\right)\left(\frac{\partial \Delta p_S}{\partial p_{X_1}}\right) B'_{p_{X_2}} B'_{p_{X_1}}\right]^{\frac{1}{2}}$$

$$= \pm\left[B^2_{p_{X_2}} + (-B_{p_{X_1}})^2 - 2\, B'_{p_{X_2}} B'_{p_{X_1}}\right]^{\frac{1}{2}} \tag{4-E-4}$$

The bias limits (calibration uncertainty) for the pressures measured by the ESP can be found in Table 4.2 (use a zero shift of ± 50 Pa) and the correlated bias limits are equal to the bias limit for each measurement.

$$B'_{p_{X_i}} = B_{p_{X_i}} \tag{4-E-5}$$

Substituting in the values for the bias limits yields the following:

$$B_{\Delta p_S} = \pm\left[58.24^2 + (-60.57)^2 - 2(58.24)(60.57)\right]^{\frac{1}{2}} = \pm 2.33 \text{ Pa} \tag{4-E-6}$$

The resulting bias limit for the incremental pressure is much smaller than the bias limits for either of the measured pressures. This illustrates how the correlated bias limit can be used to reduce the bias limit for an incremental value. Note that if the bias limits were constant over the range of measured pressures, the correlated bias limits would completely cancel the measurement bias limits.

The precision limit for the incremental pressure is calculated using the following equation.

$$P_{\Delta p_S} = \pm\left[\left(\frac{\partial \Delta p_S}{\partial p_{X_2}} P_{p_{X_2}}\right)^2 + \left(\frac{\partial \Delta p_S}{\partial p_{X_1}} P_{p_{X_1}}\right)^2\right]^{\frac{1}{2}} \quad (4\text{-E-}7)$$

Substituting the precision limits for the pressures measured by the ESP as found in Table 4.2 in the above equation yields:

$$P_{\Delta p_S} = \pm[39.27^2 + 51.63^2]^{\frac{1}{2}} = k64.87 \text{ Pa} \quad (4\text{-E-}8)$$

Notice that the resulting precision limit for the incremental pressure is larger than the precision limits for the measured pressures. This is the opposite of what occurred for the bias limit. The estimated uncertainty of the incremental pressure is determined by combining the incremental bias and precision limits.

$$U_{\Delta p_S} = \pm[B^2_{\Delta p_S} + P^2_{\Delta p_S}]^{\frac{1}{2}} = \pm[2.33^2 + 64.87^2]^{\frac{1}{2}} = k64.91 \text{ Pa} \quad (4\text{-E-}9)$$

The estimated uncertainties for the measured pressures are determined as follows (note that all of the partial derivatives are equal to 1):

$$B_{p_{S_1}} = \pm[B^2_{p_{X_1}} + B^2_{p_{REF}}]^{\frac{1}{2}} = \pm[60.57^2 + 16.76^2]^{\frac{1}{2}} = \pm 62.85 \text{ Pa} \quad (4\text{-E-}10)$$

$$B_{p_{S_2}} = \pm[B^2_{p_{X_2}} B^2_{p_{REF}}]^{\frac{1}{2}} = \pm[58.24^2 + 16.76^2]^{\frac{1}{2}} = k60.60 \text{ Pa} \quad (4\text{-E-}11)$$

$$P_{p_{S_1}} = \pm[P^2_{p_{X_1}} + P^2_{p_{REF}}]^{\frac{1}{2}} = \pm[51.63^2 + 5.03^2]^{\frac{1}{2}} = k51.87 \text{ Pa} \quad (4\text{-E-}12)$$

$$P_{p_{S_2}} = \pm[P^2_{p_{X_2}} + P^2_{p_{REF}}]^{\frac{1}{2}} = \pm[39.27^2 + 5.03^2]^{\frac{1}{2}} = k39.59 \text{ Pa} \quad (4\text{-E-}13)$$

$$U_{p_{S_1}} = \pm[B^2_{p_{S_1}} + P^2_{p_{S_1}}]^{\frac{1}{2}} = \pm[62.85^2 + 51.87^2]^{\frac{1}{2}} = \pm 81.49 \text{Pa} \quad (4\text{-E-}14)$$

$$U_{p_{S_2}} = \pm[B^2_{p_{S_2}} + P^2_{p_{S_2}}]^{\frac{1}{2}} = \pm[60.60^2 + 39.59^2]^{\frac{1}{2}} = k77239 \text{ Pa} \quad (4\text{-E-}15)$$

Comparing the results obtained in this example reveals that the estimated uncertainty of the incremental pressure was reduced by approximately 10 to 20 percent compared to those for the individual pressures. The small reduction results from the near elimination of the bias limit being offset by an increase in the precision limit. This example has shown that the reduction in the estimated uncertainty of an incremental value is a function of the ratio of the bias and precision limits of the measurements. Large reductions in the estimated uncertainty of an incremental value will result only if the bias limits of the measurements are significantly larger than the precision limits.

## 5.0 SUMMARY AND RECOMMENDATIONS

This report describes a practical approach for assessing the uncertainty of experimental measurements. Although it concentrates on aerodynamic reference data, the approach presented can be used to report data and associated uncertainties for any other condition. The methodology described is designed to facilitate communications and to encourage professional and practical analyses of complex problems. The most recent accepted technical concepts have been included in the methodology.

The report illustrates that there are many opportunities for uncertainties to exist in test results. Because the scope of error sources is large, there may be a temptation to avoid examining the test and its associated processes and uncertainty sources in detail. It is strongly recommended that any such temptation be resisted, for only by careful analysis can the quality of the test results be defended.

The benefits of applying the uncertainty assessment method can be significant. Major gains in the effective use of test resources (facilities, labor, power, budget) can be realized by more intelligent selection and planning of tests, as well as improved monitoring of results. In the longer term, the entire aerodynamics community will benefit from improved assessment, through, for example, facilities focusing resources on further improvement of their testing practices. Also, users of data will be able to make more informed judgments concerning the appropriateness of wind tunnel test results, thus minimizing misinterpretation and/or misuse.

The practical aspects of implementing uncertainty assessment as a routine procedure within an organization, obtained from the experience of working group members, lead to the following recommendations to management.

1. The above benefits will be achieved only if management is committed to implementation of the process, and this commitment is evident to the entire organization through constancy of purpose and provision of adequate resources.

2. The staff members responsible for all phases of testing shown in Fig. 1.3 must be trained to use the methodology.

3. The educational experience must be sustained beyond the initial training. Management should ensure that the methodology is used properly and routinely. Development of a database as suggested in Section 3.4 will facilitate this. It may be advantageous for organizations to develop an "Engineer's Handbook" in which the application of the methodology is tailored to the specific processes and equipment used by the facility.

Similarly, the experience of the working group members leads to the following recommendations to test engineers responsible for the application of the method.

1. Recognize that uncertainty is process dependent. Thus, changes in details of the test technique can significantly affect the uncertainty of the test results.

2. The method should be applied to all phases of the experimental process—design, planning, calibration, execution and post-test analyses.

3. Analyses of the problem should be simplified as much as possible by using prior knowledge, (e.g., the database recommended in Section 3.4), tempered with engineering judgment. Effort should be concentrated on the dominant error sources.

4. The results of the uncertainty analyses should be reported consistently and completely. Specifically, the following components of the whole uncertainty assessment process should be documented:

   a. the experimental process in block diagram form,
   b. the equipment used,
   c. the error sources considered,
   d. all estimates for bias and precision limits, and the methods used in their estimation, (e.g. manufacturer's specifications, comparison against standards, experience...), and
   e. the uncertainty methodology used to determine the stated uncertainty estimates.

Finally, it is recommended that users of wind tunnel test facilities should encourage (or require) those facilities to present analyses of the uncertainties in their test results.

## NOMENCLATURE

| | |
|---|---|
| 4T | AEDC 4-ft Aerodynamic Wind Tunnel |
| 16T | AEDC 16-ft Propulsion Wind Tunnel |
| A | Reference area, $m^2$ (Sec. 2.1) |
| $A_B$ | Base area, $m^2$ (Sec. 4.4) |
| b | Standard deviation of the bias error distribution (Annex 2-B) |
| B' | Perfectly correlated bias limit (Sec. 2.3.3) |
| B | Bias limit of a variable (Sec. 2.2.1) |
| cal | Calibration (Sec. 4.3.3) |
| $C_D$ | Drag coefficient (Sec. 2.1) |
| $C_{D_F}$ | Forebody drag coefficient (Sec. 4.4.6) |
| $C_{D_{F_{16T}}}$ | Assumed "interference-free" reference forebody drag coefficient determined in Tunnel 16T (Sec. 4.5) |
| $C_{D_{F,AR}}$ | Forebody drag coefficient adjusted to the aerodynamic reference condition (Sec. 4.5) |
| $C_{D_{WI}}$ | Incremental drag coefficient due to wall interference (Sec. 4.5) |
| DM | Delta Mach number determined during the wind tunnel calibration (Sec. 4.4.1) |
| E | Individual sample error (Sec. 4.3.2) |
| $\bar{E}$ | Average of the individual sample errors (Sec. 4.3.2) |
| $E_{MAX}$ | Bound on the maximum individual error (Sec. 4.3.2) |
| F | Force integrated from pressure measurements, N (Annex 4-D) |
| $F_A$ | Aerodynamic axial force, N (Sec. 4.4.4) |
| $F_{A_B}$ | Base axial force, N (Sec. 4.4.5) |
| $F_{A_F}$ | Forebody axial force, N (Sec. 4.4.5) |
| $F_{A_G}$ | Gross axial force, N (Sec. 4.4.3) |
| $F_{A_M}$ | Axial force measured by the balance, N (Sec. 4.4.3) |
| $F_{A_{ST}}$ | Axial force static tare, N (Sec. 4.4.4) |
| $F_N$ | Aerodynamic normal force, N (Sec. 4.4.4) |
| $F_{N_G}$ | Gross normal force, N (Sec. 4.4.3) |

| | |
|---|---|
| $F_{N_M}$ | Normal force measured by the balance, N (Sec. 4.4.3) |
| $F_{N_{ST}}$ | Normal force static tare, N (Sec. 4.4.4) |
| IU | Intermediate uncertainty (Annex 4-A) |
| $\overline{IU}$ | Average of the intermediate uncertainty values (Annex 4-A) |
| K | Coverage factor (Sec. 2.2.2) |
| L | Length, m (Annex 4-E) |
| m | Meters (1 meter = 3.2808 ft) |
| M | Number of significant elemental bias errors (Sec. 2.2.3) |
| M | Number of separate results (Sec. 2.3.2 ) |
| M | Calculated free-stream Mach number (Sec. 4.4.1) |
| N | Number of repeated measurements (Sec. 2.2.2) |
| N | Newtons (1 Newton = 0.2248 lbf) |
| P | Calculated free-stream static pressure, Pa (Sec. 4.4.1) |
| $p_B$ | Base pressure, Pa (Sec. 4.4.5) |
| $\overline{p_B}$ | Average base pressure, Pa (Sec. 4.4.5) |
| $p_{B_M}$ | Measured differential base pressure, Pa (Sec. 4.4.5) |
| $P_C$ | Plenum static pressure, Pa (Sec. 4.4.1) |
| $P_{REF}$ | Reference pressure, Pa (Sec. 4.4.5) |
| $P_X$ | Measured differential pressure, Pa (Sec. 4.3.2) |
| $P_S$ | Surface pressure, Pa (Annex 4-E)) |
| $p_T$ | Stilling chamber total pressure, Pa (Sec. 4.4.1) |
| P | Precision limit of a variable (Sec. 2.2.1) |
| $\overline{P}$ | Average precision limit (Annex 4-A) |
| $P_a$ | Pascals (1 Pascal = 0.02089 psf) |
| q | Calculated free-stream dynamic pressure, Pa (Sec. 4.4.1) |
| r | Result (Sec. 2.1) |
| r | Average result (Sec. 2.3.2.1) |

| | |
|---|---|
| S | Standard deviation of the sample of N readings of a variable (Sec. 2.2.2) |
| Sln | Standard deviation of a log-normal distribution (Annex 4-A) |
| t | Time (Sec. 2.2.2) |
| t | Value from the t distribution at a specified confidence level (Annex 2-A) |
| $t_s$ | 95 percent confidence level value from a single-tailed t distribution (Annex 4-A) |
| T | Average of a log-normal distribution (Annex 4-A) |
| $u_c$ | Combined standard uncertainty (Annex 2-A) |
| U | Uncertainty of a variable (Sec. 2.2.1) |
| V | Velocity (Sec. 2.1) |
| W | Width, m (Annex 4-D) |
| $W_A$ | Weight of model and balance as determined using the balance axial force gages, N (Sec. 4.4.3) |
| $W_N$ | Weight of model and balance as determined using the balance normal force gages, N (Sec. 4.4.3) |
| WS | Value measured by the working standard (Sec. 4.3.2) |
| X | Variable (Sec. 2.1) |
| $\bar{X}$ | Average of separate readings of a variable (Sec. 2.2.2) |
| $\alpha$ | Model angle of attack, stability axis system, deg (Sec. 4.4.2) |
| $\alpha_S$ | Support system pitch angle, deg (Sec. 4.4.2) |
| $\alpha_{S_0}$ | Support system pitch angle at the wind-off zero position, deg (Sec. 4.4.2) |
| $\gamma$ | Ratio of specific heats (Annex 4-B) |
| $\beta$ | True bias error (Sec. 2.1) |
| $\beta$ | Model angle of sideslip, stability axis system, deg (Sec. 4.4.2) |
| 6 | Kronecker delta (Annex 2-A) |
| 6 | Deviation between a sample value and the sample mean (Annex 2-B) |
| $\Delta p_S$ | Incremental surface pressure, Pa (Annex 4-E) |
| $\phi_S$ | Support system roll angle, deg (Sec. 4.4.2) |
| $\phi_{S_0}$ | Support system roll angle at the wind-off zero position, deg (Sec. 4.4.2) |
| $\mu$ | True population mean (Sec. 2.2.1) |

$\nu$ Degrees of freedom (Annex 2-A)

$\theta$ Sensitivity coefficient (Sec. 2.3.2.2)

$\rho$ Density (Sec. 2.1)

$\rho$ Correlation coefficients for bias and precision errors (Annex 2-A)

$\tau$ Value in Chauvenet's outlier criterion (Annex 2-B)

# REPORT DOCUMENTATION PAGE

| 1. Recipient's Reference | 2. Originator's Reference | 3. Further Reference | 4. Security Classification of Document |
|---|---|---|---|
| | AGARD-AR-304 | ISBN 92-835-0753-3 | UNCLASSIFIED/ UNLIMITED |

**5. Originator** Advisory Group for Aerospace Research and Development
North Atlantic Treaty Organization
7 rue Ancelle, 92200 Neuilly sur Seine, France

**6. Title** QUALITY ASSESSMENT FOR WIND TUNNEL TESTING

**7. Presented on**

**8. Author(s)/Editor(s)** Various

**9. Date** July 1994

**10. Author(s)/Editor's Address** Various

**11. Pages** 90

**12. Distribution Statement** There are no restrictions on the distribution of this document. Information about the availability of this and other AGARD unclassified publications is given on the back cover.

**13. Keywords/Descriptors**

Wind tunnels
Aerodynamics
Data accuracy
Data quality
Measurements

**14. Abstract**

The wind tunnel continues to be the main instrument for providing experimental aerodynamic dat to the aerospace industry and the aerodynamic researcher for the purpose of load and performanc evaluation of theoretical results. In both cases, it is imperative that the user has confidence in the quality of the results, which means that he must have information of what accuracy to attach to th data.

This report describes a practical approach for assessing the uncertainty of experimental measurements. Although it concentrates on aerodynamic reference data, the approach presented can be used to report data and associated uncertainties for any other condition. The methodology described is designed to facilitate communications and to encourage professional and practical analyses of complex problems. The most recent accepted technical concepts have been included i the methodology.

This report presents the results of a study by Working Group 15 of the AGARD Fluid Dynamics Panel.

AGARD Advisory Report 304
Advisory Group for Aerospace Research and Development, NATO
QUALITY ASSESSMENT FOR WIND TUNNEL TESTING
Published July 1994
90 pages

The wind tunnel continues to be the main instrument for providing experimental aerodynamic data to the aerospace industry and the aerodynamic researcher for the purpose of load and performance evaluation of theoretical results. In both cases, it is imperative that the user has confidence in the quality of the results, which means that he must have information of what accuracy to attach to the data.

This report describes a practical approach for assessing the

P.T.O.

AGARD-AR-304

Wind tunnels
Aerodynamics
Data accuracy
Data quality
Measurements

AGARD Advisory Report 304
Advisory Group for Aerospace Research and Development, NATO
QUALITY ASSESSMENT FOR WIND TUNNEL TESTING
Published July 1994
90 pages

The wind tunnel continues to be the main instrument for providing experimental aerodynamic data to the aerospace industry and the aerodynamic researcher for the purpose of load and performance evaluation of theoretical results. In both cases, it is imperative that the user has confidence in the quality of the results, which means that he must have information of what accuracy to attach to the data.

This report describes a practical approach for assessing the

P.T.O.

AGARD-AR-304

Wind tunnels
Aerodynamics
Data accuracy
Data quality
Measurements

AGARD Advisory Report 304
Advisory Group for Aerospace Research and Development, NATO
QUALITY ASSESSMENT FOR WIND TUNNEL TESTING
Published July 1994
90 pages

The wind tunnel continues to be the main instrument for providing experimental aerodynamic data to the aerospace industry and the aerodynamic researcher for the purpose of load and performance evaluation of theoretical results. In both cases, it is imperative that the user has confidence in the quality of the results, which means that he must have information of what accuracy to attach to the data.

This report describes a practical approach for assessing the

P.T.O.

AGARD-AR-304

Wind tunnels
Aerodynamics
Data accuracy
Data quality
Measurements

AGARD Advisory Report 304
Advisory Group for Aerospace Research and Development, NATO
QUALITY ASSESSMENT FOR WIND TUNNEL TESTING
Published July 1994
90 pages

The wind tunnel continues to be the main instrument for providing experimental aerodynamic data to the aerospace industry and the aerodynamic researcher for the purpose of load and performance evaluation of theoretical results. In both cases, it is imperative that the user has confidence in the quality of the results, which means that he must have information of what accuracy to attach to the data.

This report describes a practical approach for assessing the

P.T.O.

AGARD-AR-304

Wind tunnels
Aerodynamics
Data accuracy
Data quality
Measurements

uncertainty of experimental measurements. Although it concentrates on aerodynamic reference data, the approach presented can be used to report data and associated uncertainties for any other condition. The methodology described is designed to facilitate communications and to encourage professional and practical analyses of complex problems. The most recent accepted technical concepts have been included in the methodology.

This report presents the results of a study by Working Group 15 of the AGARD Fluid Dynamics Panel.

ISBN 92-835-0753-3

uncertainty of experimental measurements. Although it concentrates on aerodynamic reference data, the approach presented can be used to report data and associated uncertainties for any other condition. The methodology described is designed to facilitate communications and to encourage professional and practical analyses of complex problems. The most recent accepted technical concepts have been included in the methodology.

This report presents the results of a study by Working Group 15 of the AGARD Fluid Dynamics Panel.

ISBN 92-835-0753-3

uncertainty of experimental measurements. Although it concentrates on aerodynamic reference data, the approach presented can be used to report data and associated uncertainties for any other condition. The methodology described is designed to facilitate communications and to encourage professional and practical analyses of complex problems. The most recent accepted technical concepts have been included **in** the methodology.

This report presents the results of a study by Working Group 15 of the AGARD Fluid Dynamics Panel.

ISBN 92-835-0753-3

AGARD
NATO OTAN
7 RUE ANCELLE • 92200 NEUILLY-SUR-SEINE
FRANCE
Telecopie (1)47.38.57.99 · Telex 610 176

**DIFFUSION DES PUBLICATIONS**
**AGARD NON CLASSIFIEES**

Aucun stock de publications n'a existé a AGARD. A partir de 1993, AGARD dktiendra un stock limité des publications associées aux cycles de conferences et cours spéciaux ainsi que les AGARDographies et les rapports des groupes de travail, organisés et publiés a partir de 1993 inclus. Les demandes de renseignements doivent être adressées à AGARD par lettre ou par fax a l'adresse indiquée ci-dessus. ***Veuillez ne pas téléphoner.*** La diffusion initiale de toutes les publications de l'AGARD est effectuée auprès des pays membres de l'OTAN par l'intermédiaire des centres de distribution nationaux indiqués ci-dessous. Des exemplaires **supplémentaires** peuvent parfois dtre obtenus auprès de ces centres (à l'exception des Etats-Unis). Si vous souhaitez recevoir toutes les publications de l'AGARD, ou simplement celles qui concernent certains Panels, vous pouvez demander à dtre inclu sur la liste d'envoi de l'un de ces centres. Les publications de l'AGARD sont en vente auprils des agences indiquees ci-dessous, sous forme de photocopie ou de microfiche.

## CENTRES DE DIFFUSION NATIONAUX

ALLEMAGNE
Fachinformationszentrum,
Karlsruhe
D-7514 Eggenstein-Leopoldshafen2

BELGIQUE
Coordonnateur AGARD-VSL
Etat-Major de la Force Aérienne
Quartier Reine Elisabeth
Rue d'Evere, 1140 Bruxelles

CANADA
Directeur du Service des Renseignements Scientifiques
Ministkre de la Dkfense Nationale
Ottawa, Ontario K1A OK2

DANEMARK
Danish Defence Research Establishment
Ryvangs Allé 1
P.O. Box 2715
DK-2100 Copenhagen O

ESPAGNE
INTA (AGARD Publications)
Pintor Rosales 34
28008 Madrid

ETATS-UNIS
NASA Headquarters
Attention: CF 37, Distribution Center
300 E Street, S.W.
Washington, D.C. 20546

FRANCE
O.N.E.R.A. (Direction)
29, Avenue de la Division Leclerc
92322 Châtillon Cedex

GRECE
Hellenic Air Force
Air War College
Scientific and Technical Library
Dekelia Air Force Base
Dekelia, Athens TGA 1010

ISLANDE
Director of Aviation
c/o Flugrad
Reykjavik

ITALIE
Aeronautica Militare
Ufficio del Delegato Nazionale all'AGARD
Aeroporto Pratica di Mare
00040 Pomezia (Roma)

LUXEMBOURG
*Voir* Belgique

NORVEGE
Norwegian Defence Research Establishment
Attn: Biblioteket
P.O. Box 25
N-2007 Kjeller

PAYS-BAS
Netherlands Delegation to AGARD
National Aerospace Laboratory NLR
P.O. Box 90502
1006 BM Amsterdam

PORTUGAL
Força Aérea Portuguesa
Centro de Documentação e Informação
Alfragide
2700 Amadora

ROYAUME UNI
Defence Research Information Centre
Kentigem House
65 Brown Street
Glasgow G2 8EX

TURQUIE
Millî Savunma Başkanlığı (MSB)
ARGE Daire Başkanlığı (ARGE)
Ankara

**Le** centre de distribution national **des** Etats-Unis ne detient **PAS de** stocks des publications **de l'AGARD.** Dkventuelles demandes de photocopies doivent être formulkes directement auprils du NASA Center for Aerospace Information (CASI) à l'adresse suivante:

## AGENCES DE VENTE

NASA Center for
Aerospace Information (CASI)
800 Elkridge Landing Road
Linthicum Heights, MD 21090-2934
United States

ESA/Information Retrieval Service
European Space Agency
10, rue Mario Nikis
75015 Paris
France

The British Library
Document Supply Division
Boston Spa, Wetherby
West Yorkshire LS23 7BQ
Royaume Uni

Les demandes de microfiches ou de photocopies de documents AGARD (y compris les demandes faites auprils du CASI) doivent comporter la dénomination AGARD, ainsi que le numkro de série d'AGARD (par exemple AGARD-AG-315). Des informations analogues, telles que le titre et la date de publication sont souhaitables. Veuiller noter qu'il y a lieu de specifier AGARD-R-nnn et AGARD-AR-nnn lors de la commande des rapports AGARD et des rapports consultatifs AGARD respectivement. Des références bibliographiques complètes ainsi que des résumés des publications AGARD figurent dans les journaux suivants:

Scientifique and Technical Aerospace Reports (STAR)
publié par la NASA Scientific and Technical
Information Program
NASA Headquarters (JTT)
Washington D.C. 20546
Etats-Unis

Government Reports Announcements and Index (GRA&I)
publié par le National Technical Information Service
Springfield
Virginia 22161
Etats-Unis

(accessible kgalement en mode interactif dans la base de données bibliographiques en ligne du NTIS, et sur CD-ROM)

*Imprimé par Specialised Printing Services Limited*
*40 Chigwell Lane, Loughton, Essex IG10 3TZ*

AGARD

NATO OTAN

7 RUE ANCELLE · 92200 NEUILLY-SUR-SEINE

FRANCE

Telefax (1)47.38.57.99 · Telex 610 176

**DISTRIBUTION OF UNCLASSIFIED AGARD PUBLICATIONS**

BELGIUM
Coordonnateur AGARD — VSL
Etat-Major de la Force Aérienne
Quartier Reine Elisabeth
Rue d'Evere, 1140 Bruxelles

CANADA
Director Scientific Information Services
Dept of National Defence
Ottawa, Ontario K1A OK2

DENMARK
Danish Defence Research Establishment
Ryvangs Allé 1
P.O. Box 2715
DK-2100 Copenhagen O

FRANCE
O.N.E.R.A. (Direction)
29 Avenue de la Division Leclerc
92322 Châtillon Cedex

GERMANY
Fachinformationszentrum
Karlsruhe
D-7514 Eggenstein-Leopoldshafen 2

GREECE
Hellenic Air Force
Air War College
Scientificand Technical Library
Dekelia Air Force Base
Dekelia, Athens TGA 1010

ICELAND
Director of Aviation
c/o Flugrad
Reykjavik

ITALY
Aeronautica Militare
Ufficio del Delegato Nazionale all'AGARD
Aeroporto Pratica di Mare
00040 Pomezia (Roma)

LUXEMBOURG
*See* Belgium

NETHERLANDS
Netherlands Delegation to AGARD
National Aerospace Laboratory, NLR
P.O. Box 90502
1006 BM Amsterdam

NORWAY
Norwegian Defence Research Establishment
Attn: Biblioteket
P.O. Box 25
N-2007 Kjeller

PORTUGAL
Força Aérea Portuguesa
Centro de Documentação e Informação
Alfragide
2700 Amadora

SPAIN
INTA (AGARD Publications)
Pintor Rosales 34
28008 Madrid

TURKEY
Milli Savunma Başkanlığı (MSB)
ARGE Daire Başkanlığı (ARGE)
Ankara

UNITED KINGDOM
Defence Research Information Centre
Kentigem House
65 Brown Street
Glasgow G2 8EX

UNITED STATES
NASA Headquarters
Attention: CF 37, Distribution Center
300 E Street, S.W.
Washington, D.C. 20546

**The United States National Distribution Centre does NOT hold stocks of AGARD publications.**
Applications for copies should be made direct to the NASA Center for Aerospace Information (CASI) at the address below.

SALES AGENCIES

NASA Center for
Aerospace Information (CASI)
800 Elkndge Landing Road
Linthicum Heights, MD 21090-2934
United States

ESA/Information Retrieval Service
European Space Agency
10, rue Mario Nikis
75015 Pans
France

The British Library
Document Supply Centre
Boston Spa, Wetherby
West Yorkshire LS23 7BQ
United Kingdom

Requests for microfiches or photocopies of AGARD documents (including requests to CASI) should include the word 'AGARD' and the AGARD serial number (for example AGARD-AG-315). Collateral information such as title and publication date is desirable. Note that

ographical

kI)


SPS

*Printed by Specialised Printing Services Limited*
*40 Chigwe* *TZ*



ISBN 92-835-0753-3